MICROTUBULE FUNCTION DURING EARLY DEVELOPMENT IN *SILVETIA COMPRESSA*

by

Nicholas Thomas Peters

A dissertation submitted to the faculty of
The University of Utah
in partial fulfillment of the requirements for the degree of

Doctor of Philosophy

Department of Biology

The University of Utah

May 2010

THE UNIVERSITY OF UTAH GRADUATE SCHOOL

SUPERVISORY COMMITTEE APPROVAL

of a dissertation submitted by

Nicholas Thomas Peters

This dissertation has been read by each member of the following supervisory committee and by majority vote has been found to be satisfactory.

4-23-10 — Chair: Darryl L. Kropf

4-23-10 — Michael Bastiani

4-23-10 — Gary N. Drews

23 Apr 2010 — David L. Gard

23 Apr 2010 — Leslie E. Sieburth

THE UNIVERSITY OF UTAH GRADUATE SCHOOL

FINAL READING APPROVAL

To the Graduate Council of the University of Utah:

I have read the dissertation of Nicholas Thomas Peters in its final form and have found that (1) its format, citations, and bibliographic style are consistent and acceptable; (2) its illustrative materials including figures, tables, and charts are in place; and (3) the final manuscript is satisfactory to the supervisory committee and is ready for submission to The Graduate School.

4-23-10
Date

Darryl L. Kropf
Chair: Supervisory Committee

Approved for the Major Department

Neil J. Vickers
Chair/Dean

Approved for the Graduate Council

Charles A. Wight
Dean of The Graduate School

ABSTRACT

Embryonic development is one of the most critical stages of the life cycle for most eukaryotic organisms. Extrinsic and intrinsic signals must be perceived and transduced to facilitate proper organization of a body plan. Cellular components must then be selectively segregated to different parts of the embryo and accompanying morphological changes must be precisely positioned. To aid the cell in orchestration of these dynamic events, the cytoskeleton performs many tasks, including structural support, organelle positioning, vesicle transport, and localization of polarity molecules. While microtubules have been extensively examined in vascular plants and animals, much less is known about their roles in the stramenopile lineage. In the brown alga *Silvetia compressa*, I examined the structural and functional roles of microtubules during early development. In contrast to previous reports, I found that microtubule arrays become asymmetrically oriented toward the apex of the rhizoid pole during polarization. These microtubule arrays organize the endoplasmic reticulum and target it toward the rhizoid pole. I also showed that the phospholipase D and phospholipase C signaling pathways are functional in brown algae and are needed for organization of the cytoskeleton. Finally, I examined the microtubule-associated motor protein Kinesin-5 (Eg5) during spindle assembly and highlighted its functional similarities and differences with vascular plants and animals. This work has yielded insights into conserved and novel traits possessed

solely by brown algae and has led to a significant revision of the model for early development.

This dissertation is dedicated to the concept that

good things really can happen to bad people

TABLE OF CONTENTS

ACKNOWLEDGEMENTS

I would first like to thank Darryl Kropf for being an excellent mentor and a friend. He worked with me every step of the way and has made me a much better scientist, writer, and person. I would also like to thank my family, friends, and Stephanie Peters for their continued support. Chapter 2 is reprinted with permission from Cell Motility and the Cytoskeleton, N.T. Peters and D. L. Kropf. Asymmetric Microtubule Arrays Organize The Endoplasmic Reticulum During Polarity Establishment In the Brown Alga *Silvetia compressa.* Copyright (2009), with permission from Wiley-Blackwell.

CHAPTER 1

INTRODUCTION: EARLY DEVELOPMENT IN *SILVETIA COMPRESSA*

Establishment of polarity and asymmetric cell division are crucial for growth and differentiation of many cell types. *Silvetia compressa* is a model system uniquely suited to examine how a polar axis is established and maintained. Importantly, *S. compressa* possesses a labile polar axis that facilitates examining the cellular and physiological mechanisms of polarization. By contrast, studying polarity establishment in most model organisms is due to the germ cells already possessing a fixed polar axis. Extensive studies have shown that the F-actin cytoskeleton plays a major role in determining and maintaining a polar axis in *S. compressa*. However, the functional roles of microtubules during polarization are not well understood and almost nothing is known about how microtubule arrays are regulated. In order to better understand how a polar axis is established and maintained to facilitate proper expression of a complex multicellular body plan, my experiments were designed to 1) examine the microtubule-based functions during axis establishment, 2) study the signaling pathways which regulate microtubules, and 3) explore the roles of microtubule-associated proteins (MAPs) that facilitate spindle assembly.

1.1 Studying stramenopiles

S. compressa, a member of the stramenopiles or heterokonts, which are a crown group, radiated about 300 million years ago, after the cretaceous period (Medlin, 1997). The lineage is composed of over 100,000 known species, including photosynthetic and nonphotosynthetic organisms. The name heterokont, from the Greek words "heteros" meaning different and "kont" meaning tail, describes the hallmark feature of two unequal flagella, one of which is covered with small hairs or mastigonemes (Bouck, 1969). Notable members include brown algal seaweeds, diatoms, and oomycetes. The

photosynthetic capacity of brown algae is thought to be derived from a secondary endosymbiotic event from red algal lineages (Le Corguille et al., 2009). The hundreds of millions of years that separate the stramenopiles from more extensively studied lineages (e.g., higher plants or animals) provides a unique opportunity to compare and contrast developmental mechanisms, and to discover novel pathways.

1.2 Early development in *S. compressa*

Polarization and asymmetric cell division are critical for organization of a complex, multicellular body plan in *S. compressa*. Zygotes must perceive and transduce vectorial cues from their environment to facilitate formation of a polar axis (Kropf et al., 1999). Subsequent localized growth and asymmetric cell division are positioned by polar axis components (Bisgrove et al., 2003; Hable et al., 1998). The first cell division forms rhizoid and thallus cells, which have different developmental fates. The cell lineage derived from the thallus cell becomes the vegetative stipe and reproductive fronds of the alga, and the rhizoid cell, from the shaded hemisphere, becomes the holdfast which anchors the alga down in the rocks (Brownlee et al., 2001).

The monecious intertidal marine brown alga *S. compressa* undergoes oogamous fertilization in which large sessile egg cells and small motile sperm are released into the surrounding seawater (Kropf, 1994). Chemoattractants guide the sperm to the egg (Kochert, 1978). The egg cell is apparently nonpolar with no signs of asymmetry. Symmetry is initially broken by sperm entry. An F-actin patch assembles in the cortex at the site of sperm entry and marks the default polar axis (Hable and Kropf, 2000). By about 3 hours after fertilization (AF), the zygotes begin to excrete a polyphenolic- and polysaccharide-based adhesive to anchor them down to the rocks in their intertidal

environment (Hable and Kropf, 1998; Vreeland et al., 1993). At this point zygotes begin to perceive cues from their external environment and typically abandon their default axis and build a new polar axis in accordance with environmental vectors (Hable et al., 2003). During polarization, the zygotes can perceive cues such as chemical, temperature, and ion gradients as well as unidirectional light in the UV and blue spectrums (Brownlee et al., 2001; Jaffe, 1968; Weisenseel, 1979). Light cues are quite strong and the polar axis can be modified in the laboratory simply by changing the orientation of a light source (Kropf, 1992). Recently a light-oxygen-voltage (LOV)-sensing photoreceptor was identified in fucoid algae, and may be involved in photopolarization (Takahashi et al., 2007). The polar axis determines the growth site of the zygote; when light is used to photopolarize, the rhizoid pole assembles on the shaded hemisphere and is the site of localized tip growth (Kropf, 1992).

Many constituents of the polarization machinery have been described, but little is known about their functional interactions. Several processes have been shown to be localized to the rhizoid pole early on during polarity establishment; reactive oxygen species (ROS), cytosolic calcium and pH gradients, and cortical F-actin all accumulate at the developing rhizoid pole (Alessa and Kropf, 1999; Coelho et al., 2008; Kropf et al., 1995; Pu and Robinson, 2003). F-actin is necessary for perception of polarizing cues as well as facilitating endo- and exocytosis (Hable and Kropf, 1998; Hadley et al., 2006). More work will be needed to properly address the temporal order and functional interactions between these constituents.

The polar axis becomes fixed around 10 hours AF and is concurrent with physical breaking of symmetry (germination) (Belanger and Quatrano, 2000b). By 24 hours AF,

rhizoid outgrowth has given the zygote a pear-shaped appearance. At this point in development the zygote undergoes an invariant, asymmetric cell division (Belanger and Quatrano, 2000a; Bisgrove and Kropf, 2004a). The positioning of the division plane is dictated by the orientation of the mitotic spindle (Bisgrove et al., 2003). The mitotic spindle undergoes two stages of alignment before and during mitosis, with telophase nuclei ultimately positioned parallel to the long axis of the cell (Bisgrove and Kropf, 1998). Interdigitating microtubules from telophase nuclei define the division plane where a zone of F-actin promotes membrane accumulation and fusion in a centripetal direction (Bisgrove and Kropf, 2004a).

1.3 Microtubules: structure and function

Microtubules are polar structures. Three physical aspects of microtubules dictate their polarity: the orientation of their subunits, presence or absence of GTP bound to their subunits, and localization of the nucleation complex (Wade, 2009). Microtubules are hollow tubes or cylinders built primarily from dimers of α- and β-tubulin (Meurer-Grob et al., 2001). The alternating dimers of α- and β-tubulin, bound through noncovalent interactions, stack into long protofilaments. Typically a microtubule is composed of 13 protofilaments, arranged in parallel and bound laterally to form the characteristic hollow tube shape (Wade, 2009). Microtubule subunits, dimers of α- and β-tubulin, exhibit polarity with the β subunit at the growing end (plus end) and α subunit oriented toward the origin of nucleation (minus end). The plus end of microtubules is typically highly dynamic, and undergoes rapid growth and shrinkage, termed dynamic instability (Mitchison and Kirschner, 1984). A growing microtubule rapidly adds dimers of α- and β-tubulin to the plus end, with GTP bound to the β subunit (Meurer-Grob et al., 2001). In

a growing microtubule hydrolysis of GTP to GDP is slower than the addition of subunits, resulting in a cap of dimers with GTP bound at the plus end (Howard and Hyman, 2009). When GTP hydrolysis exceeds the addition of new GTP-bound dimers, the GTP cap becomes hydrolyzed, destabilizing the plus end, and the microtubule depolymerizes (Howard and Hyman, 2009). A ring of γ-tubulin, which promotes nucleation and microtubule outgrowth, marks the minus end of a microtubule (Oakley, 1989). The γ-tubulin ring complex (γ-TuRC) forms a lock washer-shaped structure that has a high affinity for the α subunit of the dimer.

The organization of microtubule arrays is not the same for all lineages. In animals, and most other lineages including brown algae, microtubules are anchored at their minus ends in the centrosome (Motomura, 1989). Centrosomes are microtubule organizing centers (MTOCs) that usually reside in perinuclear positions (Cuschieri, 2007). Centrosomes are composed of hundreds of different proteins, with a pair of centrioles at the core. Centrioles are somewhat mysterious microtubule-based structures resembling basal bodies and their exact functions are still being uncovered. During interphase, centrosomes nucleate radial microtubule arrays with the plus end toward the cortex. These arrays can carry MAPs, attached to the plus end of microtubules, thereby moving the MAPs toward subcellular destinations as microtubules elongate (Bisgrove and Kropf, 2004b). Microtubules can also be used as molecular highways by motor proteins that carry vesicles along them (Hehnly and Stamnes, 2007). Centrosomes duplicate in preparation for mitosis (Nagasato et al., 1999). Entry into mitosis leads to disassembly of the radially oriented perinuclear microtubule array, separation of centrosomes, and formation of a bipolar, interdigitating spindle (Kollu et al., 2009).

During metaphase, interactions between microtubule-plus ends and the kinetocores of chromosomes ensure proper chromosomal segregation during anaphase. Astral microtubules maintain the position of the mitotic spindle and thereby ensure proper placement of the cell division plane (Takayama et al., 2002).

Higher plant cells lack centrioles and centrosomes (Wasteneys, 2000). Without centrosomes, higher plants do not possess discreet MTOCs like most other lineages. The loss of centrioles during the course of higher plant evolution may have occurred because higher plants evolved a fertilization strategy that does not require motile gametes. Motility requires basal bodies, which are functionally equivalent to centrosomes (Shimamura et al., 2004). The evolution of pollen for fertilization may have therefore rendered motile sperm, and centrioles, expendable. Rather than perinuclear centrosomes, higher plants in interphase possess γ-TuRCs scattered throughout the cortical regions of the cell (Schmit, 2002). These complexes function in a similar fashion to their homologues in animals, but give rise to a unique interphase microtubule array consisting of parallel microtubules just beneath the plasma membrane (Schmit, 2002). Interactions between microtubules align them into parallel arrays (Cyr and Palevitz, 1995; Lucas and Shaw, 2008).Whereas microtubules in nonplants typically grow and shrink only from the plus end; microtubules in plants can grow from the plus end while shrinking from the minus end through a process termed treadmilling (Shaw et al., 2003). Because of this dynamic behavior, plant microtubules appear to crawl along the cell cortex.

Plant cells possess additional microtubule arrays not found in animals. Just before mitotic entry, the cortical network of microtubules condenses into a preprophase band resembling a belt around the cell, which defines the future division plane (Ambrose and

Cyr, 2008). During mitosis, plant cells form a broad, barrel-shaped spindle lacking well-defined poles (Smirnova, 2003). After the chromosomes are segregated, short, interdigitating microtubules from the daughter telophase nuclei form a phragmoplast which functions in the centripetal formation of a cell membrane and plate (Jürgens, 2005).

Since pharmacological disruption of microtubules does not block polar axis selection or rhizoid outgrowth, microtubule array morphology has not been extensively studied in stramenopiles. In the few reports of microtubule array organization in brown algae, perinuclear, centrosomally-nucleated, radial arrays as well as cortically nucleated arrays have been reported (Bisgrove and Kropf, 2001; Corellou et al., 2005). To answer these questions I have examined the morphology and functional roles of microtubules during polarity establishment and asymmetric cell division. In addition, particular attention was paid to what roles, if any, microtubules may play in organization of the endomembrane system. The results of that research are presented in Chapter 2.

1.4 Phospholipid signaling

The underlying signaling mechanisms that regulate microtubules in brown algae have not been investigated. Recent studies in vascular plants and animals suggested that microtubule arrays are regulated, in part, by the membrane bound phospholipase D (PLD) and phospholipase C (PLC) signaling pathways (Meijer and Munnik, 2003). Environmental stimuli activate both the PLD and PLC pathways through activation of heterotrimeric G-proteins (Malhó et al., 2006; Oude Weernink et al., 2007b). Both the PLD and PLC pathways ultimately produce phosphatidic acid (PA), a signaling molecule (Oude Weernink et al., 2007b). Phospholipase D cleaves head groups of structural

phospholipids such as phosphatidyl choline and phosphatidylethanolamine for generation of PA (Oude Weernink et al., 2007a). The PLC pathway cleaves phosphatidylinositol 4,5-bisphosphate (PIP_2) to inositol 1,4,5-triphosphate (IP_3) and diacylglycerol (DAG) (Wang, 2004). IP_3 and DAG are also signaling molecules. DAG is subsequently phopshorylated by diacylglycerol kinase (DAGK), yielding PA. PA is a class of signaling molecules composed of two fatty acid chains bound to glycerol with a phosphate head group (Munnik, 2001a). The length and degree of saturation of the fatty acid chains in PA is thought to impart signaling specificities (Hodgkin et al., 1998; Wang et al., 2006). Thus, PA produced by the PLD and PLC pathways may have unique cellular effects due to variations in fatty acid side chains (Hodgkin et al., 1998; Testerink and Munnik, 2005). Interestingly, in both vascular plants and animals, the PLD and PLC pathways can regulate microtubule, F-actin, and endomembrane organization, ultimately affecting a multitude of downstream developmental processes (Jenkins and Frohman, 2005; Meijer and Munnik, 2003; Munnik, 2001b; Oude Weernink et al., 2007a).

I investigated PLD and PLC signaling to microtubules using pharmalogical tools. Primary alcohols, like 1-butanol, are preferred transphosphatidylation substrates of PLD, leading to formation of P-butanol, which is not a signaling molecule, at the expense of PA production. I examined the microtubule and developmental effects of PLD signaling disruption in *S. compressa* by treatment with 1-butanol. The results of these experiments showed that PLD regulates microtubules and are described in Chapter 3. The PLC signaling pathway is insensitive to primary alcohols, but a chemical inhibitor, R59022, is commercially available to block the phosphorylation capacity of DAGK, thus eliminating PA production through DAGK. I applied R59022 to young zygotes; the results of these

experiments suggested an extensive role for the PLC pathway in brown algae, and are described in Chapter 4.

1.5 Microtubule-associated proteins

To complement my initial examination of the structure, function, and regulation of microtubules, I initiated analysis of the role of MAPs in *S. compressa*. Since spindle position determines the site of the cell division plane, I investigated how a bipolar spindle is formed and maintained during chromosomal capture. One class of MAPs, known to function during mitosis in other systems, is the kinesin family of motor proteins. The evolutionarily conserved kinesins are found in metazoans, plants, fungi, and protozoans (Miki et al., 2005). Kinesin motor domains use the energy from ATP hydrolysis to "walk" along microtubules, usually towards the plus end. Kinesin tail domains are more varied and can form higher order associations with other kinesins or mediate interactions with cargo to be transported along microtubules (Miki et al., 2005). Human and fly kinesins have been systematically examined to ascertain their myriad functions, but plant kinesins have been much more difficult to study (Goshima and Vale, 2003). Higher plants are thought to lack an additional class of motor proteins termed dyneins, and instead have a vast and functionally redundant assortment of kinesins (Zhu et al., 2005).

The kinesin Eg5 (Kinesin-5) regulates spindle assembly and bipolarity in animals and higher plants (Bannigan et al., 2007; Maliga et al., 2002). Eg5 is a homotetramer with two motor domains on each end of the complex (Cole et al., 1994). Eg5 is localized to the nucleus during interphase in animals and becomes associated with the spindle poles during mitosis (Sharp et al., 2000). In higher plants, Eg5 is localized along the length of microtubules during interphase and to the spindle poles during metaphase (Bannigan et

al., 2007). In both animals and higher plants, Eg5 functions to help maintain spindle bipolarity; without it the spindle poles collapse together to form a monaster (Bannigan et al., 2007; Mayer et al., 1999). Monastrol, a small molecule inhibitor, blocks Eg5 function by binding in the ATPase domain, thereby blocking processivity (Maliga et al., 2002). Monastrol, though, is not thought to inhibit the microtubule binding capacity of Eg5. In animal systems, monstrol treatment leads exclusively to the formation of monasters, due to an inability to maintain spindle bipolarity (Mayer et al., 1999).

I used antibody labeling and monastrol treatment to examine the localization and function of Eg5 during early development. Interestingly I found similarities but also striking differences for Eg5 localization and function in brown algae, compared to animals and higher plants. The results of these studies are described in Chapters 5 and 6.

1.6 References

Alessa, L., and Kropf, D.L. (1999). F-actin marks the rhizoid pole in living *Pelvetia compressa* zygotes. Development *126*, 201-209.

Ambrose, J.C., and Cyr, R. (2008). Mitotic spindle organization by the preprophase band. Mol. Plant *1*, 950-960.

Bannigan, A., Scheible, W.-R., Lukowitz, W., Fagerstrom, C., Wadsworth, P., Somerville, C., and Baskin, T.I. (2007). A conserved role for kinesin-5 in plant mitosis. J. Cell Sci. *120*, 2819-2827.

Belanger, K.D., and Quatrano, R.S. (2000a). Membrane recycling occurs during asymmetric cell growth and cell plate formation in *Fucus distichus* zygotes. Protoplasma *212*, 24-37.

Belanger, K.D., and Quatrano, R.S. (2000b). Polarity: The role of localized secretion. Curr. Op. Plant Biol. *3*, 67-72.

Bisgrove, S.R., Henderson, D.C., and Kropf, D.L. (2003). Asymmetric division in fucoid zygotes is positioned by telophase nuclei. Plant Cell *15*, 854-862.

Bisgrove, S.R., and Kropf, D.L. (1998). Alignment of centrosomal and growth axes is a late event during polarization of *Pelvetia compressa* zygotes. Dev. Biol. *194*, 246-256.

Bisgrove, S.R., and Kropf, D.L. (2001). Asymmetric cell division in fucoid algae: a role for cortical adhesions in alignment of the mitotic apparatus. J. Cell Sci. *114*, 4319-4328.

Bisgrove, S.R., and Kropf, D.L. (2004a). Cytokinesis in brown algae: studies of asymmetric division in fucoid zygotes. Protoplasma *223*, 163-173.

Bisgrove, S.R., and Kropf, D.L. (2004b). +TIPs and microtubule regulation: The beginning of the plus end in plants. Plant Physiol. *136*, 3855-3863.

Bouck, G.B. (1969). Extracellular microtubules : The origin, structure, and attachment of flagellar hairs in Fucus and Ascophyllum antherozoids. JCB *40*.

Brownlee, C., Bouget, F.-Y., and Corellou, F. (2001). Choosing sides: establishment of polarity in zygotes of fucoid algae. Cell Dev. Biol. *12*, 345-351.

Coelho, S., Brownlee, C., and Bothwell, J. (2008). A tip-high, Ca2+-interdependent, reactive oxygen species gradient is associated with polarized growth in Fucus serratus zygotes. Planta *227*, 1037-1046.

Cole, D., Saxton, W., Sheehan, K., and Scholey, J. (1994). A "slow" homotetrameric kinesin-related motor protein purified from Drosophila embryos. J. Biol. Chem. *269*, 22913-22916.

Corellou, F., Coelho, S.M.B., Bouget, F.-Y., and Brownlee, C. (2005). Spatial re-organisation of cortical microtubules in vivo during polarisation and asymmetric division of *Fucus* zygotes. J. Cell Sci. *118*, 2723-2734.

Cuschieri, L., Nguyen, T., Vogel, J. (2007). Control at the cell center: the role of spindle poles in cytoskeletal organization and cell cycle regulation. Cell Cycle *6*, 2788-2794.

Cyr, R.J., and Palevitz, B.A. (1995). Organization of cortical microtubules in plant cells. Curr. Opin. Cell Biol *7*, 65-71.

Goshima, G., and Vale, R.D. (2003). The roles of microtubule-based motor proteins in mitosis: comprehensive RNAi analysis in the *Drosophila* S2 cell line. JCB *162*, 1003-1016.

Hable, W.E., Bisgrove, S.R., and Kropf, D.L. (1998). To shape a plant-The cytoskeleton in plant morphogenesis. Plant Cell *10*, 1772-1774.

Hable, W.E., and Kropf, D.L. (1998). Roles of secretion and the cytoskeleton in cell adhesion and polarity establishment in *Pelvetia compressa* zygotes. Dev. Biol. *198*, 45-56.

Hable, W.E., and Kropf, D.L. (2000). Sperm entry induces polarity in fucoid zygotes. Development *127*, 493-501.

Hable, W.E., Miller, N.R., and Kropf, D.L. (2003). Polarity establishment requires dynamic actin in fucoid zygotes. Protoplasma *221*, 193-204.

Hadley, R., Hable, W.E., and Kropf, D.L. (2006). Polarization of the endomembrane system is an early event in fucoid zygote development. BMC Plant Biol. *6*, 1-10.

Hehnly, H., and Stamnes, M. (2007). Regulating cytoskeleton-based vesicle motility. FEBS Letters *581*, 2112-2118.

Hodgkin, M.N., Pettitt, T.R., Martin, A., Michell, R.H., Pemberton, A.J., and Wakelam, M.J.O. (1998). Diacylglycerols and phosphatidates: which molecular species are intracellular messengers? Trends in Biochemical Sciences *23*, 200-204.

Howard, J., and Hyman, A.A. (2009). Growth, fluctuation and switching at microtubule plus ends. Nat. Rev. Mol. Cell Biol. *10*, 569-574.

Jaffe, L.F. (1968). Localization in the developing *Fucus* egg and the general role of localizing currents. Adv. Morphol. *7*, 295-328.

Jenkins, G., and Frohman, M. (2005). Phospholipase D: a lipid centric review. CMLS *62*, 2305-2316.

Jürgens, G. (2005). Plant cytokinesis: fission by fusion. Trends Cell Biol. *15*, 277-283.

Kochert, G. (1978). Sexual pheromones in algae and fungi. Ann. Rev. Plant Physiol. *29*, 461-486.

Kollu, S., Bakhoum, S.F., and Compton, D.A. (2009). Interplay of microtubule Dynamics and sliding during bipolar spindle formation in mammalian cells. Curr. Biol. *11*, 21-32.

Kropf, D.L. (1992). Establishment and expression of cellular polarity in fucoid zygotes. Microbiol. Rev. *56*, 316-339.

Kropf, D.L. (1994). Cytoskeletal control of cell polarity in a plant zygote. Dev. Biol. *165*, 361-371.

Kropf, D.L., Bisgrove, S.R., and Hable, W.E. (1999). Establishing a growth axis in fucoid algae. Trends Plant Sci. *4*, 490-494.

Kropf, D.L., Henry, C.A., and Gibbon, B.C. (1995). Measurement and manipulation of cytosolic pH in polarizing zygotes. Eur. J. Cell Biol. *68*, 297-305.

Le Corguille, G., Pearson, G., Valente, M., Viegas, C., Gschloessl, B., Corre, E., Bailly, X., Peters, A., Jubin, C., Vacherie, B., *et al.* (2009). Plastid genomes of two brown algae, *Ectocarpus siliculosus* and *Fucus vesiculosus*: further insights on the evolution of red-algal derived plastids. BMC Evol. Biol. *9*, 253.

Lucas, J., and Shaw, S.L. (2008). Cortical microtubule arrays in the *Arabidopsis* seedling. Curr. Opin. Plant Biol. *11*, 94-98.

Malhó, R., Liu, Q., Monteiro, D., Rato, C., Camacho, L., and Dinis, A. (2006). Signalling pathways in pollen germination and tube growth. Protoplasma *228*, 21-30.

Maliga, Z., Kapoor, T.M., and Mitchison, T.J. (2002). Evidence that Monastrol Is an Allosteric Inhibitor of the Mitotic Kinesin Eg5. Chem. & Biol. *9*, 989-996.

Mayer, T.U., Kapoor, T.M., Haggarty, S.J., King, R.W., Schreiber, S.L., and Mitchison, T.J. (1999). Small molecule inhibitor of mitotic spindle bipolarity identified in a phenotype-based screen. Science *286*, 971-974.

Medlin, L.K., Kooistra, W. H. C. F., Potter, D., Saanders, G., Wandersen, R. A. (1997). Phylogenetic relationships of the 'golden algae' (haptophytes, heterokont chromophytes) and their plastids. Plant System. and Evol. *11*, 187-219.

Meijer, H., and Munnik, T. (2003). Phospholipid-based signaling in plants. Annu. Rev. Plant Biol. *54*, 265-306.

Meurer-Grob, P., Kasparian, J., and Wade, R.H. (2001). Microtubule Structure at Improved Resolution†. Biochem. *40*, 8000-8008.

Miki, H., Okada, Y., and Hirokawa, N. (2005). Analysis of the kinesin superfamily: insights into structure and function. Trends Cell Biol. *15*, 467-476.

Mitchison, T., and Kirschner, M. (1984). Dynamic instability of microtubule growth. Nature *312*, 237-242.

Motomura, T. (1989). Ultrastructural study of sperm in Laminaria angustata (Laminariales, Phaeophyta), especially on the flagellar apparatus. Jpn. J. Phycol. *37*, 105-116.

Munnik, T. (2001a). Phosphatidic acid: An emerging plant lipid second messenger. Trends Plant. Sci. *6*, 227-233.

Munnik, T., Musgrave, A. (2001b). Phospholipid signaling in plants: holding on to phospholipase D. Sci. Signal. *4*, 42.

Nagasato, C., Motomura, T., and Ichimura, T. (1999). Influence of centriole behavior on the first spindle formation in zygotes of the brown alga *Fucus distichus* (Fucales, Phaeophyta). Dev. Biol. *208*, 200-209.

Oakley, C.E.O., B. R. (1989). Identification of γ-tubulin, a new member of the tubulin superfamily encoded by mipA gene of *Aspergillus nidulans*. Nature *338*, 662-664.

Oude Weernink, P., López de Jesús, M., and Schmidt, M. (2007a). Phospholipase D signaling: orchestration by PIP2 and small GTPases. Naunyn-Schmiedeberg's Arch. Pharmacol. *374*, 399-411.

Oude Weernink, P.A., Han, L., Jakobs, K.H., and Schmidt, M. (2007b). Dynamic phospholipid signaling by G protein-coupled receptors. BBA Biomem. *1768*, 888-900.

Pu, R., and Robinson, K.R. (2003). The involvement of Ca^{2+} gradients, Ca^{2+} fluxes, and CaM kinase II in polarization and germination of *Silvetia compressa* zygotes. Planta *217*, 406-416.

Schmit, A.C. (2002). Acentrosomal microtubule nucleation in higher plants. Int. Rev. Cytol. *220*, 257-289.

Sharp, D.J., Brown, H.M., Kwon, M., Rogers, G.C., Holland, G., and Scholey, J.M. (2000). Functional coordination of three mitotic motors in *Drosophila* embryos. Mol. Biol. Cell *11*, 241-253.

Shaw, S.L., Kamyar, R., and Ehrhardt, D.W. (2003). Sustained microtubule treadmilling in *Arabidopsis* cortical arrays. Science *300*, 1715-1718.

Shimamura, M., Brown, R.C., Lemmon, B.E., Akashi, T., Mizuno, K., Nishihara, N., Tomizawa, K.-I., Yoshimoto, K., Deguchi, H., Hosoya, H., *et al.* (2004). Gamma-tubulin in basal land plants: characterization, localization, and implication in the evolution of acentriolar microtubule organizing centers. Plant Cell *16*, 45-59.

Smirnova, E.A. (2003). Spindle pole formation in higher plant cells. Cell Biol. Int. *27*, 273-274.

Takahashi, F., Yamagata, D., Ishikawa, M., Fukamatsu, Y., Ogura, Y., Kasahara, M., Kiyosue, T., Kikuyama, M., Wada, M., and Kataoka, H. (2007). AUREOCHROME, a photoreceptor required for photomorphogenesis in stramenopiles. Proc. Natl. Acad. Sci. *104*, 19625-19630.

Takayama, M., Noguchi, T., Yamashiro, S., and Mabuchi, I. (2002). Microtuble organization in *xenopus* eggs during the first cleavage and its role in cytokinesis. Cell Str. Funct. *27*, 163-171.

Testerink, C., and Munnik, T. (2005). Phosphatidic acid: a multifunctional stress signaling lipid in plants. Trends Plant Sci. *10*, 368-375.

Vreeland, V., Grotkopp, E., Espinosa, S., Quiroz, D., Laetsch, W.M., and West, J. (1993). The pattern of cell wall adhesive formation by *Fucus* zygotes. Hydrobiologia *260/261*, 485-491.

Wade, R. (2009). On and around microtubules: An overview. Molec. Biotech. *43*, 177-191.

Wang, X. (2004). Lipid signaling. Cur. Opin. Plant Biol. *7*, 329-336.

Wang, X., Devaiah, S.P., Zhang, W., and Welti, R. (2006). Signaling functions of phosphatidic acid. Prog. Lipid Res. *45*, 250-278.

Wasteneys, G.O. (2000). The cytoskeleton and growth polarity. Curr. Opin. Plant Biol. *3*, 503-511.

Weisenseel, M.H. (1979). Induction of polarity. In Encyclopedia of Plant Physiology, W. Haupt, and M.E. Feinleib, eds. (Berlin, Springer-Verlag), pp. 485-505.

Zhu, C., Zhao, J., Bibikova, M., Leverson, J.D., Bossy-Wetzel, E., Fan, J.-B., Abraham, R.T., and Jiang, W. (2005). Functional analysis of human microtubule-based motor proteins, the kinesins and dyneins, in mitosis/cytokinesis using RNA interference. Mol. Biol. Cell *16*, 3187-3199.

CHAPTER 2

ASYMMETRIC MICROTUBULE ARRAYS ORGANIZE THE ENDOPLASMIC RETICULUM DURING POLARITY ESTABLISHMENT IN THE BROWN ALGA *SILVETIA COMPRESSA*

RESEARCH ARTICLE
Cytoskeleton, Month 2010 000:000–000 (doi: 10.1002/cm.20427)

Asymmetric Microtubule Arrays Organize the Endoplasmic Reticulum During Polarity Establishment in the Brown Alga *Silvetia compressa*

Nick T. Peters* and Darryl L. Kropf
Department of Biology, University of Utah, Salt Lake City, Utah

Received 15 October 2009; Revised 14 December 2009; Accepted 16 December 2009
Monitoring Editor: Makoto Kinoshita

Polarity is a fundamental characteristic of most cell types, and is crucial to early development of the brown alga *Silvetia compressa*. In eukaryotes the cytoskeleton plays an important role in generating cellular asymmetries. While it is known that F-actin is required for polarization and growth in most tip-growing cells, the roles of microtubules are less clear. We examined the distribution and function of microtubules in *S. compressa* zygotes as they polarized and initiated tip growth. Microtubules formed asymmetric arrays oriented toward the rhizoid hemisphere early in the polarization process. These arrays were spatially coupled with polar adhesive deposition, a marker of the rhizoid pole. Reorientation of the light vector during polarization led to sequential redistribution of polar axis components, with the microtubules and the polar axis reorienting nearly simultaneously, followed by cell wall loosening and then deposition of new polar adhesive. These findings suggested that microtubules may organize and target endomembrane arrays. We therefore examined the distribution of the endoplasmic reticulum during polarization and found it colocalized with microtubules and became targeted toward the rhizoid pole as microtubule asymmetry was generated. Endoplasmic reticulum association with microtubules remained fully intact following pharmacological disruption of F-actin, whereas microtubule disruption led to aggregation of the endoplasmic reticulum around the nucleus. We propose that brown algae utilize microtubules for organization of the endoplasmic reticulum and migration of exocytotic components to the rhizoid cortex, and present a model for polarity establishment to account for these new findings.

Additional Supporting Information may be found in the online version of this article.

*Address correspondence to: Nick T. Peters, Department of Biology, University of Utah, Salt Lake City, Utah 84112. E-mail: nicktpeters@gmail.com or Darryl L. Kropf, Department of Biology, University of Utah, Salt Lake City, Utah 84112. E-mail: Kropf@bioscience.utah.edu

Published online 00 Month 2010 in Wiley InterScience (www.interscience.wiley.com).

Key Words: microtubules, endoplasmic reticulum, polarity establishment, brown algae, development

Introduction

The asymmetries that define cell polarity are manifested as unequal distribution of cellular components or molecules, many times accompanied by differences in cell morphology. Perhaps the clearest examples of highly polar cells are tip-growing cells where growth is restricted to a narrow zone in the cellular cortex, as in neurons, pollen tubes, fungal hyphae, and algal rhizoids. While many of the molecules and mechanisms required for maintenance of cell polarity are well known, much less is known about how cells establish polarity during development. This is due to the fact that the zygotes of most model organisms already possess a fixed polar axis inherited from the egg cell. To overcome this obstacle, researchers have sought model systems in which the polar axis can be established and modified in the laboratory.

The brown alga, *Silvetia compressa*, is uniquely suited for studies of polarity establishment and maintenance [Quatrano, 1997; Brownlee et al., 2001; Bisgrove and Kropf, 2008]. The site of sperm entry establishes the default axis of the zygote [Hable and Kropf, 2000]. Around 3 h after fertilization (AF) zygotes begin to secrete a polyphenolic-based adhesive, which becomes targeted toward the rhizoid hemisphere by 4 h AF [Vreeland et al., 1998]. The adhesive is used to anchor zygotes down to the rocky substratum in their aquatic environment. Once attached, the zygotes monitor their external environment and reorient the axes according to perceived cues, most commonly light direction [Jaffe, 1968]. The axis remains labile until 10 h AF when it becomes fixed and zygotes begin growing a rhizoid via tip growth [Belanger and Quatrano, 2000b]. By 24 h AF, the zygotes undergo an asymmetric cell division, yielding two daughter cells of different developmental fates [Bisgrove and Kropf, 2004]. The rhizoid cell lineage becomes the holdfast and anchors the alga to the rocky substratum, and the thallus cell lineage becomes the vegetative stipe and reproductive fronds. Because of these attributes, fucoid algae have

been utilized as a model organism for studying early development for well over 100 years [Bower, 1880].

Extensive studies of polarizing vectors, signaling molecules, and the cytoskeleton during polarity establishment have provided many insights into the mechanisms of the polarization process in fucoid algae [Katsaros et al., 2006; Bisgrove and Kropf, 2008]. Still, fundamental questions about polarization and the role of the cytoskeleton remain. Polarization studies have not focused on microtubule function because microtubule inhibitors do not block polarization or rhizoid outgrowth [Quatrano, 1973], and because microtubule arrays have been reported to be uniformly distributed throughout polarity establishment [Kropf et al., 1990]. Interestingly though, it has been recently noted that disruption of microtubules leads to a loss of endomembrane asymmetry in polarizing zygotes, a reduction of polar adhesive deposition, and bulged rhizoid outgrowth [Hadley et al., 2006; Peters and Kropf, 2006].

These observations have prompted us to examine what roles, if any, microtubules play in polarity establishment. In this study, we investigated the morphology and organization of microtubule arrays throughout the polarization process. The functional roles of microtubules in organizing the endomembrane system were also examined. The results of these investigations have identified important functions for microtubules during early development in brown algae.

Materials and Methods

Algal Culture and Pharmacological Agents

Receptacles of the fucoid alga *S. compressa* were collected near Santa Cruz, California and cultured as described before [Peters and Kropf, 2006]. Zygotes were grown in artificial seawater (ASW) under unilateral light, unless otherwise noted. Pharmacological agents were dissolved in dimethylsulfoxide (DMSO) to make stock solutions, and applied to zygotes in ASW as follows: Latrunculin B (Calbiochem, La Jolla, CA), 50 μM stock, 30 nM final; oryzalin (Sigma-Aldrich), 10 mM stock, 3 μM final; Brefeldin A (Sigma-Aldrich), 2.5 mg/ml stock, 5 μg/ml final. Appropriate controls were carried out using DMSO.

Experimental Design

For all experiments, sexually mature fronds of *S. compressa* were potentiated in ASW under unilateral light for 1–5 h, depending on their degree of ripeness. Potentiation prepares the fronds for subsequent release of eggs and sperm. Potentiated fronds were then placed in the dark for 30 min, to induce synchronous release of eggs and sperm. Fertilization takes place almost immediately after release. Time zero is considered the midpoint of the dark period. The age of zygotes, given in hours AF, is hours after this zero time. Zygotes were harvested immediately after the dark period, and were plated and placed under unilateral light. Harvesting and plating were completed by 0.5 h AF. A population of zygotes develops synchronously through the first cell cycle.

The polar axis of zygotes is labile from the time of sperm entry until germination around 10 h AF. For light reversal experiments, (Figs. 3 and 7, Assays 2 and 3) the original light source (Light 1) was reoriented 180° (Light 2).

Quantification of Polarity

For population studies, microtubules, adhesive or localized cell wall loosening was classified as polarized when preferential localization was observed at one hemisphere. For experiments in which the light vector was reoriented, the percent polarization was ascertained by scoring the number of zygotes polarized to Light 2, minus the number polarized to Light 1, divided by the total number of zygotes scored, and then multiplied by 100 [(# Light 2–# Light 1/total) × 100]. Therefore, a polarization of 100% indicates that all zygotes polarized to Light 2, 0% indicates that the population polarized randomly, and 100% indicates that every zygote polarized to Light 1. All experiments were conducted in triplicate and representative images are shown in all figures. For quantification of microtubule and endoplasmic reticulum distribution in individual zygotes, the Zeiss LSM510's image software package was used to ascertain pixel intensity. The rhizoid pole was defined by the region with the thickest deposition of polar adhesive. This position was never more that 30° from parallel to the orienting light. For each time point, five representative zygotes were divided into octants and the raw pixel intensity of microtubules and/or HDEL was assessed for each section. For microtubule analysis, the nuclear region was excluded due to the intense labeling of this microtubule organizing center. The resulting data was normalized by defining the octant with the highest pixel intensity as 1.0.

High-Pressure Freezing

Zygotes were grown in 150 mm petri dishes for varying times AF. They were then gently scraped into 300 μm aluminum planchettes with a glass coverslip; excess artificial seawater was dabbed away with a paper towel. Samples were cryoimmobilized using a Bal-Tec HPM 010 high-pressure freezer and subsequently fixed and substituted in and a Leica AFS freeze substitution unit with acetone plus 3% glutaraldehyde. Substitution was done at −80°C for 5 days, followed by warming to −20°C over 12 h; after an additional 24 h at −20°C, samples were warmed to 4°C over 12 h. Samples were transferred in 10% steps into methanol, and then into modified phosphate-buffered saline containing 1% DMSO, again in 10% steps. Zygotes were then processed for immunoflourescence as described previously [Peters and Kropf, 2006].

For conventional fixation, zygotes were fixed in PHEM [60 mM piperazine-N, N0-bis(2-ethanesulfonic acid), 25 mM HEPES, 10 mM EGTA, 2 mM $MgCl_2$, pH adjusted to 7.5 with KOH] containing 3% paraformaldehyde and 0.5% glutaraldehyde. Zygotes were processed as previously described [Peters and Kropf, 2006].

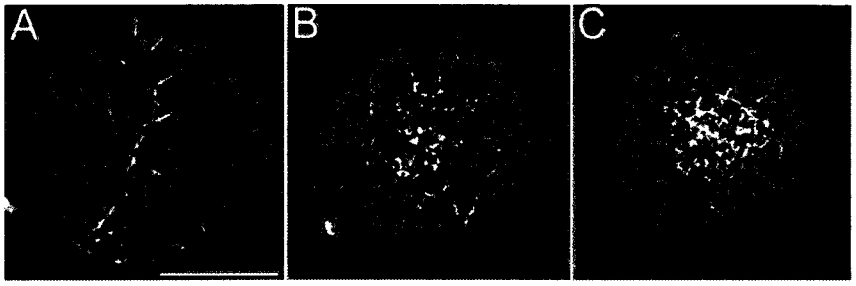

Fig. 1. Microtubule arrays in 8-h old zygotes. A: An individual bundle of microtubules in a single confocal section (~ 0.5 μm thickness). Arrows track the microtubule bundle from the perinuclear region out to and along the plasma membrane. **B**: Tangential section of the first 7 μm of the thallus cortex. Microtubule distribution was relatively even throughout the thallus hemisphere. **C**: The first 7 μm of the rhizoid cortex. The microtubules in the rhizoid cortex appeared greater in number and were more focused toward the pole. Long linear microtubules in B and C represent arrays that extended along the plasma membrane of the cortex, while punctate dots represent microtubule bundles that terminated at or near the plasma membrane (directly into the plane of view). Images depict representative zygotes. Scale bar equals 50 μm.

Imaging

Bright field images were captured with a coolSNAP digital camera (Roper Scientific Photometrics, Tucson, AZ) on an Olympus IMT2 microscope. For immunofluorescence, single labeling of microtubules was performed using a monoclonal anti-alpha-tubulin antibody (DM1A: Sigma-Aldrich, St. Louis, MO) and Alexa 488 goat anti-mouse secondary antibody (Invitrogen, Eugene, OR), or a polyclonal anti-tubulin antibody (ab18251: Abcam, Cambridge, MA) followed by Alexa 546 goat anti-rabbit secondary antibody. For double-labeled zygotes, the polyclonal tubulin antibody followed by Alexa 546 goat anti-rabbit secondary antibody was used for microtubules, and endoplasmic reticulum labeling was carried out using a monoclonal HDEL (2E7) antibody (sc-53472: Santa Cruz Biotechnology, Santa Cruz, CA) and Alexa 488 goat anti-mouse secondary antibody. Primary antibodies were added simultaneously, as were secondary antibodies. Images were collected on a LSM510 (Carl Zeiss, Thornwood, NY) confocal laser-scanning microscope using a narrow bandpass filter for the green channel (500–530 nm) and a Meta adjustable bandpass filter for the red channel (558–601 nm). Images represent individual confocal sections of approximately 0.5 μm in thickness, unless otherwise noted.

Results

Microtubules Radiate from the Perinuclear Region and Extend to and Along the Plasma Membrane

Previous research has identified both centrosomal [Bisgrove et al., 1997] and cortical [Corellou et al., 2005] microtubule arrays in zygotes. To assess the relationship between these arrays, both conventional fixation and high-pressure freezing/freeze substitution protocols were employed (see Materials and Methods). Individual microtubule bundles could be followed from the perinuclear region out to and along the plasma membrane following conventional fixation (Fig. 1A, Supporting Information Movie 1). To examine microtubule distribution in the first few microns of the rhizoid or thallus cortex, unidirectional light was applied from above or below zygotes so that the rhizoid or thallus poles, respectively, formed at the interface with the coverslip. This allowed confocal imaging of the first few grazing (tangential) sections of either hemisphere (Figs. 1B and 1C). As expected, cortical microtubule arrays were present in both hemispheres, but microtubules in the rhizoid cortex appeared more concentrated than those in the thallus cortex.

To confirm that individual bundles of microtubules extended from the centrosome out to and along the cortex, the organization of microtubule arrays was examined utilizing high-pressure freezing/freeze substitution of 18 h-old zygotes. This procedure provides the best preservation of cellular structure currently available. High-pressure freezing allows cryoimmobilization within milliseconds, reducing or eliminating the formation of ice crystals that damage cytoarchitecture. The continuity of individual microtubule bundles, from nucleation to their point of termination on the plasma membrane was confirmed (Supporting Information Movie 2). In addition, a dense network of microtubules was observed to extend into the very tip (first 2 μm) of the rhizoid cortex of germinated zygotes (Supporting Information Fig. 1). Microtubule arrays that appeared cortically nucleated were not observed at any time point.

Microtubule Arrays Become Asymmetric During Polarization

To investigate the organization of microtubule arrays throughout the polarization process (2–10 h AF), microtubule distributions were examined using conventional fixation (Fig. 2A). No detectable microtubule asymmetry was observed for the first few hours of development. By 4 h AF the rhizoid hemisphere began to exhibit preferential microtubule accumulation. These asymmetric microtubule arrays

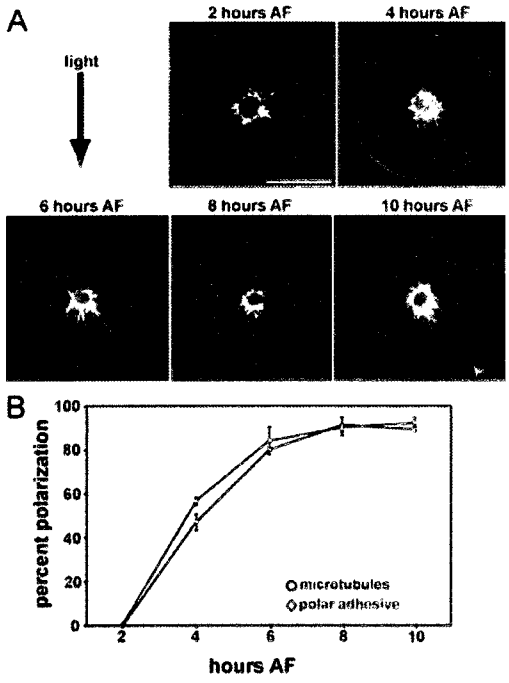

Fig. 2. Microtubule arrays and adhesive deposition during polarization. Zygotes were grown in unilateral light (arrow) to induce rhizoid formation on the shaded hemisphere. **A:** Microtubule arrays appeared uniform at 2 h AF. Microtubules began to exhibit asymmetric distribution toward the rhizoid (shaded) hemisphere by 4 h AF, and the asymmetry intensified throughout polarization. The arrowhead indicates the site of maximum polar adhesive deposition; note that maximum adhesive and the focus of the microtubule array are slightly offset with respect to the light vector. Scale bar equals 50 μm. **B:** Percent of population with asymmetric microtubules (circles) or polar adhesive (diamonds). Zygotes were scored as polarized in accordance with (away from) the light vector or uniform in appearance; polarization toward the light was observed in less than 1% of zygotes, and thus omitted from the analysis. At least 300 zygotes were scored for each time point.

increased in frequency within a population and became more focused toward the rhizoid pole as development progressed. Visual assessment of microtubule asymmetry was scored in populations by hemisphere and showed that by 10 h AF approximately 90% of zygotes displayed microtubule arrays polarized toward the rhizoid pole (Fig. 2B). Deposition of polar adhesive was strongly spatially correlated with microtubule arrays in over 99% of zygotes ($N > 1000$), with maximum adhesive at the site of maximum microtubule accumulation. Importantly, when the focus of a microtubule array was slightly offset from the light vector, polar adhesive deposition was also offset accordingly (see last panel in Fig. 2A). Therefore, the microtubule array is oriented by the developmental axis, and not directly by the light vector. Temporally, polar adhesive deposition lagged slightly behind formation of asymmetric microtubule arrays (Fig. 2B).

Reorienting the Light Vector Sequentially Redistributes Components of the Polar Axis

To test whether the strong spatiotemporal correlation between microtubule asymmetry and polar adhesive deposition target the exocytotic machinery to the rhizoid pole, axis reversal experiments were performed. Zygotes were polarized for 6 h in unilateral light (Light 1), then the light vector was reoriented 180°(Light 2) and polar axis components were assayed hourly thereafter (Fig. 3A). The polar axis and microtubule array reoriented nearly simultaneously, with about 80% reoriented by 4 h after turnaround (Fig. 3B). Cell wall loosening, a proxy for localized exocytosis of cell wall degrading enzymes, lagged behind the polar axis and microtubule turnaround by about 30 min. Deposition of asymmetric adhesive trailed the polar axis and microtubule turnaround by about 1 h. As microtubule arrays reoriented from Light 1 to Light 2, the intermediate microtubule arrays did not exhibit any clear asymmetries (Fig. 3B, inset), suggesting disassembly of the initial asymmetric array and reassembly of a new polar array, rather than rotation of the initial array. These results are consistent with microtubule arrays rapidly reorienting in accordance with the new axis and guiding local exocytosis.

The Endoplasmic Reticulum is Highly Spatially and Temporally Correlated with Microtubule Asymmetry

Microtubules may guide local exocytosis by organizing the endomembrane system. To investigate the possible spatial relationship between microtubules and endoplasmic reticulum, zygotes were double labeled for microtubules and endoplasmic reticulum. A monoclonal antibody to the endoplasmic reticulum retention signal (HDEL), which has been used for successful localization studies in other species of brown algae [Varvarigos et al., 2007], was used to visualize endoplasmic reticulum. Both HDEL and microtubule signal intensity appeared uniform at 2 h AF, but as polarization proceeded microtubule and HDEL asymmetry increased (Fig. 4). Asymmetry was quantitated by analyzing microtubule and HDEL pixel intensity on five individual zygotes at each time point. Each zygote was divided into octants and pixel intensities were measured for each octant (see Materials and Methods). This analysis confirmed that both microtubule and endoplasmic reticulum distributions were initially uniform, but by 4 h AF microtubules were significantly enriched at the rhizoid pole (Fig. 5). However, at this time endoplasmic reticulum was primarily perinuclear and was not significantly asymmetric. From 6 h AF onward, both microtubule and endoplasmic reticulum arrays were preferentially localized in the rhizoid region (octants I and VIII in Fig. 5), and their asymmetries were highly significant. The finding that microtubule asymmetry slightly preceded asymmetry in the endoplasmic reticulum is consistent with microtubules organizing this endomembrane system.

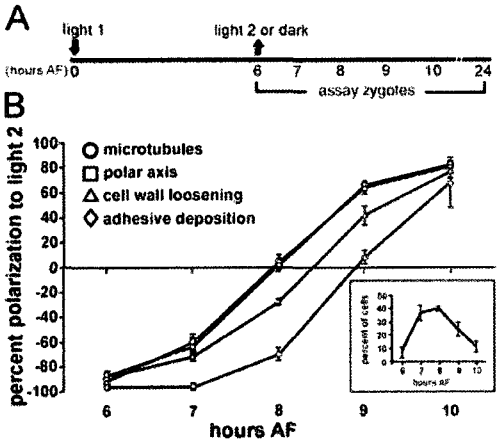

Fig. 3. Temporal correlations of polar axis component realignment to a new polarity vector. *A: Experimental design.* All zygotes were grown in Light 1 for 6 h; at 6 h, some samples were assayed for asymmetries in microtubules, cell wall loosening and adhesive deposition. Microtubules and adhesive deposition were assayed as in Fig. 2. Cell wall loosening was measured by placing zygotes in hypotonic ASW and scoring the position of cell lysis. To measure polar axis orientation, other samples were placed in the dark and the orientation of rhizoid outgrowth was assayed at 24 h AF. Yet a third set of dishes containing zygotes were reoriented to Light 2 at 6 h and assayed at hourly intervals thereafter as described above. **B:** Percent polarization to Light 2 was calculated as described in the Materials and Methods. A polarization of 100% indicates that all zygotes polarized to Light 2, 0% indicates that the population polarized randomly, and 100% indicates that every zygote polarized to Light 1. Microtubules (circles) and polar axes (squares) reoriented rapidly followed by cell wall loosening (triangles) and asymmetric adhesive (diamonds). The inset shows the percent of cells without any clear asymmetry in microtubule array orientation. Each point represents an $N > 300$.

Cortical HDEL signal also increased throughout polarization, but as zygotes entered mitosis the endoplasmic reticulum aggregated and associated with the astral microtubules of spindles (Fig. 4, 17 h AF). During cytokinesis, interdigitating microtubules emanating from telophase centrosomes define the division plane [Bisgrove et al., 2003]. HDEL was observed at the cell division zone and in the perinuclear regions facing the developing partition membrane (Fig. 4, 24 h AF). Less-bundled microtubules were also present in these regions [Bisgrove and Kropf, 2004]. HDEL was present in the subapex of the rhizoid, but was absent from the rhizoid tip, an area known to be comprised of post-Golgi exocytotic vesicles [Belanger and Quatrano, 2000a].

Microtubule Disruption Decreases Asymmetric Adhesive Deposition and Reduces Tip Growth

To test the functional roles of microtubules in organizing endomembranes and targeting exocytosis, microtubules were disrupted with oryzalin [Katsaros et al., 2006]. While the effects of microtubule disrupting agents on asymmetric adhesive deposition and rhizoid outgrowth have been reported [Hadley et al., 2006; Peters and Kropf, 2006], their significance has not been appreciated. Asymmetric adhesive deposition was reduced following microtubule depolymerization, yet it was still localized to the rhizoid pole (Figs. 6A and 6B). Rhizoid outgrowth was also impaired, but not inhibited, in the absence of microtubules (Figs. 6C and 6D). Thus, local exocytosis is mediated by factors other than microtubules, likely a patch of F-actin localized to the rhizoid cortex [Alessa and Kropf, 1999; Hable and Kropf, 2000].

Microtubules are Required for Formation and Maintenance of the Asymmetric Distribution of Endoplasmic Reticulum

Pharmacological agents were used to test functional relationships between microtubules and the endoplasmic reticulum. Three different protocols were used to test the effects of microtubule disruption (Fig. 7A). In Assay 1, oryzalin was added at 6 h AF and HDEL signal was assayed at 10 h AF. The HDEL signal was aggregated around the nucleus and no discernable asymmetry was detected (Fig. 7B), indicating that maintenance of HDEL asymmetry requires microtubules. In Assay 2, oryzalin was added at 6 h AF and then the light vector was reoriented 180° at 6.5 h AF. When assayed at 10 h AF, the HDEL signal was again aggregated symmetrically in the perinuclear region but, as expected, some deposition of polar adhesive was observed in accordance with Light 2 (Fig. 7C). In Assay 3, oryzalin was applied at 6 h AF, followed by reorientation of the light vector at 6.5 h AF, and zygotes were assayed at 16 h AF. Zygotes deposited asymmetric adhesive and germinated in accordance with Light 2, but the endoplasmic reticulum remained uniformly distributed around the nucleus (Fig. 7D). The results of Assays 2 and 3 indicate that microtubules are needed to establish endoplasmic reticulum asymmetry in accordance with a new developmental axis. In all oryzalin-treated zygotes, microtubules were absent and cortical localization of the HDEL signal was greatly reduced.

In order to address whether F-actin also plays a role in organizing the endoplasmic reticulum, zygotes were treated with Latrunculin B at 6 h AF using Assay 2. Latrunculin B depolymerizes most F-actin and severely inhibits F-actin dependent processes in *S. compressa* [Hable and Kropf, 1998]. The endoplasmic reticulum remained tightly colocalized with microtubule arrays in the absence of functional F-actin (Fig. 7E). Neither the endoplasmic reticulum nor the microtubules reoriented to the new light vector. This is consistent with the finding that Latrunculin B treatment prevents axis reorientation [Hable and Kropf, 1998]. Interestingly, microtubule arrays were broadened and the nucleus was displaced following Latrunculin B treatment. The cortical microtubule array remained extensive (Fig. 7F). Thus, microtubules are the principal cytoskeletal organizing factor for the endoplasmic reticulum, and F-actin acts upstream of microtubule array polarization.

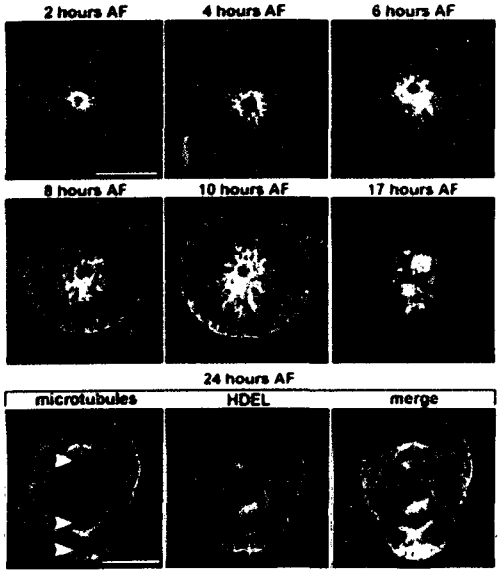

Fig. 4. Organization of the endoplasmic reticulum during early development. HDEL (green) and microtubules (red) signals colocalize during polarization (6–10 h AF), mitosis (17 h AF) and cytokinesis (24 h AF). During cytokinesis HDEL is associated with perinuclear microtubules (arrowheads), the subapex of the rhizoid, and the division zone. Images depict single confocal sections of representative zygotes. Scale bar equals 50 μm.

Zygotes were also treated with brefeldin A, an endomembrane trafficking disrupter [Shaw and Quatrano, 1996; Hable and Kropf, 1998; Hadley et al., 2006] that binds an ARF-GEF in metazoans and plants [Helms and Rothman, 1992; Tanaka et al., 2009]. The effects of BFA treatment were analyzed using Assay 2. Microtubule and endoplasmic reticulum asymmetries were lost, but their spatial colocalization remained (Fig. 7G). Since endomembrane trafficking is necessary for polar axis reorientation and maintenance [Bisgrove and Kropf, 2004], no new asymmetric adhesive was deposited in accordance with Light 2.

Discussion

Microtubule Arrays Become Asymmetric Toward the Rhizoid Pole During Polarization

Our examination of microtubules during polarization uncovered previously undescribed polar arrays emanating from the perinuclear region and extending out to and along the plasma membrane. However, a recent study examining microtubule arrays during early development using rhodamine-tubulin injected into live cells found cortical microtubule arrays that appeared to be nucleated from cortical microtubule organizing centers during polarization [Corellou et al., 2005]. Although we cannot rule out cortical nucleation, two observations suggest that the results presented here are likely to represent the bona fide organization of microtubules during polarization in brown algae. First, our chemical fixation technique preserves microtubules throughout the entire cell, from the perinuclear region out to the plasma membrane. The perinuclear arrays are difficult to image in live cells due to the opacity of the large zygotes. Secondly, we have confirmed the extensive microtubule array using high-pressure freezing and freeze substitution, the most reliable technique currently available.

The extensive microtubule array became increasing targeted to the rhizoid pole as polarization progressed. This asymmetry was not observed in previous studies [Kropf et al., 1990], probably due to poor preservation of cytoarchitecture. In light reversal experiments, microtubules became targeted in accordance with the new light direction as soon as the axis reoriented, suggesting rapid signaling from polar axis components to microtubules. One possibility is that cortical polarity markers that capture and stabilize microtubules rapidly concentrate at the new rhizoid pole, perhaps by interaction with a cortical patch of F-actin that marks the rhizoid pole [Alessa and Kropf, 1999; Hable and Kropf, 2000]. Search and capture is a common mechanism for selectively stabilizing microtubules in the context of cell polarity [Miller et al., 2000; Gundersen, 2002].

Asymmetric Microtubule Arrays Organize the Endomembrane System

The observation that microtubule array asymmetry preceded local cell wall loosening and deposition of polar adhesive led us to hypothesize that microtubules organize the endomembrane system and target exocytosis of vesicles containing wall degrading enzymes or adhesive to the rhizoid pole. Targeted exocytosis followed axis and microtubule reorientation by *only an hour or two, perhaps reflecting the relatively short* period of time in which these intertidal organisms must secrete adhesive toward the rocky substratum to securely anchor themselves before the onset of strong tidal forces.

Several findings indicate that organization and inheritance of the endoplasmic reticulum in *S. compressa* is a microtubule-based process. At all stages of the first cell cycle, the endoplasmic reticulum co-localized with microtubule arrays. Microtubule arrays and endoplasmic reticulum were initially uniformly distributed, and then became increasingly focused on the rhizoid pole as polarization progressed. Endoplasmic reticulum associated with astral microtubules during mitosis and the interdigitating microtubule array that defines the division plane during cytokinesis [Bisgrove et al., 2003]. Disrupting microtubules caused the endoplasmic reticulum to collapse around the nucleus, while actin disruption did not affect microtubule-endoplasmic reticulum associations.

Microtubule-based organization of the endomembrane system has been observed in a variety of organisms, most notably metazoans. In animals, the endoplasmic reticulum travels along microtubules with F-actin playing only a minor role in the peripheral cortical regions of some cell types [Bart, 2002;

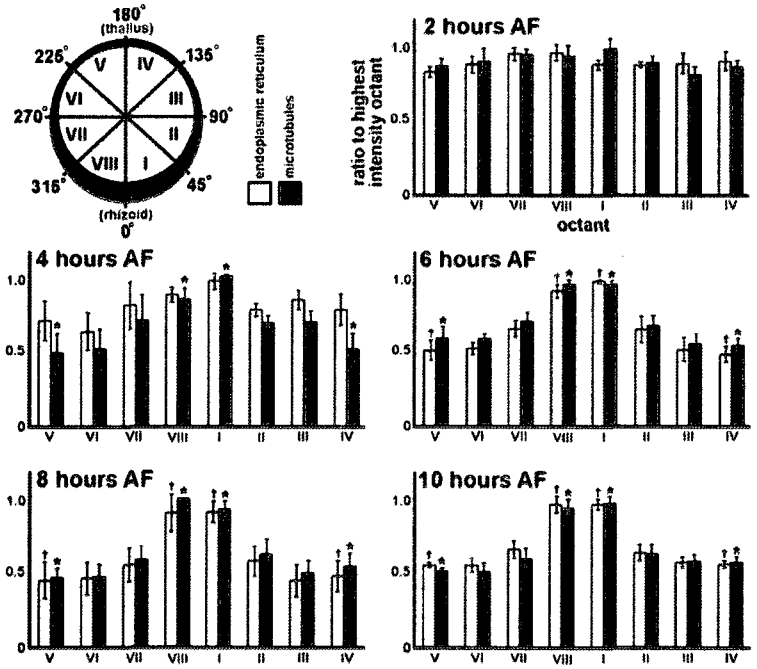

Fig. 5. Quantification of microtubule and endoplasmic reticulum asymmetry during polarization. For each histogram, five representative images of double-labeled zygotes were divided into octants and analyzed for microtubule and HDEL pixel intensity (see Materials and Methods). To quantitate asymmetries in rhizoid versus thallus regions, pixel intensities in octants I and VIII were combined and compared to the combined intensities of octants IV and V. There was no significant difference between rhizoid and thallus regions for microtubule or HDEL intensity at 2 h AF ($P > 0.1$). By 4 h AF, the microtubule signal intensities in the rhizoid (octants I and VIII) were significantly higher than those in the thallus (octants IV and V). However, the HDEL signal intensities were not significantly different between rhizoid and thallus at this time ($P > 0.01$). From 6 h AF onward, both microtubule and HDEL intensities were significantly higher in the rhizoid than in the thallus. For any individual octant at any time point, the microtubule intensity was not significantly different from HDEL intensity. Asterisks indicate significance to $P < 0.001$ between rhizoid and thallus regions for microtubule intensities, and daggers indicate significance to $P < 0.001$ for HDEL intensities.

Du et al., 2004]. Rapid extension of the endoplasmic reticulum is dependent on microtubule arrays, molecular motors or polymerization itself [Waterman-Storer and Salmon, 1998; Lane and Allan, 1999]. Much as we observe in *S. compressa* zygotes, microtubules are required for proper inheritance of the endoplasmic reticulum [Terasaki, 2000], and microtubule disruption causes the endoplasmic reticulum to aggregate around the nucleus [Terasaki et al., 1986; Terasaki, 2000].

There is evidence for microtubules organizing the endoplasmic reticulum in plants, as well. The endoplasmic reticulum becomes disorganized following microtubule perturbation in moss protonema [Pressel et al., 2008] and in leaf and root tip cells of the gymnosperms *Asplenium nidus* and *Pinus brutia* [Zachariadis et al., 2001; Zachariadis et al., 2003]. F-actin disruption has little effect on endoplasmic reticulum in these organisms. In angiosperms, the association of microtubules with endoplasmic reticulum appears to be dependent on the stage of the cell cycle [Gupton et al., 2006]. Endoplasmic reticulum associates with spindle poles and phragmoplasts to ensure proper segregation during cell division [Hepler, 1980; Gupton et al., 2006], but F-actin is responsible for organizing the endoplasmic reticulum and trafficking vesicles during interphase [Sheahan et al., 2007]. Likewise, green algae and budding yeast have been shown to use myosin-based movement of vesicles and endoplasmic reticulum along F-actin [Kachar and Reese, 1988; Yoshida et al., 2003; Du et al., 2004]. More recently, studies in characean algae found that while the endoplasmic reticulum streams along F-actin cables in the endoplasm, the cortical endoplasmic reticulum uses microtubule-based motility mechanisms [Foissner et al., 2009]. Thus, evolution has apparently established two relatively distinct cytoskeletal-based systems for endomembrane organization and inheritance, one based on microtubules and one based on F-actin.

F-actin may also contribute to endoplasmic reticulum organization in some brown algae. In contrast to our findings, a recent study found spatial association of HDEL signal with

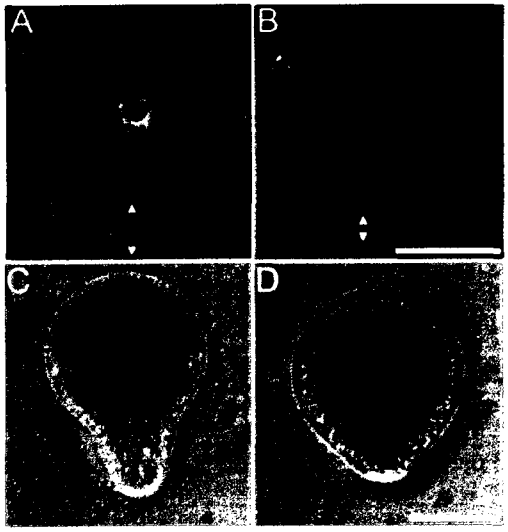

Fig. 6. The effect of oryzalin treatment on asymmetric adhesive deposition and tip growth. **A** and **B**: Medial confocal sections of 8-h old zygotes antibody-labeled for microtubules. A: Control zygote with polar adhesive (arrow) and microtubule arrays polarized toward the rhizoid hemisphere. B: Zygote treated continuously with oryzalin beginning 30 min AF. No microtubule arrays were observed and deposition of asymmetric adhesive (arrow) was strongly reduced. **C** and **D**: Brightfield images of zygotes at 24 h AF. C: A well-developed rhizoid tip of a control zygote exhibiting normal morphology. D: Zygote treated with oryzalin from 30 min AF. Tip growth was reduced and poorly focused in the absence of functional microtubule arrays. Scale bars equal 50 μm.

cortical F-actin but not with microtubule arrays in *Macrocystis pyrifera*, *Splachnidium rugosum*, and *Choristocarpus tenellus* [Varvarigos et al., 2007]. Furthermore, disruption of microtubules had no effect on radial endoplasmic reticulum organization, while disruption of F-actin abolished the radial endoplasmic reticulum arrays in *M. pyrifera*. Hence, different species of brown algae may utilize different mechanisms of endomembrane organization, and perhaps vesicle trafficking as well. Addressing the mechanistic and functional similarities and differences of endomembrane organization and vesicle trafficking in brown algae will be an important avenue of future research.

The Role of Microtubules in Tip Growing Cells

Asymmetric microtubule arrays organize the endoplasmic reticulum and are necessary for maintaining rhizoid morphology and the rate of tip growth in *S. compressa*. Similar microtubule-based requirements have been observed in other tip growing cells. In root hairs of Arabidopsis and the legume *Medicago truncatula*, and in fungal hyphae of *Aspergillus nidulans*, microtubule depolymerization leads to defects in the rate of tip growth, tip morphology, and in some instances cytoplasmic organization [Bibikova et al., 1999; Horio and Oakley, 2005; Sieberer et al., 2005; Antonius et al., 2006]. In *M. truncatula*, microtubules are also needed for asymmetric distribution of the cortical polarity marker, Ebl [Antonius et al., 2006]. These results suggest that

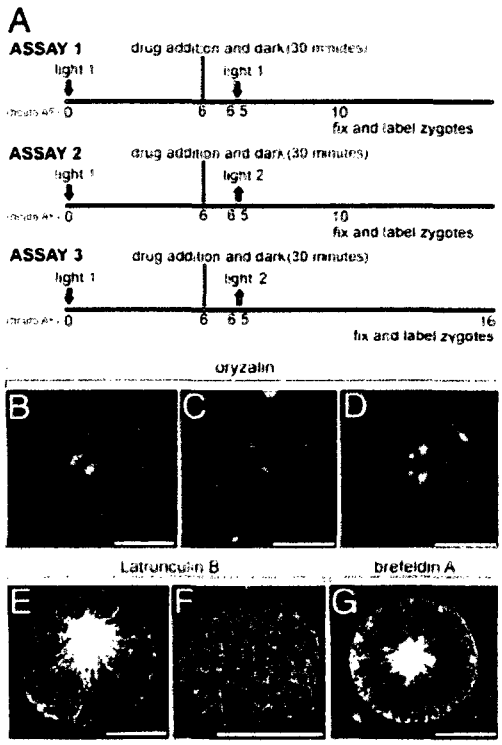

Fig. 7. Cellular requirements for asymmetric endoplasmic reticulum organization. **A**: Experimental design. Assay 1: zygotes were grown in unilateral light (Light 1) for 6 h AF at which point inhibitors were added and dishes were placed in the dark for 30 min to permit inhibitor uptake. At 6.5 h AF samples were returned to Light 1 and were fixed at 10 h AF. Assay 2: zygotes were grown in unilateral light (Light 1) until 6 h AF at which point inhibitors were added and dishes were placed in the dark for 30 min. At 6.5 h AF, the light vector was reoriented 180° (Light 2), and zygotes were fixed at 10 h AF. Assay 3: Zygotes were treated as in Assay 2 except that zygotes were fixed at 16 h AF. **B–G**: HDEL signal is shown in (green) and microtubules in (red) for all panels. B: Zygote was treated with oryzalin following Assay 1. C: Zygote treated with oryzalin following Assay 2. D: Zygote treated with oryzalin following Assay 3. In B–D, no microtubules were observed, and the HDEL signal became aggregated with minimal cortical localization. E: Zygote treated with Latrunculin B following Assay 2. The microtubule arrays appeared broad and remained polarized to Light 1. The HDEL signal colocalized with microtubules. F: Cortical Z-series stack (approximately 7 μm) of a zygote treated with Latrunculin B. The microtubules extended for considerable distances along the plasma membrane. G: Zygote treated with brefeldin A following Assay 2. Microtubule and HDEL signal remained colocalized but symmetric. No polar adhesive deposition was observed in accordance with Light 2. Scale bars equal 50 μm.

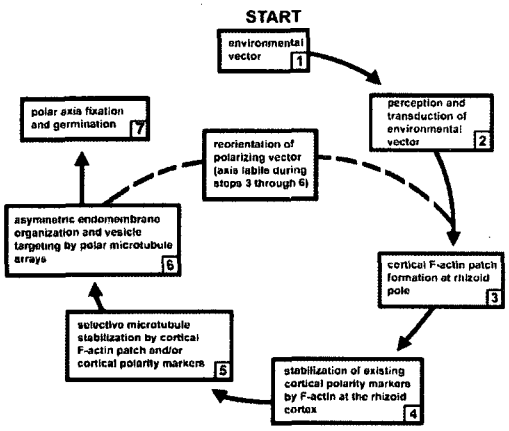

Fig. 8. Polarization model for *S. compressa* (See text for details).

microtubules regulate polarized growth by controlling the localization of tip growth components, but are not required *per se* for vesicle fusion and tip extension. Thus, microtubules may directly organize the endomembrane system that supplies vesicles for tip growth, and may facilitate the movement of polar axis components to the cell cortex. Without functional microtubules, the endomembrane system becomes disorganized and vesicle trafficking becomes inefficient, leading to reduced, delocalized tip growth.

Model of Early Development

Our current study and past research lead to a new model of polarity establishment in *S. compressa*. Polarization occurs sequentially during the first 10 h of development, depicted by boxes and arrows in Fig. 8. (Step 1) The sperm-induced polar axis is usually overridden by an environmental vector, typically light [Hable and Kropf, 2000], which is likely detected by aureochrome photoreceptors [Takahashi et al., 2007]. (Step 2) The polarizing signal is transduced from the plasma membrane for modification of polar axis components [Takahashi et al., 2007]. (Step 3) Signal transduction leads to formation of gradients of reactive oxygen species [Coelho et al., 2008], calcium [Bothwell et al., 2008], and protons [Kropf et al., 1995], with highest concentrations at the rhizoid pole. A cortical F-actin patch also forms at the rhizoid pole [Alessa and Kropf, 1999; Hable and Kropf, 2000]. As in most organisms, the cortical F-actin functions in endo- and exocytosis. (Step 4) The actin patch stabilizes hypothesized cortical polarity markers. (Step 5) Microtubules are captured and selectively stabilized by F-actin and/or cortical polarity markers at the rhizoid pole. In the absence of F-actin, the microtubule array is less focused due to compromised cortical stabilization. (Step 6) Polar microtubule arrays organize the endoplasmic reticulum and mediate vesicle targeting, likely by transporting vesicles to the rhizoid pole. Local vesicle fusion is dependent upon the cortical F-actin and may insert additional polarity markers, further amplifying the axis. The polar axis is labile through Step 6 and detection of a new environmental vector leads to repositioning of cortical F-actin, polarity markers, microtubules and endomembranes (dashed line). (Step 7) The polar axis becomes fixed and tip growth commences with rhizoid germination.

Acknowledgment

The authors thank Ed King for his continued help developing a protocol for high-pressure freezing and Kyle Logan for helpful discussions. This work was supported by NSF awards IOB-0414089 and IOS 0817045.

References

Alessa L, Kropf DL. 1999. F-actin marks the rhizoid pole in living *Pelvetia compressa* zygotes. Development 126:201–209.

Antonius CJ, Timmers AC, Vallotton P, Heym C, Menzel D. 2006. Microtubule dynamics in root hairs of *Medicago truncatula*. Eur J Cell Biol 86(2): 69–83.

Barr FA. 2002. Inheritance of the endoplasmic reticulum and golgi apparatus. Curr Opin Cell Biol 14(4):496–499.

Belanger KD, Quatrano RS. 2000a. Membrane recycling occurs during asymmetric cell growth and cell plate formation in *Fucus distichus* zygotes. Protoplasma 212:24–37.

Belanger KD, Quatrano RS. 2000b. Polarity: The role of localized secretion. Curr Opin Plant Biol 3:67–72.

Bibikova TN, Blancaflor EB, Gilroy S. 1999. Microtubules regulate tip growth and orientation in root hairs of *Arabidopsis thaliana*. Plant J 17(6): 657–665.

Bisgrove SR, Henderson DC, Kropf DL. 2003. Asymmetric division in fucoid zygotes is positioned by telophase nuclei. Plant Cell 15:854–862.

Bisgrove SR, Kropf DL. 2004. Cytokinesis in brown algae: Studies of asymmetric division in fucoid zygotes. Protoplasma 223:163–173.

Bisgrove SR, Kropf DL. 2008. Asymmetric cell divisions: Zygotes of fucoid algae as a model system. In: Verma DPS, Hong Z, editors. Cell Division Control in Plants. Heidelberg: Springer-Verlag. pp324–341.

Bisgrove SR, Nagasato C, Motomura T, Kropf DL. 1997. Immunolocalization of centrin during fertilization and the first cell cycle in *Fucus distichus* and *Pelvetia compressa* (Fucales. Phaeophyceae). J Phycol 33(5):823–829.

Bothwell JHF, Kisielewska J, Genner MJ, McAinsh MR, Brownlee C. 2008. Ca2+ signals coordinate zygotic polarization and cell cycle progression in the brown alga *Fucus serratus*. Development 135(12):2173–2181.

Bower FO. 1880. On the development of the conceptacle in the Fucaceae. Q J Microsc Sci 20:36–49.

Brownlee C, Bouget F-Y, Corellou F. 2001. Choosing sides: Establishment of polarity in zygotes of fucoid algae. Cell Dev Biol 12:345–351.

Coelho S, Brownlee C, Bothwell J. 2008. A tip-high. Ca2+-interdependent, reactive oxygen species gradient is associated with polarized growth in *Fucus serratus* zygotes. Planta 227(5):1037–1046.

Corellou F, Coelho SMB, Bouget F-Y, Brownlee C. 2005. Spatial re-organisation of cortical microtubules in vivo during polarisation and asymmetric division of Fucus zygotes. J Cell Sci 118:2723–2734.

Du Y, Ferro-Novick S, Novick P. 2004. Dynamics and inheritance of the endoplasmic reticulum. J Cell Sci 117(14):2871–2878.

Foissner I, Mendel D, Wasteneys GO. 2009. Microtubule-dependent motility and orientation of the cortical endoplasmic reticulum in elongating characean internodal cells. Cell Motil Cytoskeleton 66:142–155.

Gundersen GG. 2002. Evolutionary conservation of microtubule-capture mechanisms. Nat Rev Mol Cell Biol 3(4):296–304.

Gupton SL, Collings DA, Allen NS. 2006. Endoplasmic reticulum targeted GFP reveals ER organization in tobacco NT-1 cells during cell division. Plant Physiol Biochem 44(2–3):95–105.

Hable WE, Kropf DL. 1998. Roles of secretion and the cytoskeleton in cell adhesion and polarity establishment in *Pelvetia compressa* zygotes. Dev Biol 198:45–56.

Hable WE, Kropf DL. 2000. Sperm entry induces polarity in fucoid zygotes. Development 127:493–501.

Hadley R, Hable WE, Kropf DL. 2006. Polarization of the endomembrane system is an early event in fucoid zygote development. BMC Plant Biol 6: 1–10.

Helms JB, Rothman JE. 1992. Inhibition by brefeldin A of a golgi membrane enzyme that catalyses exchange of guanine nucleotide bound to ARF. Nature 360(6402):352–354.

Hepler P. 1980. Membranes in the miotic apparatus of barley cells. J Cell Biol 86(2):490–499.

Horio T, Oakley BR. 2005. The role of microtubules in rapid hyphal tip growth of *Aspergillus nidulans*. Mol Biol Cell 16(2):918–926.

Jaffe LF. 1968. Localization in the developing Fucus egg and the general role of localizing currents. Adv Morphol 7:295–328.

Kachar B, Reese T. 1988. The mechanism of cytoplasmic streaming in characean algal cells: Sliding of endoplasmic reticulum along actin filaments. J Cell Biol 106(5):1545–1552.

Katsaros C, Karyoophyllis D, Galatis B. 2006. Cytoskeleton and morphogenesis in brown algae. Ann Bot 97:679–693.

Kropf DL, Henry C, Gibbon BC. 1995. Measurement and manipulation of cytosolic pH in polarizing zygotes. Eur J Cell Biol 68(3):297–305.

Kropf DL, Maddock A, Gard DL. 1990. Microtubule distribution and function in early Pelvetia development. J Cell Sci 97:545–552.

Lane JD, Allan VJ. 1999. Microtubule-based endoplasmic reticulum motility in *Xenopus laevis*: Activation of membrane-associated kinesin during development. Mol Biol Cell 10(6):1909–1922.

Miller RK, Cheng S-C, Rose MD. 2000. Bim1p/Yeb1p mediates the Kar9p-dependent cortical attachment of cytoplasmic microtubules. Mol Biol Cell 11(9):2949–2959.

Peters NT, Kropf DL. 2006. Kinesin-5 motors are required for organization of spindle microtubules in *Silvetia compressa* zygotes. BMC Plant Biol 6:19: 1–10.

Pressel S, Ligrone R, Duckett JG. 2008. Cellular differentiation in moss protonemata: A morphological and experimental study. Ann Bot 102(2): 227–245.

Quatrano RS. 1973. Separation of processes associated with differentiation of two-celled Fucus embryos. Dev Biol 30:209–213.

Quatrano RS. 1997. Cortical asymmetries direct the establishment of cell polarity and the plane of cell division in the Fucus embryo. In: Cold Spring Harbor Symposium on Quantitative Biology. Cold Spring Harbor, NY: Cold Spring Harbor Laboratory Press. Vol.62, pp65–70.

Shaw SL, Quatrano RS. 1996. The role of targeted secretion in the establishment of cell polarity and the orientation of the division plane in Fucus zygotes. Development 122:2623–2630.

Sheahan MB, Rose RJ, McCurdy DW. 2007. Mechanisms of organelle inheritance in dividing plant cells. J Integr Plant Biol 49(8):1208–1218.

Sieberer BJ, Timmers AC, Emons AM. 2005. Nod factors alter the microtubule cytoskeleton in *Medicago truncatula* root hairs to allow root hair reorientation. Mol Plant Microbe Interact 18(11):1195–1204.

Takahashi F, Yamagata D, Ishikawa M, Fukamatsu Y, Ogura Y, Kasahara M, Kiyosue T, Kikuyama M, Wada M, Kataoka H. 2007. AUREOCHROME, a photoreceptor required for photomorphogenesis in stramenopiles. Proc Natl Acad Sci USA 104:19625–19630.

Tanaka H, Kitakura S, De Rycke R, De Groodt R, Friml J. 2009. Fluorescence imaging-based screen identifies ARF GEF component of early endosomal trafficking. Curr Biol 19(5):391–397.

Terasaki M. 2000. Dynamics of the endoplasmic reticulum and golgi apparatus during early sea urchin development. Mol Biol Cell 11(3):897–914.

Terasaki M, Chen L, Fujiwara K. 1986. Microtubules and the endoplasmic reticulum are highly interdependent structures. J Cell Biol 103(4): 1557–1568.

Varvarigos V, Galatis B, Katsaros C. 2007. Radial endoplasmic reticulum arrays co-localize with radial F-actin in polarizing cells of brown algae. Eur J Phycol 42:253–262.

Vreeland V, Waite JH, Epstein L. 1998. Polyphenols and oxidases in substratum adhesion by marine algae and mussels. J Phycol 34:1–8.

Waterman-Storer CM, Salmon ED. 1998. Endoplasmic reticulum membrane tubules are distributed by microtubules in living cells using three distinct mechanisms. Curr Biol 8(14):798–807.

Yoshida K, Inoue N, Sonobe S, Shimmen T. 2003. Involvement of microtubules in rhizoid differentiation of Spirogyra species. Protoplasma 221(3–4): 227–235.

Zachariadis M, Quader H, Galatis B, Apostolakos P. 2001. Endoplasmic reticulum preprophase band in dividing root-tip cells of *Pinus brutia*. Planta 213:824–827.

Zachariadis M, Quader H, Galatis B, Apostolakos P. 2003. Organization of the endoplasmic reticulum in dividing cells of the gymnosperms *Pinus brutia* and *Pinus nigra*, and of the pterophyte *Asplenium nidus*. Cell Biol Int 27(1): 31–40.

CHAPTER 3

PHOSPHOLIPASE D SIGNALING REGULATES MICROTUBULE ORGANIZATION IN THE FUCOID ALGA *SILVETIA COMPRESSA*

Plant Cell Physiol. 48(12): 1764–1774 (2007)
doi:10.1093/pcp/pcm149, available online at www.pcp.oxfordjournals.org

Phospholipase D Signaling Regulates Microtubule Organization in the Fucoid Alga *Silvetia compressa*

Nick T. Peters *, Kyle O. Logan, Anne Catherine Miller and Darryl L. Kropf
University of Utah, Department of Biology, 257 South 1400 East, Salt Lake City, UT 84112, USA

Recent studies in higher plants or animals have shown that phospholipase D (PLD) signaling regulates many aspects of development, including organization of microtubules (MTs), actin and the endomembrane system. PLD hydrolyzes structural phospholipids to form the second messenger phosphatidic acid (PA). To begin to understand the signaling pathways and molecules that regulate cytoskeletal and endomembrane arrays during early development in the brown alga, *Silvetia compressa*, we altered PLD activity by applying butyl alcohols to zygotes. 1-Butanol activates PLD and is a preferred substrate, primarily forming phosphatidyl butanol (P-butanol), which is not a signaling molecule. Treatment with 1-butanol inhibited cell division and cytokinesis but not photopolarization or germination, suggesting an MT-based effect. Immunolabeling revealed that 1-butanol treatment rapidly disrupted MT arrays and caused zygotes to arrest in metaphase. MT arrays recovered rapidly following butanol washout, but subsequent development depended on the timing of the treatment regime. Additionally, treatment with 1-butanol early in development disrupted endomembrane organization, known to require functional MTs. Interestingly, treatment with higher concentrations of 2-butanol, which also activates PLD, mimicked the effects of 1-butanol. In contrast, the control *t*-butanol had no effect on MTs or development. These results indicate that *S. compressa* zygotes utilize PLD signaling to regulate MT arrays. In contrast, PLD signaling does not appear to regulate actin arrays or endomembrane trafficking directly. This is the first report describing the signaling pathways that regulate cytoskeletal organization in the stramenopile (heterokont) lineage.

Keywords: Brown algae — Cytoskeleton — Development — Endomembrane — Phosphatidic acid — Phospholipase D.

Abbreviations: AF, after fertilization; ASW, artificial sea water; CLSM, confocal laser scanning microscope; DMSO, dimethylsulfoxide; L1, unidirectional light; L2, light oriented 180° from L1; MAP, microtubule-associated protein; MT, microtubule; MTOC, microtubule-organizing center; PA, phosphatidic acid; P-butanol, phosphatidyl butanol; PLD, phospholipase D.

Introduction

Silvetia compressa, a fucoid marine brown alga in the stramenopile lineage, has been utilized for investigating many aspects of cell biology for more than a hundred years (Bower 1880). Fucoid algae are particularly useful model organisms for studying polarity establishment and asymmetric cell division (Quatrano 1997, Brownlee et al. 2001, Bisgrove and Kropf 2007). The cytoskeleton and endomembrane system are critical for polarization of the zygote; targeting the endomembrane system to the future growth site relies upon dynamic microtubules (MTs) and a cortical actin patch that marks the rhizoid pole (Alessa and Kropf 1999, Hable and Kropf 2005, Hudley et al. 2006). Targeted vesicle trafficking leads to polar deposition of adhesive and localized rhizoid outgrowth (Hable and Kropf 1998, Belanger and Quatrano 2000). Rhizoid morphogenesis, nuclear positioning and subsequent formation of a bipolar spindle require reorganization of MT arrays (Bisgrove and Kropf 1998). Cytokinesis proceeds from the cell interior toward the cortex as in higher plants (Bisgrove and Kropf 2001b). The plane of division is determined by an interdigitating MT array and a plate of actin that assembles in the cytokinetic plane (Bisgrove et al. 2003). Both cytoskeletal arrays and vesicle trafficking are needed for deposition of partition membranes and the cell wall (Belanger and Quatrano 2000, Bisgrove and Kropf 2004). While the organization of the cytoskeletal arrays and endomembranes in *S. compressa* has been documented, little is known about the signaling mechanisms that regulate these arrays. In this study we begin to address whether the phospholipase D (PLD) signaling pathway regulates cytoskeletal rearrangements and/or endomembrane organization during brown algal development.

PLD signaling affects numerous developmental processes in higher plants, yeast and animals (Meijer and Munnik 2003, Jenkins and Frohman 2005). Environmental stimuli activate G-proteins that, in turn, stimulate PLD activity (Malho et al. 2006, Oude Weernink et al. 2007b).

*Corresponding author: E-mail, npeters@biology.utah.edu; Fax, +1-801-581-4668.

PLD removes the head group of structural phospholipids and forms a covalent bond with the remaining phosphatidyl moiety (Munnik and Musgrave 2001). This intermediate is subsequently converted to phosphatidic acid (PA) via PLD, transferring the phosphatidyl moiety to water (Oude Weernink et al. 2007a). PA can also be formed by the phospholipase C pathway through phosphorylation of diacylglycerol or by dephosphorylation of diacylglycerol pyrophosphate (Wang 2004). PA remains in the membrane and binds to and activates a host of target molecules that regulate cellular physiology (Meijer and Munnik 2003, Oude Weernink et al. 2007a).

PLD signaling has been most extensively studied in yeast and animal cells where it primarily regulates actin arrays and trafficking of vesicles to and from the plasma membrane (Oude Weernink et al. 2007a). PLD and PA are also thought to play important roles in higher plants, which have many more PLD genes (12 in Arabidopsis) than humans (two genes) or yeast (one gene), allowing for gene-specific regulation of cellular responses (Munnik 2001). In plants, embryo maturation, cell elongation, germination, senescence (reviewed in Meijer and Munnik 2003) and a host of stress responses (de Jong et al. 2004, Vergnolle et al. 2005) have been shown to be regulated by the PLD pathway. As with animals, cellular targets of PLD signaling in plants include actin arrays (Motes et al. 2005, Huang et al. 2006) and endomembrane trafficking (Monteiro et al. 2005); in addition, PLD regulates cortical MT arrays in plants (Dhonukshe et al. 2003, Motes et al. 2005).

PLD can be activated experimentally by treating zygotes with alcohols that stimulate G-proteins by promoting GTP binding (Munnik 2001). Primary alcohols, such a 1-butanol, can promote PLD activity by this mechanism and are also transphosphatidylation substrates (Fig. 1) (Munnik et al. 1995). Since the primary alcohol is the preferred substrate, application of 1-butanol produces more phosphatidyl butanol (P-butanol) than PA (Munnik et al. 1995). P-butanol is not a signaling molecule (Munnik and Musgrave 2001). Secondary alcohols, such as 2-butanol, also stimulate G-proteins that activate PLD, but are not transphosphatidylation substrates (Munnik et al. 1995). Tertiary alcohols, such as *t*-butanol, do not activate G-proteins nor are they transphosphatidylation substrates (Dhonukshe et al. 2003).

To begin addressing whether the PLD-based signaling pathway is responsible for cytoskeletal and endomembrane rearrangements during development in brown algae, we applied butyl alcohols to *S. compressa* zygotes. We found that 1-butanol disrupted cell division but not germination or photopolarization, suggesting that PLD primarily signals MTs rather than actin arrays or endomembrane trafficking. Indeed, 1-butanol treatment rapidly and reversibly disorganized MT arrays. Treatment early in development also prevented polarization of endomembranes, presumably by disorganizing MTs. Prolonged treatment resulted in developmental arrest at the spindle assembly checkpoint. These results suggest that disrupting PLD activity in *S. compressa* quickly and dramatically alters MT organization, which in turn disrupts endomembrane organization and early development.

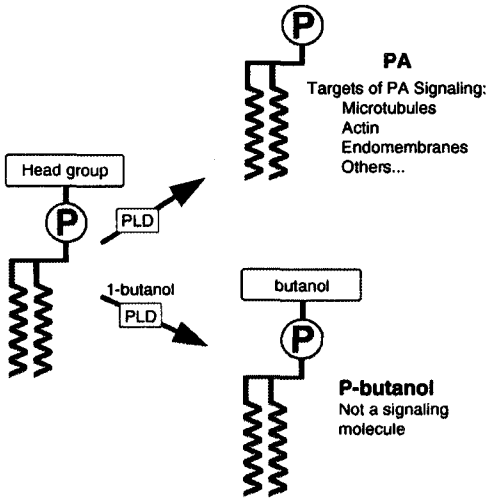

Fig. 1 Formation and functional roles of phosphatidic acid (PA) and phosphatidyl-butanol (P-butanol). PA is formed by phospholipase D (PLD)-catalyzed hydrolysis of the head group of phosphatidylcholine or phosphatidylethanolamine, followed by transfer of the phosphatidyl moiety to water. Since 1-butanol is a preferred transphosphatidylation substrate, its presence preferentially leads to formation of P-butanol. P-butanol is not a signaling molecule.

Results

1-Butanol does not affect germination but blocks cell division

Zygotes treated with 1-butanol, 2-butanol and *t*-butanol were examined for effects on development. Application of 1-butanol to *S. compressa* zygotes at 1 h after fertilization (AF) did not affect rhizoid germination at concentrations up to 0.2%, and only slightly reduced germination at higher concentrations (Fig. 2A). 2-Butanol and *t*-butanol treatments did not affect germination of zygotes.

In contrast, 0.1% 1-butanol treatment significantly reduced cell division, and concentrations of $\geq$0.2% inhibited nearly all division (Fig. 2B). Treatment with 2-butanol had much less effect and only reduced division by

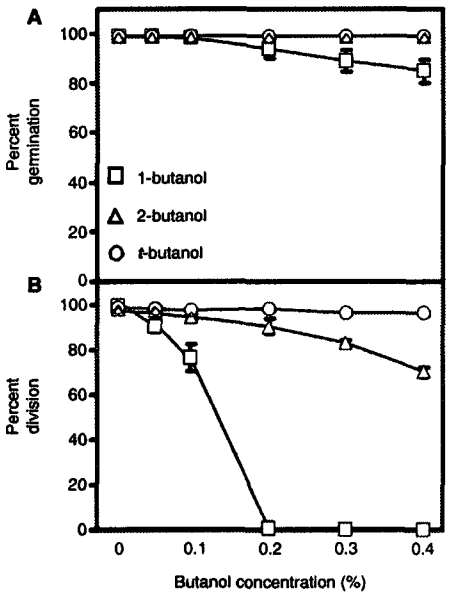

Fig. 2 1-Butanol treatment blocks cell division. 1-, 2- and *t*-butanol were tested for effects on germination (A) and division (B). Experiments were performed in triplicate; standard error bars are shown.

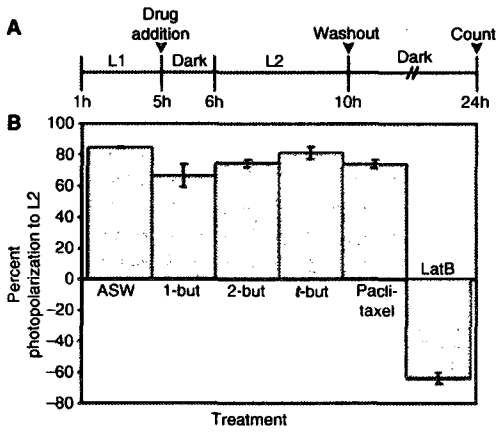

Fig. 3 Photopolarization of zygotes is not inhibited by butanol treatment. (A) Experimental design; zygotes were photopolarized with unidirectional light (L1), and then placed in the dark and incubated with drugs for 1 h. Next, zygotes were exposed to a second light vector (L2) followed by drug washout and incubation in the dark to allow germination. Zygotes were scored for photopolarization in accordance with L2. (B) Zygotes in ASW, 1-butanol (1-but), 2-butanol (2-but), *t*-butanol (*t*-but) and paclitaxel were able to reorient their photopolarization axis to L2. Latrunculin B (LatB) prevented axis reorientation. Experiments were performed in triplicate; standard error bars are shown. See text for details.

30±2.1% at 0.4% alcohol concentration, while *t*-butanol had no effect. We chose to utilize 0.2% butyl alcohol treatments for all further experiments, unless otherwise stated, because it was the lowest 1-butanol concentration that had maximal effect. Previous work has shown that cell division is dependent on MTs, actin arrays and endomembrane trafficking, while physical germination is dependent primarily on filamentous actin arrays and endomembrane trafficking (Kropf et al. 1999, Bisgrove and Kropf 2007). Therefore, the observation that 0.2% 1-butanol inhibits division but not germination suggests that PLD primarily signals to MTs rather than to filamentous actin or endomembrane trafficking.

Photopolarization is not affected by butanol treatment

In order to discriminate further between PLD-based signaling to MTs, filamentous actin arrays and the endomembrane organization and trafficking system, we investigated butanol effects on photopolarization. Photopolarized zygotes germinate away from the light vector. Like germination, photopolarization requires dynamic actin arrays and endomembrane trafficking, but MTs play a more subtle role and are dispensable for physical outgrowth of the rhizoid tip (Quatrano 1973, Hable and Kropf 1998). We tested the ability of butanol-treated zygotes to reverse their polar axes in response to reorientation of a light cue. Zygotes were photopolarized by exposure to unidirectional light (L1), treated with butanol and then exposed to L2, which was oriented 180° from L1 (see Materials and Methods and Fig. 3A). Following drug washout, zygotes were allowed to germinate in the dark and assayed for photopolarization to L2. Artificial seawater (ASW) controls, 1-butanol-, 2-butanol- and *t*-butanol-treated zygotes reoriented their rhizoid poles in accordance with the L2 vector (Fig. 3B). As expected, the microtubule-stabilizing drug paclitaxel also had no effect on axis reorientation. In contrast, zygotes treated with the actin-depolymerizing drug latrunculin B failed to reorient and remained polarized in accordance with the L1 vector, as indicated by negative polarization values. These data further suggest that PLD primarily signals to MTs rather than to filamentous actin arrays.

1-Butanol treatment disrupts MT arrays

To determine whether MT arrays are affected by 1-butanol, 8-hour-old zygotes were incubated with 1-butanol and then chemically fixed, antibody labeled

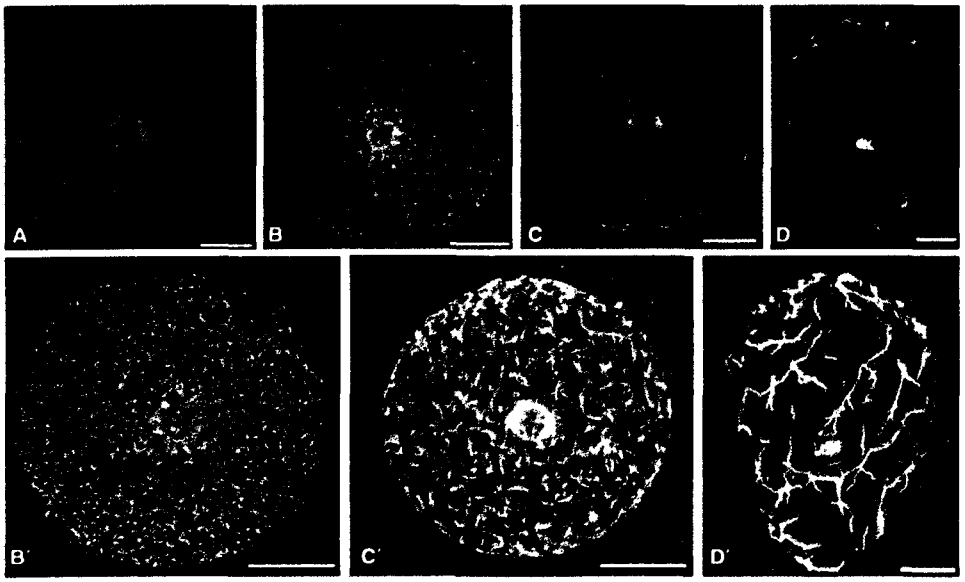

Fig. 4 1-Butanol treatment disrupts MT arrays. Zygotes were double labeled for MTs (green) and phosphorylated histone H3 (red), a marker of condensed chromatin. (A) A medial CLSM section taken from a control zygote at 8 h AF. MT arrays emanate from the nucleus and centrosomes toward the cell cortex. (B–D') Zygotes treated with 0.2% 1-butanol for increasing durations, beginning 8 h AF. B–D are single, medial CLSM sections, and B'–D' are projections from the cell cortex to the nucleus of the corresponding cells. (B) An 8.5-hour-old zygote treated for 30 min. MTs are in short fragments scattered uniformly throughout the cytoplasm. (B') Projection demonstrating the extreme number of MT fragments. (C) A 10-hour-old zygote treated for 2 h. MTs are in fragments mostly in the cell cortex and immediately surrounding the nucleus. (C') A projection clearly revealing the numerous cortical MT fragments. (D) A 24-hour-old zygote treated for 16 h. MT bundles are present in the cell cortex and fragments are localized near condensed chromatin. (D') Heavily bundled, branching MT fragments at the cell cortex are apparent in the CLSM projection. Bars = 25 μm. Single CLSM sections were 1–2 μm thick.

for MTs and condensed chromatin, and viewed by confocal laser scanning microscopy (CLSM; Fig. 4). Untreated control zygotes displayed normal MT arrays; MTs nucleated from microtubule-organizing centers (MTOCs) associated with the nuclear envelope and extended radially through the cytoplasm to the cellular cortex (Fig. 4A). Within 5 min of treatment with 1-butanol, MTs began to appear fragmented, and by 30 min zygotes displayed numerous, very short MTs scattered throughout the cytoplasm (Fig. 4B, B'). Over the next 1.5 h, the short fragmented MTs became longer and less numerous, and accumulated preferentially in the cell cortex (Fig. 4C, C'). Zygotes treated with 1-butanol progressed through the cell cycle up to metaphase of mitosis. At this point, the zygotes arrested, unable to form a bipolar metaphase spindle, and appeared to possess bundled MTs at the cortex and condensed nuclear chromatin (Fig. 4D). A cortex to nucleus projection showed MT fragments located exclusively in the cortex, with the exception of a small amount of diffuse MT labeling near the condensed chromatin (Fig. 4D').

Zygotes treated with 2-butanol did not exhibit any MT disruption at concentrations of $\leq$0.2% (data not shown). However, higher concentrations of 2-butanol mimicked the effects of 1-butanol treatment. Zygotes treated with 0.4% 2-butanol displayed prominent cortical MT arrays, and at 2-butanol concentrations of 0.6% MT arrays appeared nearly identical to those observed in zygotes treated with 0.2% 1-butanol. This finding is consistent with the observation that 2-butanol significantly reduced division at 0.4% (Fig. 2B), and blocked division nearly completely at 0.6% (data not shown). In contrast, zygotes treated with *t*-butanol did not show any evidence of cortical MT arrays, even at alcohol concentrations up to 2.0% (data not shown). Butanol concentrations of $\geq$0.7% were increasingly toxic. As noted earlier, butanols were used at 0.2% in developmental experiments, and at this concentration only MTs in 1-butanol-treated zygotes were compromised. Together, these data confirm that disrupting PLD signaling leads to dramatic effects on MT arrays.

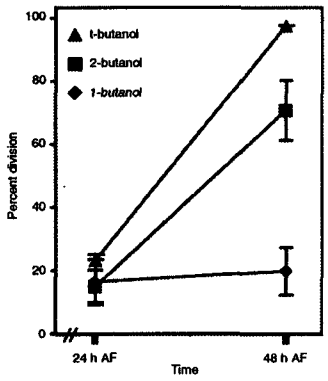

Fig. 5 1-Butanol treatment blocks cytokinesis. Zygotes were treated with 0.2% butanol when approximately 20% of the population had completed cell division. Zygotes were again scored for cell division at 48 h AF. Experiments were performed in triplicate; standard error bars are shown.

1-Butanol treatment inhibits cytokinesis

Since treatment with 1-butanol prior to mitosis activated the spindle assembly checkpoint (Fig. 4D, D′), the inhibition of cell division observed in Fig. 2 was probably due to metaphase arrest. To examine whether disruption of PLD signaling inhibited cytokinesis directly, butyl alcohols were added after zygotes had successfully completed metaphase of mitosis. Alcohols were added when approximately 20% of zygotes had completed cell division (around 24 h AF). Addition of 0.2% 2-butanol or *t*-butanol had minor effects on cytokinesis, with 70.8 ± 15.1 and $97.6 \pm 0.1\%$, respectively, of zygotes completing cell division by 48 h AF (Fig. 5). In contrast, the addition of 1-butanol blocked further division nearly completely, consistent with rapid PLD-based signaling to MTs during cytokinesis.

Reversibility of 1-butanol is influenced by developmental timing

In order to determine whether the effects of 1-butanol were reversible, zygotes were treated with 1-butanol at 1 or 15 h AF, followed by washout at 24–24.5 h AF and evaluation of division (Fig. 6A). ASW controls and 2-butanol-treated zygotes had nearly all divided by 48 h AF (Fig. 6B). Interestingly, the ability of 1-butanol-treated zygotes to recover after washout depended on the treatment regimen. At the time of washout, zygotes were arrested at the spindle assembly checkpoint, regardless of whether 1-butanol was added at 1 h AF (prior to germination) or at 15 h AF (after germination). However, when 1-butanol was added at 1 h AF, only $29 \pm 6.8\%$ of zygotes were able to

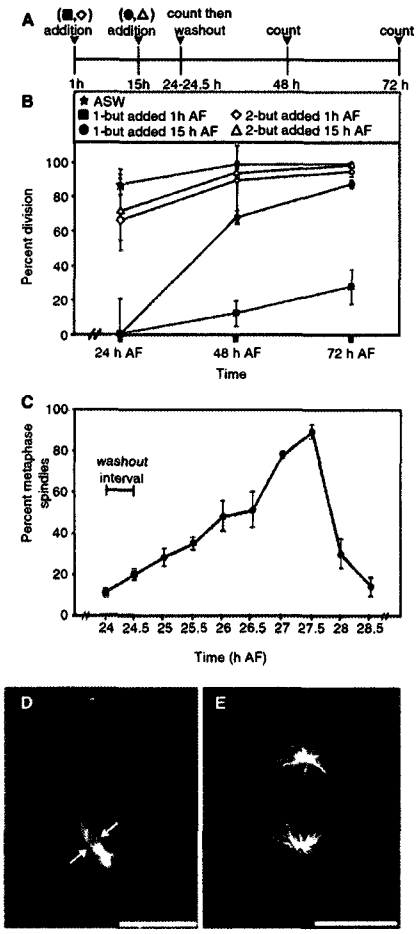

Fig. 6 Reversibility of the effect of 1-butanol. (A) Experimental design; 0.2% 1- and 2-butanol were added at either 1 or 15 h AF. Drugs were washed out from 24 to 24.5 h AF and zygotes were scored for division at 24 (before washout), 48 and 72 h AF. (B) Percentage division of recovering zygotes. Division was inhibited in zygotes treated with 1-butanol at 1 h AF, whereas zygotes treated with 1-butanol at 15 h AF recovered and divided following washout. (C–E) MT arrays in zygotes that did not divide following 1-butanol washout. 1-Butanol was added at 1 h AF and washed out from 24 to 24.5 h AF. (C) Progress of spindle formation. (D) A median projection (approximately 25 μm thick) showing a well-formed, but poorly aligned, metaphase spindle 3 h after drug washout. The spindle is double labeled for MTs and condensed chromatin, with arrows indicating chromosomes at the metaphase plate. (E) A projection of an entire zygote labeled for MTs 48 h after washout, showing a well-aligned telophase array. All experiments were performed in triplicate; standard error bars are shown. Scale bars in D and E equal 50 μm.

complete division after washout. In contrast, addition of 1-butanol at 15 h AF did not block recovery; following washout 90.6 ± 3.3% of zygotes continued development and divided normally by 72 h AF (Fig. 6B). Apparently, PLD signaling early in development is required for subsequent division.

To investigate the cellular mechanisms that prevent recovery when zygotes were treated early in development, MT arrays were examined during recovery. 1-Butanol was added at 1 h AF and washed out from 24 to 24.5 h AF. Surprisingly, MT arrays quickly recovered. Within 3 h following washout (27.5 h AF), nearly all zygotes possessed a well-formed spindle (Fig. 6C, D), indicating that development resumed synchronously. However, spindle alignment was aberrant. In untreated zygotes, metaphase spindles are moderately well aligned with the growth axis, and by telophase the alignment is nearly perfect (Bisgrove and Kropf 1998). The first cell division bisects the telophase array, and is therefore transverse to the growth axis (Bisgrove et al. 2003). Zygotes recovering from 1-butanol treatment had nearly random metaphase spindle alignments (Fig. 6D), averaging 59.8 ± 27.9° ($n = 234$) from parallel to the growth axis of the zygote. As recovering zygotes progressed through mitosis they were able to correct the misalignment, and by telophase the alignment angle was 5.3 ± 11.9° ($n = 90$) (Fig. 6E). Most zygotes arrested in telophase had MT arrays that appeared morphologically normal, but with fewer MTs than untreated controls (Fig. 6E). Arrested zygotes stained with FM4-64 did not to appear to possess any membranous material at the position of the presumptive division plane. The relatively few zygotes that divided possessed a well-aligned, transverse division plane (83.56 ± 15.4°, $n = 38$). In summary, the removal of 1-butanol permitted rapid recovery of PLD signaling, illustrated by the swift reformation of morphologically normal MT arrays. Therefore, the inability of zygotes treated at 1 h AF to divide after washout may not be directly caused by MT disruption.

1-Butanol affects endomembrane organization in young zygotes but not in germinated zygotes

Since MTs have recently been shown to organize endomembranes in young zygotes (Hadley et al. 2006), we further investigated the differential temporal effects of 1-butanol treatment by examining endomembrane organization in zygotes treated at 1 and 15 h AF. Prior to germination, the endomembrane system gradually reorganizes from a uniform to a polar array, with preferential membrane accumulation in the rhizoid hemisphere (Hadley et al. 2006). Following germination, the endomembrane system further consolidates into a cone radiating from the nucleus to the rhizoid tip (Belanger and Quatrano 2000). 2-Butanol-treated zygotes possessed a well-developed endomembrane cone at 16 and 24 h AF (Fig. 7A, B). However, the endomembrane organization of zygotes treated with MT-disrupting drugs was dependent on the developmental stage at the time of treatment. Endomembranes in zygotes treated with 1-butanol at 1 h AF were uniformly distributed throughout the zygote when assessed at 24 h AF (Fig. 7C). In contrast, treatment with 1-butanol at 15 h AF, after endomembrane polarity was established, appeared to have little or no effect on organization of the endomembrane system at 24 h AF (Fig. 7D). In order to exclude the possibility that the differential effects of 1-butanol treatment on endomembranes and development were due to the duration of drug incubation, zygotes were treated at 15 h AF and incubated for an additional 24 h. These zygotes displayed normal endomembranes and most successfully divided following washout (data not shown).

Treatment with the MT-stabilizing drug paclitaxel had effects on endomembrane organization similar to those of 1-butanol, preventing endomembrane localization to the rhizoid when added at 1 h AF, but having little effect when added at 15 h AF (Fig. 7E, F). Similar effects were also observed when MTs were depolymerized by treatment with oryzalin (Fig. 7G, H). Zygotes with disorganized endomembranes germinated, but their rhizoids were broader (Fig. 7C, E, G) than rhizoids of zygotes with polarized endomembranes (Fig. 7A, B, D, F, H). Previous results have shown that disrupting MT arrays in polarizing zygotes leads to delocalization of endomembranes within 30 min of treatment (Hadley et al. 2006). We were therefore surprised to find that MT perturbation after polarity had been fixed had little effect on endomembrane organization. This suggests that MTs are fundamental to organization of endomembranes in polarizing zygotes, but play a less significant role in endomembrane organization following germination. These data further suggest that the inability of zygotes treated early in development to divide following washout may be related to disorganization of the endomembrane system.

MTs are required for separation of centrosomes

In fucoid zygotes, centrosomes are inherited paternally and separate around the zygotic nucleus following karyogamy (Bisgrove et al. 1997). It has been difficult to examine the role of MTs in centrosomal separation because most agents that perturb MTs are poorly reversible. However, the rapid reversibility of 1-butanol treatment on MT arrays provides a unique opportunity to examine the role of MTs in centrosomal separation directly.

A typical zygote nucleates MTs from the entire surface of the nucleus until the paternally inherited centrioles become MTOCs (centrosomes) at about 4 h AF (Bisgrove and Kropf 1998). At this time, the two centrosomes appear

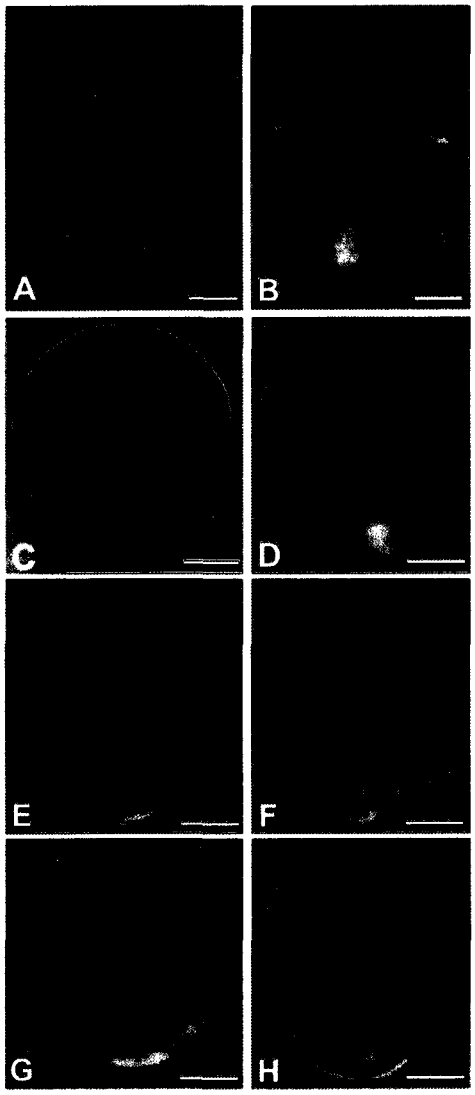

Fig. 7 Pharmacological agents that disrupt MTs affect endomembrane organization only in young zygotes. The vital stain FM4-64 was used to assess the morphology of the endomembrane system at 24 h AF in zygotes that were treated with drugs beginning at 1 or 15 h AF. Zygotes treated with 0.2% 2-butanol at 1 h AF and stained with FM4-64 at 16 h (A) or 24 h AF (B). The transverse band in B is endomembrane associated with cytokinesis. Treatment with 0.2% 1-butanol at 1 h AF (C) or 15 h AF (D) Treatment with 5 μM paclitaxel at 1 h (E) or 15 h (F) AF. Treatment with 3 μM oryzalin at 1 h (G) or 15 h (H) AF. See text for details.

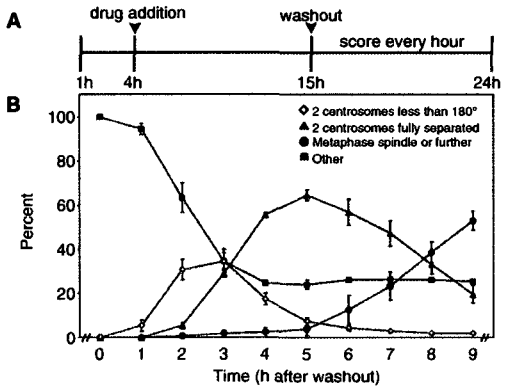

Fig. 8 Microtubules are required for centrosomal separation. (A) Experimental design; 0.2% 1-butanol was added to zygotes at 4 h AF. The drug was washed out at 15 h AF and cells were chemically fixed and antibody labeled for MTs every hour from 15 to 24 h AF. (B) Transitions in MT arrays following washout. Just after drug washout, as MTs began to reform, the centrosomes appeared as a single focus, or were not discernible as the MTs had yet to form distinct arrays. These arrays were classified as 'other'. MT arrays then rapidly transited from two centrosomes <180° apart to two centrosomes fully separated, to metaphase spindles. The experiment was done in triplicate, and bars represent standard errors.

as a single focus and MTs nucleated from the nuclear envelope gradually disappear. The centrosomes slowly separate around the nuclear envelope and by 15 h AF they reside on opposite sides, 180° apart (Bisgrove and Kropf 1998). To examine the role of MTs in centrosomal separation, 1-butanol was applied in a pulse from 4 to 15 h AF and centrosomal positioning was measured at the end of the treatment and during recovery (Fig. 8A). At the time of washout, 15 h AF, few if any zygotes displayed two distinct centrosomes, suggesting that centrosomes failed to separate when MTs were disrupted. The appearance of two distinct centrosomes began 1 h after drug washout and peaked at 3 h after washout (Fig. 8B). By 5 h after drug washout, two centrosomes, fully separated to 180°, were present in most zygotes. Beyond 5 h, bipolar spindles appeared as zygotes entered metaphase of mitosis. Thus, centrosome separation can occur very rapidly and is clearly dependent upon functional MTs. It is likely that centrosome separation also requires motor proteins which slide interdigitating MTs apart (Peters and Kropf 2006).

Discussion

PLD signals to MTs

Chemical fixation and immunolabeling of *S. compressa* zygotes revealed that 1-butanol treatment severely disrupted

MT arrays, resulting in rapid MT fragmentation followed by formation of heavily bundled cortical MTs. The developmental effects of 1-butanol were consistent with abnormal MT arrays; treatment prevented endomembrane polarization, induced broadening of the rhizoid tip, led to metaphase arrest and blocked cytokinesis. Each of these is known to result from MT disruption (Bisgrove and Kropf 2004, Hadley et al. 2006, Peters and Kropf, 2006), and our current results demonstrate that centrosomal separation around the nuclear envelope is also MT dependent. Taken together, these findings indicate that the PLD pathway signals to the MT cytoskeleton and thereby regulates MT-dependent developmental processes. In contrast, PLD is unlikely to signal directly to actin or to endomembranes. Disruption of actin arrays or vesicle trafficking blocks photopolarization and rhizoid outgrowth (Hable and Kropf 1998, Hable et al. 2003), but 1-butanol-treated zygotes photopolarized and germinated properly. Since the inhibition of endomembrane polarization by 1-butanol was mimicked by other MT inhibitors, it is likely that endomembrane polarization requires functional MTs, but is not regulated through PLD signaling directly.

In animals, PLD has been shown to work in concert with phosphoinositide 5-kinase (PIP5K) and is regulated by protein kinase C (PKC), small GTPases of the ARF, Rho and Ras families, and by phosphatidylinositol-4,5-bisphosphate (PIP_2) (Powner and Wakelam 2002, Oude Weernink et al. 2007a, Oude Weernink et al. 2007b). Disrupting PLD signaling affects many receptor-mediated cellular processes including actin organization, endocytosis, exocytosis, vesicle trafficking, calcium mobilization, glucose transport, superoxide production, mitogenesis and cell survival (reviewed in Oude Weernink et al. 2007a, Oude Weernink et al. 2007b). However, evidence for PLD signaling to MTs in animals is lacking.

Research on PLD signaling in higher plants has been complicated by the fact that plants have 12 PLD genes, many of which possess overlapping functions (Munnik and Musgrave 2001). Since production of mutants with distinct phenotypes has been slow, utilizing chemical disrupters of PLD signaling, such as 1-butanol, has commonly been employed. These studies indicate that higher plants, like animals, utilize PLD signaling for complex regulation of actin arrays (Kusner et al. 2003, Motes et al. 2005) and endomembrane organization (Monteiro et al. 2005). In addition, PLD appears to signal MTs in plant cells (Dhonukshe et al. 2003, Motes et al. 2005, Hirase et al. 2006).

Interphase plant cells possess an extensive cortical MT array that girdles the cell with MTs oriented transverse or helical to the cellular growth axis (Wasteneys 2002, Paradez et al. 2006, Murata and Hasebe 2007). During division, MTs form a cortical pre-prophase band that accurately predicts the division plane, and following mitosis a MT-based phragmoplast guides deposition of a partition membrane. Several studies have described the effects of 1-butanol treatment on these plant MT arrays (Dhonukshe et al. 2003, Gardiner et al. 2003, Motes et al. 2005, Hirase et al. 2006, Komis et al. 2006). Treatment with 1-butanol led to disruption of interphase, pre-prophase and phragmoplast MTs, while not affecting spindle MTs in tobacco BY-2 cells (Dhonukshe et al. 2003). Interphase cortical MT arrays of BY-2 cells became dissociated from the cell cortex following 1-butanol treatment, and partially depolymerized (Dhonukshe et al. 2003, Hirase et al. 2006). MT arrays in Arabidopsis roots, hypocotyls and cotyledons also became disorganized following 1-butanol treatment, but they did not appear to depolymerize (Gardiner et al. 2003, Motes et al. 2005). As expected, 1-butanol treatment perturbed several MT-based processes in plant growth and development, including cell expansion, root elongation, root hair formation and cell viability (Gardiner et al. 2003, Motes et al. 2005).

Two models have been proposed to explain the effects of 1-butanol on MTs in higher plants. The first model focuses on PA levels downstream of PLD. 1-Butanol is preferred over water as a transphosphatidylation substrate for PLD (Munnik et al. 1995), resulting in formation of more P-butanol than PA (Munnik et al. 1995). It has been suggested that the effects on plant development and MT arrays is due to a reduction in PA levels (Gardiner et al. 2003). This is an attractive hypothesis since PA is a second messenger and has been shown to regulate seed germination, stomatal movements, senescence and responses to osmotic stress, wounding and pathogens (Meijer and Munnik 2003, de Jong et al. 2004, Vergnolle et al. 2005). Further support is provided by the observation that the developmental defects caused by 1-butanol treatment can, in some cases, be reversed with addition of exogenous PA (Potocký et al. 2003, Komis et al. 2006). However, this model is based on the assumption that 1-butanol treatment lowers PA levels, which has not yet been demonstrated.

The second model proposed to explain the effects of 1-butanol on plant cells postulates that the effects on cortical MT arrays are due directly to activation of PLD (Dhonukshe et al. 2003). A 90 kDa microtubule-associated protein (MAP) was recently identified as a PLD in Arabidopsis and was shown to decorate MTs at every stage of the cell cycle (Gardiner et al. 2001). Interestingly, it was also found to be closely associated with the plasma membrane in the absence of MTs (Gardiner et al. 2001). Based on these observations, it has been suggested that the reaction intermediate, in which PLD is covalently bonded to the substrate phospholipid, also binds MTs. In this way PLD would link MTs to the plasma membrane, providing stability to cortical MT arrays and a means for rapid

signaling to MTs (Dhonukshe et al. 2003). PLD activation is postulated to release the MT–plasma membrane link, forming PA. While the observation that activating PLD by 1-butanol disrupts cortical MT arrays supports the PLD activation hypothesis, direct evidence has yet to show that PLD links MTs to the plasma membrane. On the contrary, Hirase et al. (2006) observed that MTs in membrane ghosts of BY-2 cells were still closely associated with the membrane after 1-butanol treatment.

How might 1-butanol induce the dramatic effects observed in *S. compressa* zygotes? Unlike higher plants, *S. compressa* zygotes have centrosomally nucleated MT arrays. However, the two arrays are similar in that MTs interact laterally with the plasma membrane. Using CLSM, we have observed MTs that extend from centrosomes to the cell cortex and then turn and run along the inner membrane surface (Bisgrove and Kropf 2001a). Recently, cortical MTs were described in living zygotes of the closely related fucoid alga, *Fucus serratus*, and these MTs were thought to be nucleated cortically (Corellou et al. 2005). At present we can only speculate on the mechanism by which 1-butanol induces loss of endoplasmic MTs and formation of cortical bundles. Initially 1-butanol induces a rapid fragmentation of MTs throughout the cytoplasm, from cortex to nucleus. This fragmentation may be due to a diffusible signal that globally activates MT severing. This signal is unlikely to be PA itself since PA remains membrane bound. MT fragments have uncapped ends and are therefore unstable, and probably depolymerize. However, fragments in the cell cortex may be stabilized by interactions with plasma membrane proteins that normally anchor cortical MTs. These fragments could then polymerize and become bundled by as yet unknown MAPs. In addition, it is plausible that new MTs are nucleated cortically.

Effects of 1- and 2-butanol on MTs may be due to PLD activation

1-Butanol activates PLD and is a preferred transphosphatidylation substrate (Munnik et al. 1995). Addition of 2-butanol has been shown to activate PLD, while not being a transphosphatidylation substrate (Munnik et al. 1995), and is therefore used as a PLD activation control (Gardiner et al. 2003). We found that the MT-based effects of 2-butanol at a concentration of 0.6% appeared to mimic the effects of 1-butanol at 0.2%. Neither of these concentrations was toxic to zygotes. Also, *t*-butanol, which does not activate PLD and is not a transphosphatidylation substrate, did not disrupt MT arrays even at a concentration of 2.0%. Since both 1- and 2-butanol activate PLD but have unknown effects on PA levels, their primary effects on MTs may be due to PLD activation. The higher concentration of 2-butanol needed to disrupt MTs may indicate that it is a less potent activator than 1-butanol. To address these issues, we plan to examine the effects of other activators of PLD, such as mastoparan (Munnik et al. 1998), on MT arrays and to use thin-layer chromatography to examine the levels of PA and P-butanol following 1- and 2-butanol and mastoparan treatments.

Conclusions

We have found that the PLD pathway directly signals to MTs, and indirectly affects organization of endomembrane arrays in polarizing zygotes. Inhibitor studies suggest that the PLD pathway does not play a major role in signaling to actin-dependent processes. However, subtle effects of butanol treatment on actin organization and function have not yet been examined. This is the first report of a signaling pathway responsible for cytoskeletal organization in stramenopiles.

Materials and Methods

Sexually mature receptacles of the fucoid algae *S. compressa* were collected near Santa Cruz, California and cultured as in Peters and Kropf (2006). Zygotes were grown in ASW with unidirectional light until harvest, unless otherwise noted.

Pharmacological agents were dissolved in dimethylsulfoxide (DMSO) to make stock solutions, and applied to zygotes in ASW as follows: latrunculin B (Calbiochem, La Jolla, CA, USA), 50 μM stock, 30 nM final; paclitaxel (Sigma-Aldrich, St Louis, MO, USA), 10 mM stock, 5 μM final; oryzalin (Sigma-Aldrich), 10 mM stock, 3 μM final. Butyl alcohols (Sigma-Aldrich) were applied directly. Appropriate controls were carried out using DMSO or non-primary butyl alcohols.

Photopolarization was analyzed as follows. Zygotes were initially photopolarized by exposure to unidirectional light (L1) until 5 h AF; butanols were then applied and the zygotes were placed in the dark for 1 h. Beginning 6 h AF, zygotes were exposed to L2, which was oriented 180° from L1, for 4 h. Drugs were washed out at 10 h AF and zygotes were placed in the dark. At 24 h AF, photopolarization to L2 was assayed. The percentage photopolarization was ascertained by scoring the number of zygotes germinated on the hemisphere shaded during L2 minus the number of zygotes germinated on the hemisphere shaded during L1, divided by the total number of zygotes scored, and then multiplied by 100 [(#L2 − #L1/total) × 100]. Therefore, a photopolarization of 100% indicates that all zygotes polarized to L2, 0% indicates that the population polarized randomly, and negative 100% indicates that every zygote polarized to L1.

To image endomembranes, zygotes treated with the vital membrane stain FM4-64 (Molecular Probes Inc., Eugene OR, USA; 20 mM stock in DMSO, 5 μM final) for 30 min were subsequently imaged using conventional epifluorescence microscopy with a 577.5–632.5 nm bandpass emission filter (Chroma Technologies, Brattleboro, VT, USA). Images were captured with a coolSNAP digital camera (Roper Scientific Photometrics, Tucson, AZ, USA) on an Olympus IMT2 microscope.

Zygotes prepared for immunofluorescence microscopy of MTs and condensed chromatin were fixed in PHEM [60 mM piperazine-*N*, *N*′-bis(2-ethanesulfonic acid), 25 mM HEPES,

10 mM EGTA, 2 mM $MgCl_2$] containing 3% paraformaldehyde and 0.5% glutaraldehyde. Zygotes were processed as previously described (Peters and Kropf, 2006). MTs were labeled with a monoclonal anti-α-tubulin antibody (DM1A: Sigma) and Alexa 488 goat anti-mouse secondary antibody (Invitrogen, Eugene, OR, USA). Condensed chromosomes were labeled with a polyclonal anti-histone H3 (pSer10) antibody (Calbiochem, San Diego, CA, USA), followed by Alexa 546 goat anti-rabbit secondary antibody. For double labeling, primary antibodies were added simultaneously, as were secondary antibodies. Images were collected on an LSM510 (Carl Zeiss Inc., Thornwood, NY, USA) confocal laser scanning microscope using a narrow bandpass filter for MTs ($\lambda = 500$–530 nm) and a Meta adjustable bandpass filter ($\lambda = 558$–601 nm) for condensed chromatin.

Acknowledgments

We would like to thank Coby Price for his preliminary work testing the effects of butyl alcohol treatments, and Teun Munnik for his helpful discussions about phospholipid signaling. This work was supported by NSF award IOB-0414089 and a University of Utah Undergraduate Research Opportunity Program award to A.C.M.

References

Alessa, L. and Kropf, D.L. (1999) F-actin marks the rhizoid pole in living *Pelvetia compressa* zygotes. *Development* 126: 201–209.

Belanger, K.D. and Quatrano, R.S. (2000) Membrane recycling occurs during asymmetric cell growth and cell plate formation in *Fucus distichus* zygotes. *Protoplasma* 212: 24–37.

Bisgrove, S.R., Henderson, D.C. and Kropf, D.L. (2003) Asymmetric division in fucoid zygotes is positioned by telophase nuclei. *Plant Cell* 15: 854–862.

Bisgrove, S.R. and Kropf, D.L. (1998) Alignment of centrosomal and growth axes is a late event during polarization of *Pelvetia compressa* zygotes. *Dev. Biol.* 194: 246–256.

Bisgrove, S.R. and Kropf, D.L. (2001a) Asymmetric cell division in fucoid algae: a role for cortical adhesions in alignment of the mitotic apparatus. *J. Cell Sci.* 114: 4319–4328.

Bisgrove, S.R. and Kropf, D.L. (2001b) Cell wall deposition during morphogenesis in fucoid algae. *Planta* 212: 648–658.

Bisgrove, S.R. and Kropf, D.L. (2004) Cytokinesis in brown algae: studies of asymmetric division in fucoid zygotes. *Protoplasma* 223: 163–173.

Bisgrove, S.R. and Kropf, D.L. (2007) Asymmetric cell divisions: zygotes of fucoid algae as a model system. *In* Cell Division Control in Plants. Edited by Verma, D.P.S. and Hong, Z. in press. Springer-Verlag, Heidelberg.

Bisgrove, S.R., Nagasato, C., Motomura, T. and Kropf, D.L. (1997) Immunolocalization of centrin during fertilization and the first cell cycle in *Fucus distichus* and *Pelvetia compressa* (Fucales, Phaeophyceae). *J. Phycol.* 33: 823–829.

Bower, F.O. (1880) On the development of the conceptacle in the Fucaceae. *Q. J. Microsc. Sci.*36–49.

Brownlee, C., Bouget, F.-Y. and Corellou, F. (2001) Choosing sides: establishment of polarity in zygotes of fucoid algae. *Cell Dev. Biol.* 12: 345–351.

Corellou, F., Coelho, S.M.B., Bouget, F.-Y. and Brownlee, C. (2005) Spatial re-organization of cortical microtubules in vivo during polarization and asymmetric division of Fucus zygotes. *J. Cell Sci.* 118: 2723–2734.

de Jong, C.F., Laxalt, A., Bargmann, B.O.R., de Wit, P.J.G.M., Joostein, M.H.A.J. and Munnik, T. (2004) Phosphatidic acid accumulation is an early response in the Cf-4/Avr4 interaction. *Plant J.* 39: 1–12.

Dhonukshe, P., Laxalt, A.M., Goedhart, J., Gadella, T.W.J. and Munnik, T. (2003) Phospholipase D activation correlates with microtubule reorganization in living plant cells. *Plant Cell* 15: 2666–2679.

Gardiner, J., Collings, D.A., Harper, J.D.I. and Marc, J. (2003) The effects of the phospholipase D-antagonist 1-butanol on seedling development and microtubule organization in Arabidopsis. *Plant Cell Physiol.* 44: 687–696.

Gardiner, J., Harper, J.D., Weerakoon, N., Collings, D.A., Ritchie, S., Gilroy, S., Cyr, R.J. and Marc, J. (2001) A 90-kD phospholipase D from tobacco binds to microtubules and the plasma membrane. *Plant Cell* 13: 2143–2158.

Hable, W.E. and Kropf, D.L. (1998) Roles of secretion and the cytoskeleton in cell adhesion and polarity establishment in *Pelvetia compressa* zygotes. *Dev. Biol.* 198: 45–56.

Hable, W.E. and Kropf, D.L. (2000) Sperm entry induces polarity in fucoid zygotes. *Development* 127: 493–501.

Hable, W.E. and Kropf, D.L. (2005) The Arp2/3 complex nucleates actin arrays during zygote polarity establishment and growth. *Cell Motil. Cytoskel.* 61: 9–20.

Hable, W.E., Miller, N.R. and Kropf, D.L. (2003) Polarity establishment requires dynamic actin in fucoid zygotes. *Protoplasma* 221: 193–204.

Hadley, R., Hable, W.E. and Kropf, D.L. (2006) Polarization of the endomembrane system is an early event in fucoid zygote development. *BMC Plant Biol.* 6: 1–10.

Hirase, A., Hamada, T., Itoh, T.J., Shimmen, T. and Sonobe, S. (2006) *n*-Butanol induces depolymerization of microtubules in vivo and in vitro. *Plant Cell Physiol.* 47: 1004–1009.

Huang, S., Gao, L., Blanchoin, L. and Staiger, C.J. (2006) Heterodimeric capping protein from Arabidopsis is regulated by phosphatidic acid. *Mol. Biol. Cell* 17: 1946–1958.

Jenkins, G. and Frohman, M. (2005) Phospholipase D: a lipid centric review. *Cell. Mol. Life Sci.* 62: 2305–2316.

Komis, G., Quader, H., Galatis, B. and Apostalakos, P. (2006) Macrotubule-dependent protoplast volume regulation in plasmolysed root-tip cells of *Triticum turgidum*: involvement of phospholipase D. *New Phytol.* 171: 737–750.

Kropf, D.L., Bisgrove, S.R. and Hable, W.E. (1999) Establishing a growth axis in fucoid algae. *Trends Plant Sci.* 4: 490–494.

Kusner, D.J., Barton, J.A., Qin, C., Wang, X. and Iyer, S.S. (2003) Evolutionary conservation of physical and functional interactions between phospholipase D and actin. *Arch. Biochem. Biophys.* 412: 231–241.

Malho, R., Liu, Q., Monteiro, D., Rato, C., Camacho, L. and Dinis, A. (2006) Signaling pathways in pollen germination and tube growth. *Protoplasma* 228: 21–30.

Meijer, H. and Munnik, T. (2003) Phospholipid-based signaling in plants. *Annu. Rev. Plant Biol.* 54: 265–306.

Monteiro, D., Liu, Q., Lisboa, S., Scherer, G.E.F., Quader, H. and Malho, R. (2005) Phosphoinositides and phosphatidic acid regulate pollen tube growth and reorientation through modulation of $[Ca^{2+}]_c$ and membrane secretion. *J. Exp. Bot.* 56: 1665–1674.

Motes, C.M., Pechter, P., Yoo, C.M., Wang, Y.-S., Chapman, K.D. and Blancaflor, E.B. (2005) Differential effects of two phospholipase D inhibitors, 1-butanol and N-acylethanolamine, on in vivo cytoskeletal organization and Arabidopsis seedling growth. *Protoplasma* 226: 109–123.

Munnik, T., Arisz, S.A., de Vrije, T. and Musgrave, A. (1995) G protein activation stimulates phospholipase D signaling in plants. *Plant Cell* 7: 2197–2210.

Munnik, T. and Musgrave, A. (2001) Phospholipid signaling in plants: holding on to phospholipase D. *Sci. STKE* 2001: pe42.

Munnik, T., van Himbergen, J.A.J., ter Riet, B., Braun, F.-J., Irvine, R.F., van den Ende, H. and Musgrave, A. (1998) Detailed analysis of the turnover of polyphosphoinositides and phosphatidic acid upon activation of phospholipases C and D in *Chlamydomonas* cells treated with non-permeabilizing concentrations of mastoparan. *Planta* 207: 133–145.

Murata, T. and Hasebe, M. (2007) Microtubule-dependent microtubule nucleation in plant cells. *J. Plant Res.* 120: 73–78.

Oude Weernink, P.A., Han, L., Jakobs, K.H. and Schmidt, M. (2007b) Dynamic phospholipid signaling by G protein-coupled receptors. *Biochim. Biophys Acta* 1768: 888–900.

Oude Weernink, P., López de Jesús, M. and Schmidt, M. (2007a) Phospholipase D signaling: orchestration by PIP2 and small GTPases. *Naunyn-Schmiedeberg's Arch. Pharmacol.* 374: 399–411.

Paradez, A., Wright, A. and Ehrhardt, D.W. (2006) Microtubule cortical array organization and plant cell morphogenesis. *Curr. Opin. Plant Biol.* 9: 571–578.

Peters, N.T. and Kropf, D.L. (2006) Kinesin-5 motors are required for organization of spindle microtubules in *Silvetia compressa* zygotes. *BMC Plant Biol.* 6: 19.

Potocký, M., Eliáš, M., Profotová, B., Novotná, Z., Valentová, O. and Žárský, V. (2003) Phosphatidic acid produced by phospholipase D is required for tobacco pollen tube growth. *Planta* 217: 122–130.

Powner, D.J. and Wakelam, M.J.O. (2002) The regulation of phospholipase D by inositol phospholipids and small GTPases. *FEBS Lett.* 531: 62–64.

Quatrano, R.S. (1973) Separation of processes associated with differentiation of two-celled *Fucus* embryos. *Dev. Biol.* 30: 209–213.

Quatrano, R.S. (1997) Cortical asymmetries direct the establishment of cell polarity and the plane of cell division in the *Fucus* embryo. *Cold Spring Harbor Symp. Quant. Biol.* 62: 65–70.

Vergnolle, C., Vaultier, M.-N., Taconnat, L., Renou, J.-P., Kader, J.-C., Zachowski, A. and Ruelland, E. (2005) The cold-induced early activation of phospholipase C and D pathways determines the response of two distinct clusters of genes in Arabidopsis cell suspensions. *Plant Physiol.* 139: 1217–1233.

Wang, X. (2004) Lipid signaling. *Curr. Opin. Plant Biol.* 7: 329–336.

Wasteneys, G.O. (2002) Microtubule organization in the green kingdom: chaos or self-order? *J. Cell Sci.* 115: 1345–1354.

(Received August 22, 2007; Accepted October 23, 2007)

CHAPTER 4

PHOSPHOLIPID SIGNALING DURING STRAMENOPILE DEVELOPMENT

[Plant Signaling & Behavior 3:6, 398-400; June 2008]; ©2008 Landes Bioscience

Article Addendum

Phospholipid signaling during stramenopile development

Nick T. Peters,* Suyog U. Pol and Darryl L. Kropf

University of Utah; Department of Biology; Salt Lake City, Utah USA

Abbreviations: DAG, diacylglycerol; DAGK, diacylglycerol kinase; DGPP, diacylglycerol pyrophosphate; IP_3, inositol 1,4,5-triphosphate; PA, phosphatidic acid; PC, phosphatidyl choline; PE, phosphatidylethanolamine; PIP_2, phosphatidylinositol 4,5-bisphosphate; PLC, phospholipase C; PLD, phospholipase D; MT, microtubule

Key words: actin, brown algae, cytoskeleton, development, endomembrane, microtubule, phosphatidic acid, phospholipase C, phospholipase D, stramenopile

Development of sessile organisms requires adaptation to an ever-changing environment. In order to respond quickly to these challenges, complex signaling mechanisms have evolved to facilitate cellular modifications. The importance of phospholipid-based signaling pathways in plants, as well as animals, has recently been gaining attention. Both the PLD and PLC pathways produce the signaling molecule PA, which modulates MTs, F-actin and endomembrane trafficking. We have examined the roles of the PLD signaling pathway during development of the marine brown alga *Silvetia compressa*. Zygotes were treated with 1- and 2-butanol, both of which activate the PLD enzyme. However, only 1-butanol competes with water as a transphosphatidylation substrate, at the expense of PA production. Interestingly, we found that 1- and 2-butanol both disrupted MT organization and thereby cell division, with 1-butanol being more potent. These findings question whether the effects of butyl alcohol treatment are due to lowered PA levels or activation of the PLD enzyme. Additionally, preliminary results show that inhibition of DAGK results in loss of centrosomal MTs and formation of cortical MT cages that are strikingly similar to those formed following 1-butanol treatment. These data suggest that perturbation of the PLD or PLC pathway leads to cortical stabilization and/or nucleation of MT arrays.

Phosphatidic Acid Production

Phosphatidic acid (PA) is a membrane-localized signaling molecule that can be produced through two distinct pathways (Fig. 1A). The phospholipase D (PLD) pathway produces PA by hydrolyzing structural phospholipids, primarily phosphatidyl choline (PC) and phosphtidylethanolamine (PE).[1] The phospholipase C (PLC) pathway cleaves phosphatidylinositol 4,5-bisphosphate (PIP_2) to inositol 1,4,5-triphosphate (IP_3) and DAG, which is phosphorylated by diacylgylcerol kinase (DAGK), yielding PA.[2] Dephosphorylation of diacylglycerol pyrophosphate (DGPP, not shown) also produces PA.[2]

*Correspondence to: Nick T. Peters; University of Utah; Department of Biology; 257 S. 1400 E.; Salt Lake City, Utah 84112 USA; Tel.: 801.581.5423; Email: npeters@biology.utah.edu

Submitted: 12/07/07; Accepted: 12/13/07

Previously published online as a *Plant Signaling & Behavior* E-publication: http://www.landesbioscience.com/journals/psb/article/5419

Addendum to: Peters NT, Logan KO, Miller AC, Kropf DL. Phospholipase D signaling regulates microtubule organization in the fucoid alga Silvetia compressa. Plant Cell Physiol 2007:48:1764-74; PMID: 17967797; DOI: 10.1093/pcp/pcm149.

Phospholipase D Signaling

PLD signaling in animals regulates vesicle trafficking and organization of actin arrays.[1] In Arabidopsis, which has 12 PLD genes, it has proven difficult to isolate mutants with aberrant phenotypes.[3] Instead, chemical disrupters such as 1-butanol have provided valuable information about PLD signaling functions.[4] A myriad of cellular and developmental processes such as germination,[5] cell elongation,[5] senescence[6] and many stress responses are regulated by PLD signaling in plants.[7-9] At the subcellular level, treatment of plant cells with 1-butanol leads to defects in actin arrays and endomembrane organization as in animals,[10-12] and also disorganizes cortical MT arrays.[13,14]

We recently examined the roles of PLD signaling during early development of the brown alga *S. compressa*.[15] A fertilized egg normally orients its growth axis in accordance with directional light (photopolarization) and germinates and grows from the rhizoid pole of that axis.[16] The first division is asymmetric and is oriented transverse to the growth axis.[17] We found that butanol treatments did not block photopolarization or germination, but cell division was inhibited.[15] This suggested that MTs, rather than actin or endomembranes, were the primary targets of drug treatment. This was a somewhat surprising finding since actin is often disrupted by 1-butanol application in plants and animals.[1,10,11] MT arrays in treated zygotes were examined by confocal microscopy. In untreated zygotes, the MT array is nucleated from perinuclear centrosomes and extends to the cell cortex. Following treatment, MTs initially appeared fragmented and, within two hours, became heavily bundled and resided exclusively in the cortex.[15] Treated algal zygotes ultimately arrested in mitosis, unable to form a bipolar metaphase spindle. MT arrays and development recovered quickly following 1-butanol removal, providing an easy method for synchronizing populations. Of particular interest, we found that application of higher levels of 2-butanol mimicked the effects of 1-butanol. This observation has

not been described in other systems. While 1-butanol is known to activate PLD and compete with water as the transphosphatidylation substrate, 2-butanol only activates PLD.[4] These findings therefore question whether 1-butanol acts exclusively by lowering PA levels.

Two models have been proposed to explain the observed effects of 1-butanol treatment. The first model suggests that 1-butanol treatment leads to dramatically lowered PA levels, thereby disrupting signaling and resulting in cellular and developmental defects.[5] This model is supported by studies showing that exogenous addition of PA rescues the effects of 1-butanol treatment.[18,19] However, to date there is no direct evidence showing a decrease in PA levels following 1-butanol application. The second model is based on work in higher plants showing PLD decoration of cortical interphase MTs and also showing PLD in close association with the plasma membrane.[20] In this model, activation of PLD by 1-butanol facilitates release of MTs from membrane-bound PLD, thereby disrupting MT organization and subsequently causing developmental defects.[13] To discriminate these models, we are currently performing radiolabeling experiments to determine whether treatments with 1- or 2-butanol reduces the level of PA derived from the PLD pathway, and immunolabeling experiments to examine the spatial relationship between MTs and PLD.

Phospholipase C Signaling

The PLC pathway produces IP_3, which regulates Ca^{2+} release from intracellular stores,[2] and DAG, which can be phosphorylated by DAGK to yield PA.[2] Mammalian DAGK has been shown though gene knockouts and chemical inhibition to function in regulation of Rac1 activity during membrane ruffling, neural and immune responses, cell proliferation and carcinogenesis.[21] In higher plants, DAGK function is not well understood. However, treatment with R59022, a chemical inhibitor of DAGK, inhibits root elongation and lateral root formation in Arabidopsis.[22]

We have very recently begun to examine the effects of R59022 on zygotic development in *S. compressa* and preliminary findings indicate that germination, division and MT arrays are severely disrupted by drug treatment. Following R59022 treatment, MTs form a cortical cage and no MTs are found near centrosomes (Fig. 1B). Interestingly, 1-butanol also eliminates centrosomal MTs and induces formation of a bundled cortical array,[15] but the significance of these localizations is presently unclear. PA derived from the PLC-pathway likely signals to more than MTs, since R59022 blocks germination, which does not require MTs. We are now examining the organization of filamentous actin arrays and the endomembrane system in R59022-treated zygotes, as well as determining PA levels derived from the PLC pathway. These studies will be reported in detail elsewhere.

Perspectives

We find that, as in plants and animals, the PLD and PLC pathways play fundamental roles in brown algal development. However, the formation of cortical MTs following perturbation of the pathways appears to be a unique observation. Why would disruption of PLD signaling or inhibition of DAGK lead to loss of centrosomal MT arrays and formation of a bundled cortical array? While centrosomally-nucleated MT arrays in brown algae have been shown to extend to the cortex and extend along it, the presence of cortical MTs arrays has only recently been reported. In *F. serratus*, a closely related brown alga, injection of fluorescent tubulin visualized centrosomal MT arrays as well as arrays residing solely in the cortex.[23] Together, these data suggest that (1) MT arrays can be stabilized by interactions with the plasma membrane, and (2) the plasma membrane may be capable of MT nucleation. Interestingly, cortical MT nucleation and MT stabilization by interaction with the plasma membrane are both characteristic of higher plant interphase MTs.[24] Further examination and understanding of phospholipid signaling in brown algae will provide valuable insights into how PLD and PLC pathways regulate development, and will illuminate how these pathways have evolved in different lineages.

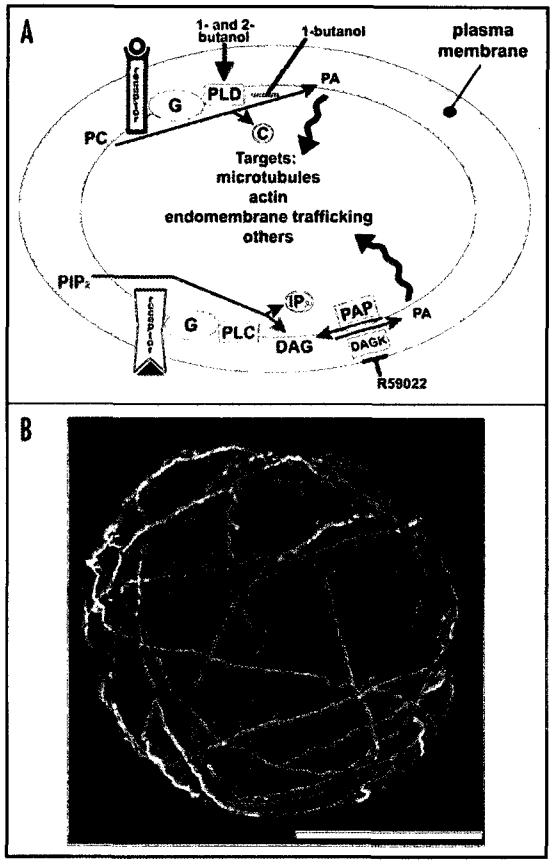

Figure 1. (A) The Phospholipase D (upper) and C (lower) pathways. Extracellular signaling activates G-protein coupled receptors; heterotrimeric G-proteins then activate PLD and PLC. PLD and PLC synthesize PA as described in the text. Both 1-butanol and 2-butanol disrupt the PLD pathway by mimicking receptor binding, while conversion of DAG to PA can be blocked by R59022, which inhibits DAGK activity. (B) Projection of confocal sections from the nucleus to the cortex of a zygote treated with 20 μM R59022 at 1 h AF, fixed and immunolabeled for MTs at 24 h AF. Scale bar equals 50 μm.

References

1. Oude Weernink P, López de Jesús M, Schmidt M. Phospholipase D signaling: orchestration by PIP2 and small GTPases. Naunyn-Schmiedeberg's Arch Pharmacol 2007; 374:399-411.
2. Wang X. Lipid signaling. Cur Opin Plant Biol 2004; 7:329-36.
3. Munnik T, Musgrave, A. Phospholipid signaling in plants: holding on to phospholipase D. Sci STKE 2001;PE42.
4. Munnik T, Arisz SA, de Vrije T, Musgrave A. G protein activation stimulates phospholipase D signaling in plants. Plant Cell 1995; 7:2197-210.
5. Gardiner J, Collings DA, Harper JDI, Marc J. The effects of the phospholipase D-antagonist 1-butanol on seedling development and microtubule organization in Arabidopsis. Plant Cell Physiol 2003; 44:687-96.
6. Meijer H, Munnik T. Phospholipid-based signaling in plants. Annu Rev Plant Biol 2003; 54:265-306.
7. de Jong CF, Laxalt A, Bargmann BOR, de Wit PJGM, Joosten MHAJ, Munnik T. Phosphatidic acid accumulation is an early response in the Cf-4/Avr4 interaction. The Plant J 2004; 39:1-12.
8. Vergnolle C, Vaultier MN, Taconnat L, Renou JP, Kader JC, Zachowski A, Ruelland E. The cold-induced early activation of phospholipase C and D pathways determines the response of two distinct clusters of genes in Arabidopsis cell suspensions. Plant Physiol 2005; 139:1217-33.
9. den Hartog M, Verhoef N, Munnik T. Nod factor and elicitors activate different phospholipid signaling pathways in suspension-cultured alfalfa cells. Plant Physiol 2003; 132:311-7.
10. Motes CM, Pechter P, Yoo CM, Wang YS, Chapman KD, Blancaflor EB. Differential effects of two phospholipase D inhibitors, 1-butanol and N-acylethanolamine, on in vivo cytoskeletal organization and Arabidopsis seedling growth. Protoplasma 2005; 226:109-23.
11. Huang S, Gao L, Blanchoin L, Staiger CJ. Heterodimeric capping protein from Arabidopsis is regulated by phosphatidic acid. Mol Biol Cell 2006; 17:1946-58.
12. Montiero D, Liu Q, Lisboa S, Scherer G, Quader H, Malho R. Phosphoinositides and phosphatidic acid regulate pollen tube growth and reorientation through modulation of $[Ca^{2+}]_c$, membrane secretion and the actin cytoskeleton. J Exp Bot 2005; 56:1665-74.
13. Dhonukshe P, Laxalt AM, Goedhart J, Gadella TWJ, Munnik T. Phospholipase D activation correlates with microtubule reorganization in living plant cells. Plant Cell 2003; 15:2666-79.
14. Hirase A, Hamada T, Itoh TJ, Shimmen T, Sonobe S. n-Butanol induces depolymerization of microtubules in vivo and in vitro. Plant Cell Physiol 2006; 47:1004-9.
15. Peters NT, Logan KO, Miller AC, Kropf DL. Phospholipase D signaling regulates microtubule organization in the fucoid alga Silvetia compressa. Plant Cell Physiol 2007; 48:1764-74.
16. Kropf DL, Bisgrove SR, Hable WE. Establishing a growth axis in fucoid algae. Trends Plant Sci 1999; 4:490-4.
17. Bisgrove SR, Kropf DL. Asymmetric cell divisions: Zygotes of fucoid algae as a model system. In: Verma DPS, Hong Z, editors. Cell Division Control in Plants. Volume in press, Plant Cell Monographs. Heidelberg: Springer-Verlag; 2007.
18. Komis G, Quader H, Galatis B, Apostolakos P. Macrotubule-dependent protoplast volume regulation in plasmolysed root-tip cells of *Triticum turgidum*: involvement of phospholipase D. New Phytol 2006; 171:737-50.
19. Potocký M, Eliáš M, Profotová B, Novotná Z, Valentová O, Žárský V. Phosphatidic acid produced by phospholipase D is required for tobacco pollen tube growth. Planta 2003; 217:122-30.
20. Gardiner J, Harper JD, Weerakoon N, Collings DA, Ritchie S, Gilroy S, Cyr RJ, Marc J. A 90-kD phospholipase D from tobacco binds to microtubules and the plasma membrane. Plant Cell 2001; 13:2143-58.
21. Sakane F, Imai SI, Kai M, Yasuda S, Kanoh H. Diacylglycerol kinases: Why so many of them? Biochim Biophys Acta-Mol Cell Biol Lipids 2007; 1771:793-806.
22. Gomez Merino FC, Arana Ceballos FA, Trejo Tellez LI, Skirycz A, Brearley CA, Dormann P, Mueller Roeber B. Arabidopsis AtDGK7, the smallest member of plant diacylglycerol kinases (DGKs), displays unique biochemical features and saturates at low substrate concentration. J Biol Chem 2005; 280:34888-99.
23. Corellou F, Coelho SMB, Bouget FY, Brownlee C. Spatial re-organization of cortical microtubules in vivo during polarisation and asymmetric division of *Fucus* zygotes. J Cell Sci 2005; 118:2723-34.
24. Murata T, Sonobe S, Baskin TI, Hyodo S, Hasezawa S, Nagata T, Horio T, Hasebe M. Microtubule-dependent microtubule nucleation based on recruitment of gamma-tubulin in higher plants. Nat Cell Biol 2005; 7:961-8.

CHAPTER 5

KINESIN-5 MOTORS ARE REQUIRED FOR ORGANIZATION OF SPINDLE MICROTUBULES IN *SILVETIA COMPRESSA* ZYGOTES

BMC Plant Biology

BioMed Central

Research article

Open Access

Kinesin-5 motors are required for organization of spindle microtubules in *Silvetia compressa* zygotes

Nick T Peters* and Darryl L Kropf

Address: Department of Biology, University of Utah, Salt Lake City, UT 84112, USA

Email: Nick T Peters* - npeters@biology.utah.edu; Darryl L Kropf - kropf@bioscience.utah.edu

* Corresponding author

Published: 31 August 2006

BMC Plant Biology 2006, 6:19 doi:10.1186/1471-2229-6-19

Received: 16 June 2006

Accepted: 31 August 2006

This article is available from: http://www.biomedcentral.com/1471-2229/6/19

Abstract

Background: Monastrol, a chemical inhibitor specific to the Kinesin-5 family of motor proteins, was used to examine the functional roles of Kinesin-5 proteins during the first, asymmetric cell division cycle in the brown alga *Silvetia compressa*.

Results: Monastrol treatment had no effect on developing zygotes prior to entry into mitosis. After mitosis entry, monastrol treatment led to formation of monasters and cell cycle arrest in a dose dependent fashion. These findings indicate that Kinesin-5 motors maintain spindle bipolarity, and are consistent with reports in animal cells. At low drug concentrations that permitted cell division, spindle position was highly displaced from normal, resulting in abnormal division planes. Strikingly, application of monastrol also led to formation of numerous cytasters throughout the cytoplasm and multipolar spindles, uncovering a novel effect of monastrol treatment not observed in animal cells.

Conclusion: We postulate that monastrol treatment causes spindle poles to break apart forming cytasters, some of which capture chromosomes and become supernumerary spindle poles. Thus, in addition to maintaining spindle bipolarity, Kinesin-5 members in *S. compressa* likely organize microtubules at spindle poles. To our knowledge, this is the first functional characterization of the Kinesin-5 family in stramenopiles.

Background

Fucoid algae are model organisms uniquely suited for studies investigating cellular polarity and asymmetric division during development. The fucoid marine brown alga *Silvetia compressa*, a member of the stramenopile lineage, displays oogamous fertilization in which a large sessile egg is fertilized by a small motile sperm [1]. The eggs and zygotes are large, about 100 μm in diameter, facilitating physiological and microscopic investigations [2]. Large numbers of zygotes, released into the surrounding seawater, can be easily collected for experimentation [3]. Zygotes develop synchronously during the first division cycle, completed about 24 h after fertilization (AF) with an invariant, asymmetric cell division [4]. From fertilization through cell plate deposition, a dynamic microtubule (MT) network is utilized for multiple cellular processes including migration of the male pronucleus, separation of the centrosomes around the nuclear envelope, nuclear positioning and rotation, formation and maintenance of a properly positioned mitotic spindle, and formation of a cytokinetic plane that bisects the spindle [5]. Numerous investigations of cytoskeletal proteins in *S. compressa* have provided a framework for more detailed studies examining the function of cytoskeletal associated proteins,

including molecular motors [4,6,7]. This study examines the Kinesin-5 family of motors during early *S. compressa* development.

The kinesin superfamily proteins (KIFs) are a diverse and evolutionarily conserved group of molecular motors present in metazoans, plants, fungi, and protozoans [8]. Kinesins possess a ~360 amino acid residue globular "motor" domain that hydrolyzes ATP for movement along MTs [8]. Kinesins travel towards the plus or minus end of MTs, or perform more structural roles in MT organization and stability [9]. The "tail" domains of kinesins are much less conserved and can mediate formation of higher order structures with fellow kinesins or attachment of cargos to be transported along MTs [8]. Recent work has categorized kinesin family members into 14 different classes which function in a multitude of cellular processes [9]. While human and fly kinesins have recently been systematically examined to determine their roles in cellular and developmental processes [10,11], the functional roles of kinesins in stramenopiles have not been investigated.

Monastrol and a chemical analogue *S*-trityl-L-cysteine (STLC) are small, cell-permeable inhibitors of the Kinesin-5 family of plus-end directed motors [12]. Kinesin-5 motors are bipolar homotetramers with two motor domains at each end, separated by a stalk/tail region [13]. Kinesin-5 motors are localized to the nucleus in animal cells until nuclear envelope breakdown at the onset of mitosis [14]. Inhibition of this motor has severe effects in mitosis but little or no effect in interphase [15]. During mitosis, Kinesin-5 motors function near the spindle midzone to maintain pole to pole distance. Motor domains attach to MTs from opposite poles and translocate towards the plus ends, thereby pushing spindle poles apart [16]. Additionally, Kinesin-5 proteins have been observed at spindle poles, though their function at that location is unclear [16,17]. Monastrol acts by specifically binding to and inhibiting the motor domain of Kinesin-5 proteins, thus impeding processive movement, while not affecting MT binding interactions [18]. Inhibition of processive movement of motors at the spindle midzone leads to formation of "monaster" spindles during metaphase. Monasters are defined by collapse of the spindle poles to a single focus, with captured chromosomes at the distil, plus ends [18].

To begin addressing the functional roles of kinesins during development in *S. compressa*, we examined the effects of monastrol treatment on the first asymmetric cell division cycle. We found that monastrol treatment induced formation of monasters upon entry into mitosis, confirming previous findings with animal systems [18]. Novel structures were also observed following drug treatment; multiple cytasters were observed throughout the cytoplasm and many cells formed multipolar spindles. There was a strong correlation between the presence of cytasters and multipolar spindles. These findings suggest that monastrol induces spindle pole breakup at mitosis entry, resulting in formation of cytasters, some of which become supernumerary spindle poles. Thus, Kinesin-5 members in *S. compressa*, and perhaps in other stramenopiles, appear to function not only at the spindle midzone to generate bipolarity, but also at spindle poles to maintain pole integrity.

Results

Monastrol or STLC treatment induced formation of monasters and multipolar spindles

To determine the functions of Kinesin-5 motors in brown algal cells, monastrol (25 μM – 100 μM) and a more potent chemical analogue, STLC (0.5 μM – 10 μM), were applied to *S. compressa* zygotes at 6 h AF. Cells were subsequently fixed at 16, 24, and 48 h AF, and fluorescently labeled with antibodies to observe MTs and condensed chromatin by confocal microscopy (see Materials and Methods). Monastrol had no effect on development or MT arrays of zygotes observed 16 h AF, prior to entry into mitosis. Treated zygotes germinated in accordance with an orienting light vector and had extensive MT arrays emanating from centrosomes on opposite sides of the nucleus (Fig. 1A–C). This finding suggests nuclear sequestration of Kinesin-5 motors during interphase, as has been reported in animal cells [10,19,20].

Normal metaphase spindles are characterized by two distinct spindle poles, consisting of centrioles and a cloud of hundreds of pericentriolar matrix proteins [21], spindle MTs and condensed chromatin at a metaphase plate (Fig. 1D). Treatment with monastrol severely disrupted spindle formation and resulted in monaster formation in some zygotes (Fig. 1E–F). Monasters, astral arrays of MTs with condensed chromatin near the periphery of the array, were similar to those observed in monastrol-treated or Kinesin-5-depleted animal cells [10,19,20]. Intense labeling of MTs in monasters is consistent with large numbers of short MTs in close proximity [16]. These results indicate that monastrol and STLC specifically inhibit brown algal Kinesin-5 motors that are critical for bipolar spindle assembly and maintenance. Although both drug treatments had similar effects on zygotes, monastrol treatment produced the most consistent results and was therefore the main focus for subsequent work.

Surprisingly, most treated cells formed multipolar spindles rather than monasters at entry into mitosis. Multipolar spindles have not been observed in other organisms treated with monastrol. The structure of multipolar spindles was quite variable, ranging from three spindle poles arranged linearly with chromosomes between poles to

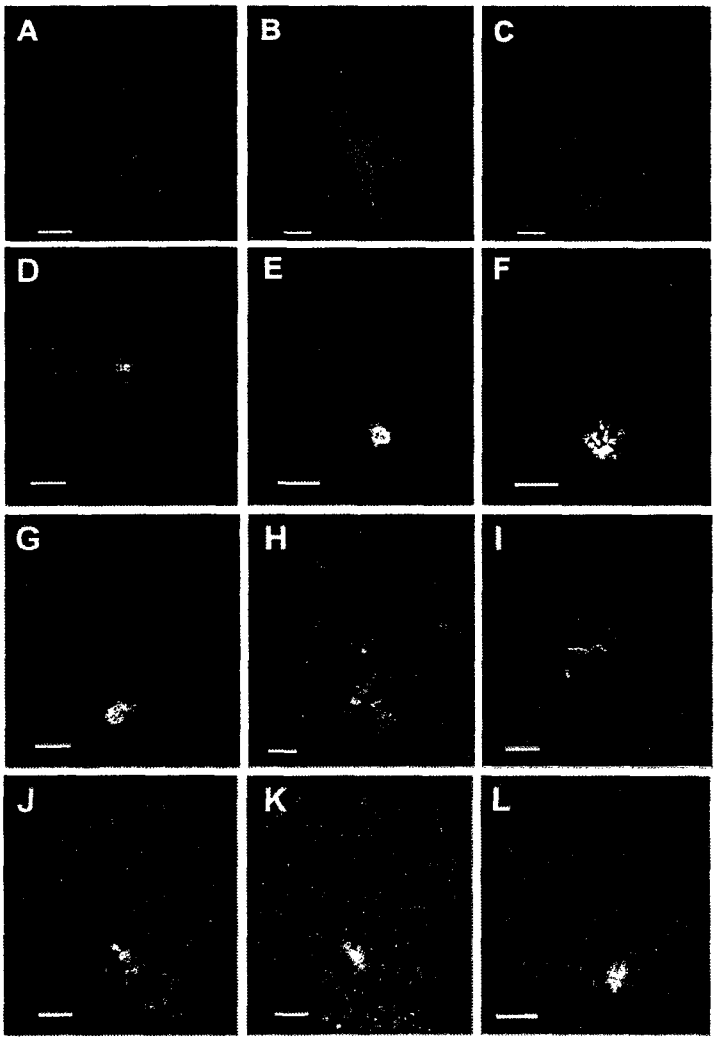

Figure 1
Monastrol and STLC treatment of *S. compressa* zygotes. (A-C) Zygotes were not sensitive to monastrol treatment during interphase (16 h AF); (A) 0.2% DMSO (B) 25 μM monastrol, (C) 50 μM monastrol. Note that the interphase zygotes in B and C exhibit elongated nuclei, indicating that they developed slightly faster than the control zygote in A. However, differences in developmental timing between treatments were not routinely observed. (D-F) Formation of monasters in mitosis (24 h AF); (D) 0.2% DMSO, (E) 25 μM monastrol, (F) 5 μM STLC. (G-I) Multipolar spindles (24 h AF); (G) 25 μM monastrol, (H) 50 μM monastrol, (I) 0.5 μM STLC. (J-L) Cytaster formation; (J) 25 μM monastrol (24 h AF), (K) 50 μM monastrol (24 h AF), (L) 100 μM monastrol (48 h AF). Cytasters were observed scattered throughout the cytoplasm. Hours in parentheses indicate times at which zygotes were fixed. MTs are depicted in green, condensed chromatin is depicted in red, and overlap between MTs and condensed chromatin is depicted in yellow. Median optical sections, 10–20 μm in total thickness, are shown. Scale bars equal 10 μm.

three or more poles in various spatial arrangements with captured chromosomes at metaphase plates (Fig. 1G–I). Chromosomes captured by a single spindle pole were also observed, but "lost" chromosomes unassociated with spindle MTs were not found. Multipolar spindles were the predominant mitotic structure in treated cells, and were observed in 70–80% of the population (Fig. 2A). The remaining 20–30% of the population had normal MT arrays or monasters in roughly equal proportions. Regardless of spindle morphology, pole-to-pole separation was reduced in a dose dependent manner by monastrol treatment (Fig. 2B), consistent with the postulated role of Kinesin-5 in generating spindle bipolarity.

Cytasters were present in most treated cells

Most treated cells observed after entry into mitosis possessed cytasters (Fig. 1H, J–L). Cytasters are supernumerary MT organizing centers (MTOCs) [22]. These structures are reminiscent of the star-shaped MT-based structures observed in the *Fucus serratus* cell cortex by Corellou *et al.* [7]; however, in our study cytasters were only observed after monastrol treatment and were distributed throughout the cytoplasm. MTs in cytasters were shorter than centrosomal MTs of untreated controls. Cytasters were present in nearly all zygotes that had multipolar spindles, while less than half of zygotes with monasters displayed cytasters (Fig. 2C). The strong correlation between multipolar spindles and cytasters suggests that cytasters may function as supernumerary spindle poles. Like multipolar spindles, cytasters have not been observed in other cell types or organisms treated with monastrol.

Monastrol treatment delays or inhibits cell division

Monastrol delayed cell division at low drug concentrations and inhibited cell division at higher concentrations (Fig. 3A). While cell division was significantly reduced by all drug treatments at 24 h AF, most zygotes treated with 25 μM monastrol had divided by 48 h AF. By contrast, treatment with higher drug concentrations (50 μM – 100 μM) resulted in sustained inhibition of cell division in a dose dependent fashion. The monastrol concentrations leading to cell cycle arrest are consistent with IC_{50} values reported for inhibition of ATP binding by a racemic mixture of monastrol [18], providing further evidence that monastrol specifically targets *S. compressa* Kinesin-5. Many undivided cells appeared to be arrested in first mitosis as judged by prolonged phosphorylation of histone H3. Histone H3 is phosphorylated from late prophase until global dephosphorylation during anaphase [23]. At 48 h AF, the percent of undivided zygotes with persistent histone H3 phosphorylation was concentration dependent in monastrol (Fig. 3B). In 100 μM monastrol, 66.5 ± 10.1 percent of the undivided cells exhibited condensed chromatin. These zygotes had likely arrested at the spindle assembly checkpoint of the first cell cycle [24]. Indeed,

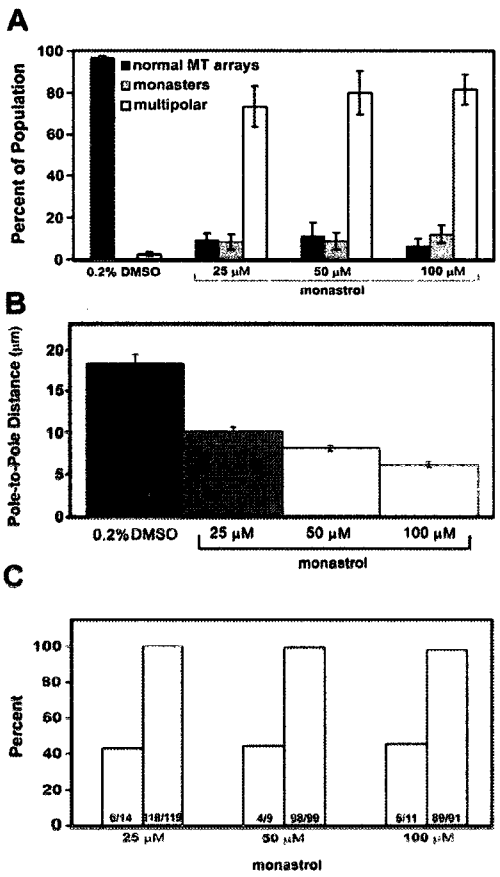

Figure 2

Monastrol or STLC treatment induced formation of multipolar spindles with reduced pole-to-pole distance at 24 h AF. (A) Incidence of monasters, multipolar spindles and normal MT arrays with increasing monastrol concentration. Zygotes with normal MT arrays had progressed beyond metaphase at 24 h AF; most were in telophase. (B) Pole-to-pole distance. For multipolar spindles, only the greatest distance between any two spindle poles sharing captured chromosomes was measured. Pole-to-pole distance was significantly ($p < 0.001$, Student's t test) shorter in all drug treatments compared to controls, and all treatments were significantly different from each other. (C) Multipolar spindles were associated with cytasters. Open bars; percent of the cells with monasters that also had cytasters. Shaded bars; percent of cells with multipolar spindles that also had cytasters.

when the spindle assembly checkpoint was activated by MT stabilization using paclitaxel or MT depolymerization

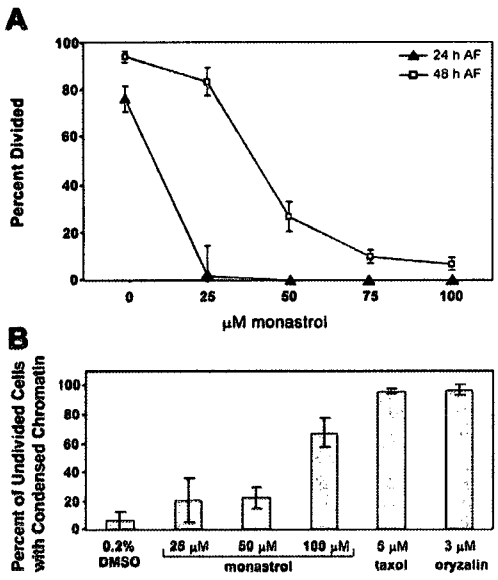

Figure 3

Monastrol treatment led to cell cycle delay at low concentrations and cell cycle arrest at high concentrations. (A) Filled triangles depict cell plate formation at 24 h AF, and open squares depict cell plate formation at 48 h AF. (B) Chromatin condensation in undivided cells at 48 h AF assayed by labeling with antibody to phosphorylated histone H3. Bars are standard errors.

using oryzalin, nearly all zygotes exhibited prolonged histone H3 phosphorylation (Fig. 3B).

Spindle and division plane alignment

Metaphase spindles in untreated cells were reasonably well aligned with the growth axis and resided near the center of the zygote (Fig. 1D). Interestingly, aberrant spindles in monastrol-treated zygotes were often displaced toward the rhizoid (Fig. 1E–L). Condensed chromatin was also incorrectly positioned following MT depolymerization by oryzalin or MT stabilization by paclitaxel, as has been previously reported [25]. However, preferential displacement toward the rhizoid was not observed in paclitaxel or oryzalin; chromatin position instead appeared more random (data not shown). Together these findings support the hypothesis that MTs are crucial for spindle positioning [26,27].

S. compressa zygotes determine division plane based on spindle position [26], so monastrol treatment was predicted to alter division patterns. The first asymmetric division in untreated zygotes bisected the spindle and therefore was transverse to the growth axis (arrowhead, Fig. 4A). Since few zygotes treated with 100 μM monastrol divided, we focused on lower drug concentrations. As expected, aberrant division planes (assessed as >30 degrees from perpendicular to the long axis of the cell) were observed in cells treated with 25 μM or 50 μM monastrol (Fig. 4B). In addition, curved planes of division were also observed (Fig. 4C). The percent of cells with abnormal division planes increased with monastrol concentration; at 50 μM approximately two thirds of divided cells displayed aberrant division planes (Fig. 4C).

MT disruption slows tip growth

Rhizoids of zygotes treated with paclitaxel, oryzalin or monastrol appeared shorter and broader than control rhizoids (Fig. 5B–E). We therefore assayed tip growth by measuring the length of the embryonic axis over a three-day period. None of the pharmacological agents affected rhizoid growth prior to mitosis; zygotes elongated at ~1 μm/h regardless of treatment (Fig. 5A). Although control embryos continued to elongate at ~1 μm/h after first division, tip elongation was severely reduced in treated zygotes following entry into first mitosis. This growth reduction was probably not due to MT disruption since treated zygotes grew normally prior to mitosis, nor was it likely caused by a cell volume checkpoint. Fucoid zygotes treated with aphidicolin activate an S-phase cell cycle checkpoint that blocks nuclear division and cytokinesis, but permits continued rhizoid tip growth [24]. This results in very large, elongated zygotes that are undivided, suggesting that zygotes do not possess a volume checkpoint. Instead, the abrupt reduction in growth rate we observed was probably caused by arrest in M phase, perhaps via activation of the spindle assembly checkpoint [28].

Discussion

Although assembly of a mitotic spindle is not well understood, the process requires dynamic MTs, plus-end and minus-end directed MT motors, and a plethora of accessory proteins, including static crosslinking molecules [29]. Kinesin-5 motors localize within the nucleus until nuclear envelope breakdown (NEB) [14] when they are released into the cytoplasm and accumulate at the midzone and poles of the forming spindle. They are required for maintenance of bipolar spindle integrity and poleward flux of MTs [30]. In the midzone, Kinesin-5 motors interact with MTs from opposite poles and move at ~20 nm s^{-1} toward MT plus-ends, effectively pushing spindle poles apart [16]. Inhibition of Kinesin-5 function by gene knockout, RNAi-mediated depletion, or treatment with pharmacological agents results in monaster formation during spindle assembly [10,11,19]. For example, mutations in *Drosophila* KLP61F, a Kinesin-5 ortholog, have

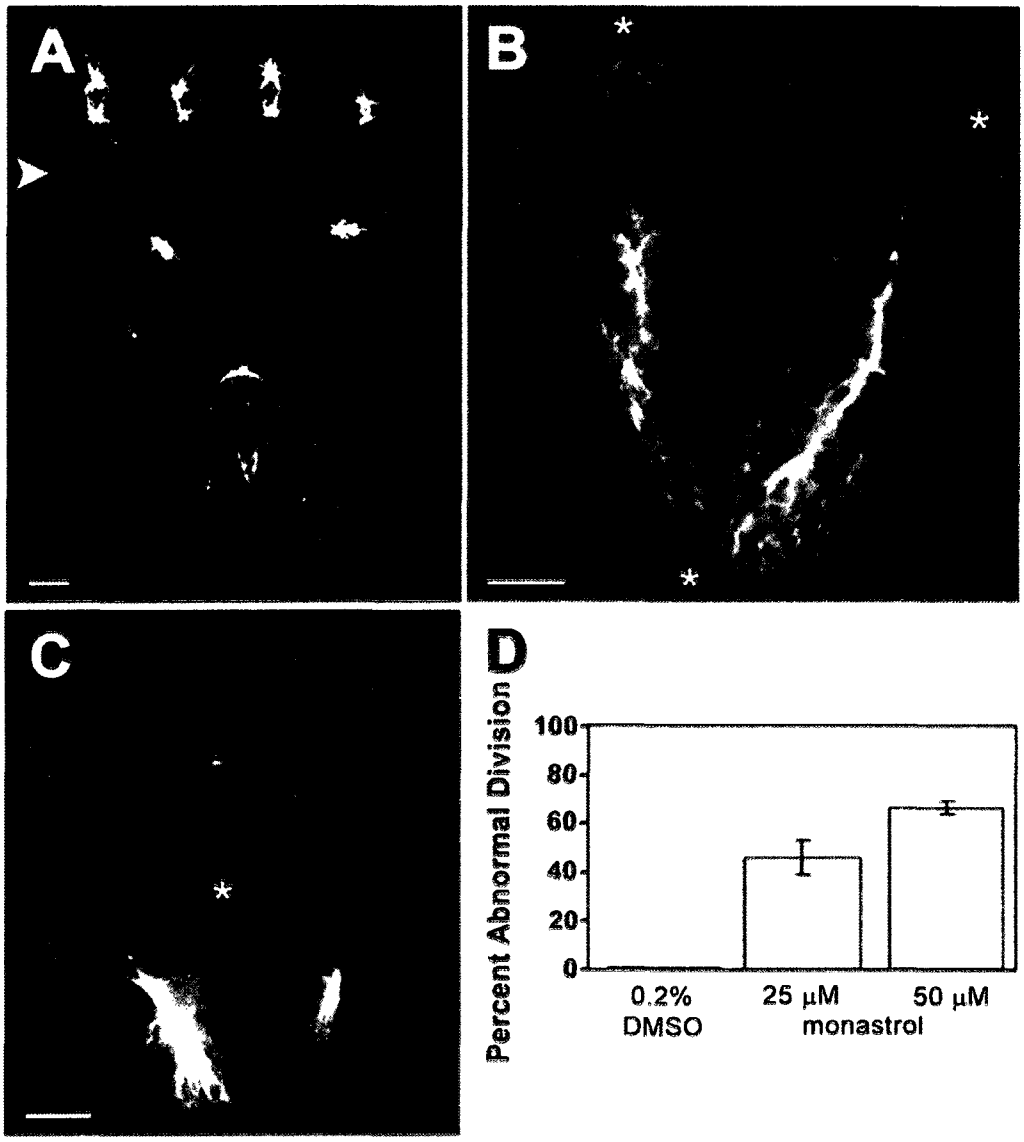

Figure 4
Monastrol concentrations permissive for cell division led to aberrant cytokinesis assayed at 48 h AF. (A) 0.2% DMSO. By 48 h AF, control zygotes had divided several times in a stereotypical pattern. Arrowhead indicates first division plane. (B-C) 25 µM monastrol. Asterisks mark aberrant division planes. (D) Percent of divided zygotes with abnormal first cytokinesis, as assessed by >30 degree deviance from perpendicular to the long axis of the cell, or by curved cell plates. Standard error bars shown. Scale bars equal 10 µm.

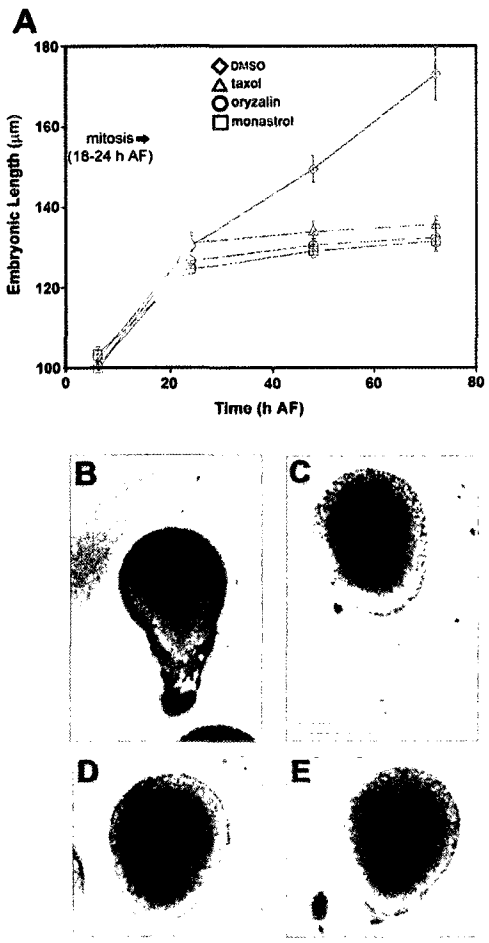

Figure 5
Monastrol, paclitaxel, and oryzalin severely reduce tip growth at first mitosis. (A) Embryonic growth over a 72 h period. Data are from one representative experiment sampling ten undivided zygotes for each treatment. Diamonds, 0.2% DMSO; triangles, 5 μM paclitaxel; squares, 3 μM oryzalin; circles, 50 μM monastrol. Standard error bars are shown. (B-E) Images of treated zygotes at 72 h AF. (B) 0.2% DMSO, (C) 50 μM monastrol (D) 5 μM paclitaxel, (E) 3 μM oryzalin. Scale bar equals 100 μm.

been shown to disrupt maintenance of spindle pole separation [31]. Kinesin-5 proteins act in concert with other spindle associated proteins to maintain proper spindle length. For example, increasing the levels of NuMA, a MT crosslinking protein, restores spindle bipolarity in mitotic extracts lacking Kinesin-5 activity [32]. In sum, animal Kinesin-5 motors function with other mitotic proteins to generate and maintain pole-to-pole separation by pushing apart antiparallel MTs at the spindle midzone.

The roles of kinesins in the stramenopile lineage have not been functionally investigated. We examined the roles of Kinesin-5 motors during the first cell division cycle in *S. compressa* by employing Kinesin-5-specific inhibitors to brown algal zygotes. *S. compressa* zygotes treated with monastrol (or STLC) appeared normal and had normal MT arrays in interphase of the first cell cycle, consistent with nuclear localization prior to NEB. Unfortunately, we were unable to confirm nuclear localization since available antibodies to animal Kinesin-5-proteins did not label fucoid zygotes. Importantly, monasters were formed upon entry into mitosis. These findings are similar to reports in animals [10,11,19] and indicate that monastrol binds and inhibits Kinesin-5 motors in *S. compressa*. However, monastrol had additional effects on zygotes not observed in animal cells; in addition to monasters, multipolar spindles and cytasters were formed at mitotic entry.

Multipolar spindles were formed at a much higher frequency than monasters, indicating that spindle poles do not fully collapse when Kinesin-5 motors are inhibited. This is unrelated to monastrol dosage since increasing concentration did not significantly increase monaster frequency. Instead, zygotes probably possess other mechanisms that work in concert with Kinesin-5 to maintain pole separation. There may be MT-based motors with overlapping function or MT crosslinking proteins, such as NuMA, that continue to function in the presence of monastrol, maintaining some pole separation. Centrosome position at the onset of mitosis may also contribute to the relatively low monaster frequency. Brown algal centrosomes are fully separated on the nuclear envelope prior to entry into mitosis, residing about 15 μm apart [33]. Animal centrosomes, however, separate concurrent with NEB so spindle poles are still close together when Kinesin-5 motors become active [34]. The greater separation of algal spindle poles may reduce the likelihood of complete spindle collapse to a monaster during drug treatment.

The presence of multipolar spindles also implies that supernumerary spindle poles are formed at entry into mitosis, and the extra poles may be derived from cytasters. Although the composition of fucoid cytasters is unknown, they are distinct small astral-like radial bursts of MTs. These are commonly associated with centrin labeling in other systems, and are likely MTOCs [22]. The observation that nearly all zygotes with multipolar spindles additionally displayed cytasters, while cytasters were only

present in about half of cells with monasters, suggests a causal a link between cytasters and supernumerary spindle poles. We speculate that monastrol treatment leads to spindle pole breakup in *S. compressa* and fragments of spindle poles nucleate MTs and become cytasters. Numerous cytasters are located throughout the cytoplasm of treated cells, and occasionally one residing close to condensed chromatin captures chromosomes, thereby becoming a supernumerary spindle pole. In this model, Kinesin-5 motors must organize and maintain the integrity of spindle poles. Kinesin-5 members residing at spindle poles have been postulated to bundle long MTs [35], sort numerous short MTs in the cloud of spindle pole proteins [16], and/or mediate attachment to a hypothesized scaffold-like spindle matrix [35]. In fucoid zygotes, one or more of these putative functions may be needed to hold pole components together.

Interestingly, the vast majority of zygotes treated with monastrol had aberrant spindles that were displaced from a central cellular position toward the rhizoid. Proper alignment of the mitotic spindle in brown algae has been shown to be a MT-dependent process [27], and we observed that condensed chromatin was displaced in zygotes treated with paclitaxel or oryzalin (data not shown). MTs that position the fucoid spindle are thought to do so by interacting with the cell cortex before and after metaphase [26]. Perhaps the dramatically prolonged metaphase during monastrol treatment permits unregulated spindle movement, resulting in aberrant spindle position. Even so, it is not clear why the spindles preferentially drift in the rhizoid direction.

Cytokinesis bisects the spindle in fucoid zygotes [27], so it was not surprising to find abnormal divisions following monastrol treatment. The preponderance of multipolar spindles likely resulted in many of the abnormal divisions. Some zygotes with multipolar spindles must still progress through mitosis because the vast majority of cells treated with 25 μM monastrol display multipolar spindles at 24 h AF but completed cell division by 48 h AF. The spindle assembly checkpoint apparently does not monitor spindle pole number. Likewise, cytokinesis proceeds in sea urchin zygotes and in vertebrate somatic cells possessing supernumerary spindle poles [36]. Since it is unlikely that monaster spindles could achieve equivalent kinetochore tension on chromosomes, these zygotes probably remained arrested in metaphase and failed to divide. Therefore, most abnormal division planes in monastrol-treated *S. compressa* zygotes are likely due to multipolar or abnormally positioned spindles that achieve balanced kinetochore attachments, permitting cell cycle progression and aberrant placement of the cytokinetic plane.

Future studies will be aided by an ongoing genomic sequencing project of closely related *Ectocarpus siliculosis* [37] and by creation of an EST database for fucoid algae. This information will permit isolation of *S. compressa* Kinesin-5 sequences for use in molecular investigations and antibody production, and may provide insight into what elements, beyond MTs, are associated with cytasters.

Conclusion

Kinesin-5 motor proteins are necessary for bipolar spindle formation during mitosis in brown algal cells, similar to what has been previously reported in animals. In addition, they appear to be involved in maintaining spindle pole integrity.

Methods

Sexually mature fronds (receptacles) of the fucoid algae *S. compressa* were collected near Santa Cruz, California, shipped cold and stored in the dark at 4°C until use. Receptacles were potentiated by placing them under 100 $\mu mol \cdot m^{-2} \cdot s^{-1}$ light at 16°C in artificial sea water (10 mM KCL, 0.45 M NaCl, 9 mM CaCl, 16 mM $MgSO_4$, 0.040 mg chloramphenicol per ml, buffered to a pH of 8.2 with Tris base) for 1 to 3 h. Potentiated receptacles were then washed with ASW and placed in the dark for 1 h to induce gamete release. The time of fertilization was taken to be the midpoint of the dark period. Zygotes were plated onto coverslips in plastic dishes and grown in ASW with unidirectional light at 16°C until harvest. All experiments were performed in triplicate. Graphs depict data compiled from three experiments, unless otherwise noted.

Pharmacological agents were dissolved in DMSO to create stock solutions of 100 mM monastrol (AG Scientific, San Diego, Ca.), 50 mM *S*-trityl-L-cysteine (Sigma, St. Louis, Mo.), 10 mM paclitaxel (taxol, Sigma, St. Louis, Mo.) and 10 mM oryzalin. Since monastrol is light sensitive, degradation was tested by exposing 100 μM monastrol in ASW in culture dishes to unilateral light for three days. Similar levels of inhibition of cell division were observed for both fresh and light-treated monastrol, indicating no significant degradation. Drugs were applied to zygotes at various times prior to mitotic entry, yielding similar results. For all work presented here, drugs were added chronically to zygotes beginning 6 hours after fertilization (h AF). Appropriate controls were performed with DMSO at concentrations corresponding to the maximum volume of drug used. These controls showed normal development.

Pharmacological effects on tip growth were evaluated by capturing sequential images of individual embryos over three days with a coolSNAP (RS Photometrics) camera on an Olympus IMT2 microscope. Embryonic length was measured using Photoshop 7.0 (Adobe, San Jose, Ca).

For immunofluorescence microscopy of MTs and condensed chromatin, zygotes were fixed in PHEM (60 mM piperazine-N, N'-bis(2-ethanesulfonic acid), 25 mM HEPES, 10 mM EGTA, 2 mM $MgCl_2$) containing 3% paraformaldehyde and 0.5% glutaraldehyde. Zygotes were processed as in Bisgrove and Kropf [26], with the following modifications. Coverslips were dipped into liquid nitrogen and removed as quickly as possible (less than 1 second) and abalone gut extract was omitted from the enzyme mixture. MTs were imaged using a monoclonal anti-α-tubulin antibody (DM1A: Sigma) with Alexa 488 goat anti-mouse secondary antibody (Invitrogen, Eugene, Or.). Condensed chromosomes were imaged using a polyclonal anti-histone H3 ($pSer^{10}$) antibody (Calbiochem, San Diego, Ca.), followed by Alexa 546 goat anti-rabbit secondary antibody. For double labeling, primary antibodies were added simultaneously, as were secondary antibodies. Images were collected on a LSM510 (Carl Zeiss Inc., Thornwood, N.Y.) laser scanning confocal microscope with a narrow band-pass filter and Meta attachment adjustable band pass filter.

Abbreviations

AF, after fertilization; ASW, artificial seawater; DMSO, dimethyl sulfoxide: NEB, nuclear envelope breakdown; MT, microtubule.

Authors' contributions

NTP conducted all of the research, DLK raised the funds, and both authors contributed equally intellectually and in writing the manuscript.

Acknowledgements

We wish to thank David L. Gard for suggesting the use of monastrol. This work was supported by award IOB-0414089 to DLK.

References

1. Kropf DL: **Cytoskeletal Control of Cell Polarity in a Plant Zygote.** *Developmental Biology* 1994, **165(2)**:361-371.
2. Kropf DL, Bisgrove SR, Hable WE: **Cytoskeletal control of polar growth in plant cells.** *Current Opinion in Cell Biology* 1998, **10(1)**:117-122.
3. Quatrano RS: **Development of Cell Polarity.** *Annual Review of Plant Physiology* 1978, **29(1)**:487-510.
4. Bisgrove SR, Kropf DL: **Cytokinesis in brown algae: studies of asymmetric division in fucoid zygotes.** *Protoplasma* 2004, **223(2 - 4)**:163-173.
5. Kropf DL, Bisgrove SR, Hable WE: **Establishing a growth axis in fucoid algae.** *Trends in Plant Sci* 1999, 4:490-494.
6. Kropf DL, Maddock A, Gard DL: **Microtubule distribution and function in early Pelvetia development.** *J Cell Sci* 1990, **97**:545-552.
7. Corellou F, Coelho SMB, Bouget FY, Brownlee C: **Spatial re-organisation of cortical microtubules in vivo during polarisation and asymmetric division of Fucus zygotes.** *Journal of Cell Science* 2005, **118(12)**:2723-2734.
8. Miki H, Okada Y, Hirokawa N: **Analysis of the kinesin superfamily: insights into structure and function.** *Trends in Cell Biology* 2005, **15(9)**:467-476.
9. Lawrence CJ, Dawe RK, Christie KR, Cleveland DW, Dawson SC, Endow SA, Goldstein LSB, Goodson HV, Hirokawa N, Howard J, Malmberg RL, McIntosh JR, Miki H, Mitchison TJ, Okada Y, Reddy ASN, Saxton WM, Schliwa M, Scholey JM, Vale RD, Walczak CE, Wordeman L: **A standardized kinesin nomenclature.** *J Cell Biol* 2004, **167(1)**:19-22.
10. Goshima G, Vale RD: **The roles of microtubule-based motor proteins in mitosis: comprehensive RNAi analysis in the Drosophila S2 cell line.** *Journal of Cell Biology* 2003, **162(6)**:1003-1016.
11. Zhu C, Zhao J, Bibikova M, Leverson JD, Bossy-Wetzel E, Fan JB, Abraham RT, Jiang W: **Functional Analysis of Human Microtubule-based Motor Proteins, the Kinesins and Dyneins, in Mitosis/Cytokinesis Using RNA Interference.** *Molecular Biology of the Cell* 2005, **16(7)**:3187-3199.
12. Brier S, Lemaire D, DeBonis S, Forest E, Kozielski F: **Identification of the Protein Binding Region of S-Trityl-L-cysteine, a New Potent Inhibitor of the Mitotic Kinesin Eg5.** *Biochemistry* 2004, **43(41)**:13072-13082.
13. Cole DG, Saxton WM, Sheehan KB, Scholey JM: **A "slow" homotetrameric kinesin-related motor protein purified from Drosophila embryos.** *J Biol Chem* 1994, **269(37)**:22913-22916.
14. Sharp DJ, Brown HM, Kwon M, Rogers GC, Holland G, Scholey JM: **Functional Coordination of Three Mitotic Motors in Drosophila Embryos.** *Molecular Biology of the Cell* 2000, **11(1)**:241-253.
15. Miyamoto DT, Perlman ZE, Mitchison TJ, Shirasu-Hiza M: **Dynamics of the mitotic spindle--potential therapeutic targets.** *Prog Cell Cycle Res* 2003, **5**:349-360.
16. Kapitein LC, Peterman EJG, Kwok BH, Kim JH, Kapoor TM, Schmidt CF: **The bipolar mitotic kinesin Eg5 moves on both microtubules that it crosslinks.** *Nature* 2005, **435(7038)**:114-118.
17. Crevel IMTC, Lockhart A, Cross RA: **Kinetic evidence for low chemical processivity in ncd and Eg5.** *Journal of Molecular Biology* 1997, **273(1)**:160-170.
18. Maliga Z, Kapoor TM, Mitchison TJ: **Evidence that Monastrol Is an Allosteric Inhibitor of the Mitotic Kinesin Eg5.** *Chemistry & Biology* 2002, **9(9)**:989-996.
19. Mayer TU, Kapoor TM, Haggarty SJ, King RW, Schreiber SL, Mitchison TJ: **Small Molecule Inhibitor of Mitotic Spindle Bipolarity Identified in a Phenotype-Based Screen.** *Science* 1999, **286(5441)**:971-974.
20. Doxsey S, Zimmerman W, Mikule K: **Centrosome control of the cell cycle.** *Trends in Cell Biology* 2005, **15(6)**:303-311.
21. Kuriyama R, Borisy GG: **Cytasters induced within unfertilized sea-urchin eggs.** *Journal of Cell Science* 1983, **61(1)**:175-189.
22. Pascreau G, Arlot-Bonnemains Y, Prigent C: **Phosphorylation of histone and histone-like proteins by aurora kinases during mitosis.** *Prog Cell Cycle Res* 2003, **5**:369-374.
23. Corellou FC, Bisgrove SR, Kropf DL, Meijer L, Kloareg B, Bouget FY: **A S/M DNA replication checkpoint prevents nuclear and cytoplasmic events of cell division including centrosomal axis alignment and inhibits activation of cyclin dependent kinase-like proteins in fucoid zygotes.** *Development* 2000, **127**:1651-1660.
24. Swope RE, Kropf DL: **Pronuclear positioning and migration during fertilization in Pelvetia.** *Dev Biol* 1993, **157**:269-276.
25. Bisgrove SR, Kropf DL: **Asymmetric cell division in fucoid algae: a role for cortical adhesions in alignment of the mitotic apparatus.** *J Cell Sci* 2001, **114**:4319-4328.
26. Bisgrove SR, Henderson DC, Kropf DL: **Asymmetric division in fucoid zygotes is positioned by telophase nuclei.** *Plant Cell* 2003, **In press:**.
27. Kapoor TM, Mayer TU, Coughlin ML, Mitchison TJ: **Probing Spindle Assembly Mechanisms with Monastrol, a Small Molecule Inhibitor of the Mitotic Kinesin, Eg5.** *J Cell Biol* 2000, **150(5)**:975-988.
28. Gaetz J, Kapoor TM: **Dynein/dynactin regulate metaphase spindle length by targeting depolymerizing activities to spindle poles.** *Journal of Cell Biology* 2004, **166(4)**:465-471.
29. Miyamoto DT, Perlman ZE, Burbank KS, Groen AC, Mitchison TJ: **The kinesin Eg5 drives poleward microtubule flux in Xenopus laevis egg extract spindles.** *Journal of Cell Biology* 2004, **167(5)**:813-818.
30. Heck MM, Pereira A, Pesavento P, Yannoni Y, Spradling AC, Goldstein LS: **The kinesin-like protein KLP61F is essential for mitosis in Drosophila.** *J Cell Biol* 1993, **123(3)**:665-679.
31. Chakravarty A, Howard L, Compton DA: **A Mechanistic Model for the Organization of Microtubule Asters by Motor and Non-Motor Proteins in a Mammalian Mitotic Extract.** *Molecular Biology of the Cell* 2004, **15(5)**:2116-2132.

32. Bisgrove SR, Kropf DL: **Alignment of centrosomal and growth axes is a late event during polarization of Pelvetia compressa zygotes.** *Dev Biol* 1998, 194:246-256.
33. Savolan MS, Rieder CL: **Mitosis in primary cultures of Drosophila melanogaster larval neuroblasts.** *J Cell Sci* 2002, 115(15):3061-3072.
34. Kapoor TM, Mitchison TJ: **Eg5 is static in bipolar spindles relative to tubulin: evidence for a static spindle matrix.** *J Cell Biol* 2001, 154(6):1125-1134.
35. Sluder G, Thompson EA, Miller FJ, Hayes J, Rieder CL: **The checkpoint control for anaphase onset does not monitor excess numbers of spindle poles or bipolar spindle symmetry.** *Journal of Cell Science* 1997, 110(4):421-429.
36. Peters AMDSDKBCJ: **Proposal of Ectocarpus Silliculosis (Ectocarpales, Phaeophyceae) as a Model Organism for Brown Algal Genetics and Genomics.** *J Phycology* 2004, 40:1079-1088.

CHAPTER 6

LOCALIZATION AND FUNCTION OF KINESIN-5-LIKE PROTEINS DURING ASSEMBLY AND MAINTENANCE OF MITOTIC SPINDLES IN *SILVETIA COMPRESSA*

BMC Research Notes

BioMed Central

Short Report

Open Access

Localization and function of Kinesin-5-like proteins during assembly and maintenance of mitotic spindles in *Silvetia compressa*

Nick T Peters*, Anne Catherine Miller and Darryl L Kropf

Address: Biology Department, University of Utah, Salt Lake City, Utah, USA

Email: Nick T Peters* - npeters@biology.utah.edu; Anne Catherine Miller - a.katie.miller@gmail.com; Darryl L Kropf - kropf@bioscience.utah.edu

* Corresponding author

Published: 15 June 2009

BMC Research Notes 2009, 2:106 doi:10.1186/1756-0500-2-106

Received: 29 December 2008
Accepted: 15 June 2009

This article is available from: http://www.biomedcentral.com/1756-0500/2/106

Abstract

Background: Kinesin-5 (Eg-5) motor proteins are essential for maintenance of spindle bipolarity in animals. The roles of Kinesin-5 proteins in other systems, such as Arabidopsis, Dictyostelium, and sea urchin are more varied. We are studying Kinesin-5-like proteins during early development in the brown alga *Silvetia compressa*. Previously, this motor was shown to be needed to assemble a bipolar spindle, similar to animals. This report builds on those findings by investigating the localization of the motor and probing its function in spindle maintenance.

Findings: Anti-Eg5 antibodies were used to investigate localization of Kinesin-5-like proteins in brown algal zygotes. In interphase zygotes, localization was predominantly within the nucleus. As zygotes entered mitosis, these motor proteins strongly associated with spindle poles and, to a lesser degree, with the polar microtubule arrays and the spindle midzone. In order to address whether Kinesin-5-like proteins are required to maintain spindle bipolarity, we applied monastrol to synchronized zygotes containing bipolar spindles. Monastrol is a cell-permeable chemical inhibitor of the Kinesin-5 class of molecular motors. We found that inhibition of motor function in pre-formed spindles induced the formation of multipolar spindles and short bipolar spindles.

Conclusion: Based upon these localization and inhibitor studies, we conclude that Kinesin-5-like motors in brown algae are more similar to the motors of animals than those of plants or protists. However, Kinesin-5-like proteins in *S. compressa* serve novel roles in spindle formation and maintenance not observed in animals.

Background

Kinesins are a diverse group of molecular motors present in protozoans, fungi, plants, and metazoans [1]. They share a globular motor domain that hydrolyses ATP to facilitate movement towards the plus or minus end of microtubules [2]. Kinesins participate in structural organization and/or stabilization of microtubules and also transport cargo throughout the cytoplasm utilizing microtubules as molecular highways [2]. The Kinesin-5 group of the kinesin superfamily consists of plus-end directed homotetramers with two motor domains on each end [1]. They have been shown to function in spindle organization during mitosis in animal cells, remaining inactive and sequestered within the nucleus during interphase [1]. Specifically, Kinesin-5 motors are thought to function at the spindle midzone and maintain spindle bipolarity by walking towards the plus ends of interdigitating microtubules from opposite poles [3]. Kinesin-5 motors are also

BMC Research Notes 2009, **2**:106 http://www.biomedcentral.com/1756-0500/2/106

present at spindle poles where they may create an outward force on parallel microtubules [4].

Monastrol is a cell permeant inhibitor of Kinesin-5 motors and is thought to function by binding the motor domains, thereby blocking normal movement [5,6]. Specifically, monastrol has been shown to bind the Kinesin-5-ADP complex and inhibit ADP release and may inhibit motor binding to microtubules [7,8]. Therefore, monastrol is a powerful tool to probe the functions of Kinesin-5 motors without the necessity of genetic manipulations. In animal cells, monastrol treatment induces spindles to collapse to monasters, while having no detectable effects during interphase [9]. In contrast, other organisms such as Dictyostelium and vascular plant cells appear to be monastrol insensitive [10,11]. Thus, sensitivity to monastrol appears to vary between different lineages.

It has previously been shown that monastrol treatment leads to malformed spindles in brown algae. Monastrol treatment of *Silvetia compressa* zygotes prior to mitosis induced the formation of mostly multipolar spindles; monasters were also formed albeit to a lesser degree [12]. Monastrol treatment also induced formation of numerous cytasters during mitosis, likely due to spindle pole fragmentation, but did not affect interphase microtubule arrays. These findings suggested that brown algal Kinesin-5-like motors, like animal Kinesin-5 motors, are sensitive to monastrol treatment. However, the specific localizations and functions of Kinesin-5-like motors remain unclear in the brown algal lineage.

Here we examine Kinesin-5-like localization during early embryonic development and utilize monastrol to assess motor function in maintaining spindle structure and function in *S. compressa* zygotes. We show that Kinesin-5-like motors are localized within the nucleus during interphase, and strongly localize to the spindle poles from the onset of mitosis until nuclear envelope reformation. These motors are also associated with polar microtubules and the spindle midzone but to a much lesser degree. Additionally, we show that inhibition of Kinesin-5-like motors during mitosis leads to the formation of multipolar and short bipolar spindles, indicating that motor function is needed to maintain spindle integrity. Many of our findings are in concert with those found in animal cells. In both brown algal zygotes and animal cells, Kinesin-5 proteins are localized within the nuclear envelope until mitosis where they strongly decorate the spindle poles, and monastrol treatment induces formation of aberrant spindles.

Methods

Zygotes were cultured as previously described [12]. Monastrol (AG Scientific, San Diego, CA) was dissolved in dimethyl sulfoxide to create a stock solution of 100 mM. 1-butanol (Sigma-Aldrich, St. Louis, MO) was applied directly into the aqueous culture medium at a concentration of 0.2%. The use of 1-butanol as a cell cycle synchronizing tool has been described elsewhere [13]. For immunofluorescence microscopy of Kinesin-5 motors, microtubules, or condensed chromatin, zygotes were fixed in PHEM (60 mM piperazine-N, N0-bis(2-ethanesulfonic acid), 25 mM HEPES, 10 mM EGTA, 2 mM $MgCl_2$, pH adjusted to 7.5 with KOH) containing 3% paraformaldehyde and 0.5% glutaraldehyde. Fixed zygotes were processed as previously described [12]. Kinesin-5 motors were labeled with polyclonal anti-Eg5 peptide primary antibody (Novus Biologicals, Littleton, CO) and Alexa 546 goat anti-rabbit secondary antibody (Invitrogen, Eugene, OR). Microtubules were labeled with a monoclonal anti-α-tubulin (DM1A) primary antibody (Sigma-Aldrich, St. Louis, MO) and Alexa 488 goat anti-mouse secondary antibody (Invitrogen, Eugene, OR). Condensed chromatin was labeled with a polyclonal anti-histone H3 (pSer10) antibody (Calbiochem, San Diego, CA), followed by Alexa 546 goat anti-rabbit secondary antibody. For double labeling of microtubules and either Kinesin-5 or condensed chromatin, primary antibodies were added simultaneously, as were secondary antibodies. Images were collected on an LSM510 (Carl Zeiss Inc., Thornwood, NY) confocal laser scanning microscope using a narrow bandpass filter for microtubules (500–530 nm) and a Meta adjustable bandpass filter (558–601 nm) for Kinesin-5 or condensed chromatin. Images were adjusted for brightness and contrast, and images shown in Fig. 1F–H were taken with increased amplifier gain to exaggerate anti-Kinesin-5 signal. All images represent single confocal sections of approximately 0.5 μm thickness. All experiments were repeated in triplicate and each data point represents a sample size of at least one hundred.

Results and Discussion

Kinesin-5-like proteins are localized to mitotic spindles

An anti-Eg5 polyclonal antibody directed towards the coiled coil domain of human Eg5 was used to establish the localization pattern of putative Kinesin-5 proteins in *S. compressa*. During interphase of the first cell cycle, anti-Kinesin-5 signal was observed exclusively within the nucleus (Fig. 1A). In prophase labeling was distributed throughout the elongated nucleus, and also distinctly localized to the forming spindle poles (Fig. 1B). During metaphase, localization was mainly observed at spindle poles (Fig. 1C, E, F, H) but weak signal was also occasionally observed at the spindle midzone in images taken with increased amplifier gain (Fig. 1F, H). Note that in Fig. 1F–H the spindle poles are out of the focal plane, allowing for better visualization of faint anti-Kinesin-5-positive signal at the spindle midzone.

The subcellular localization of Kinesin-5-like motors described above is generally similar to localization pat-

BMC Research Notes 2009, 2:106 http://www.biomedcentral.com/1756-0500/2/106

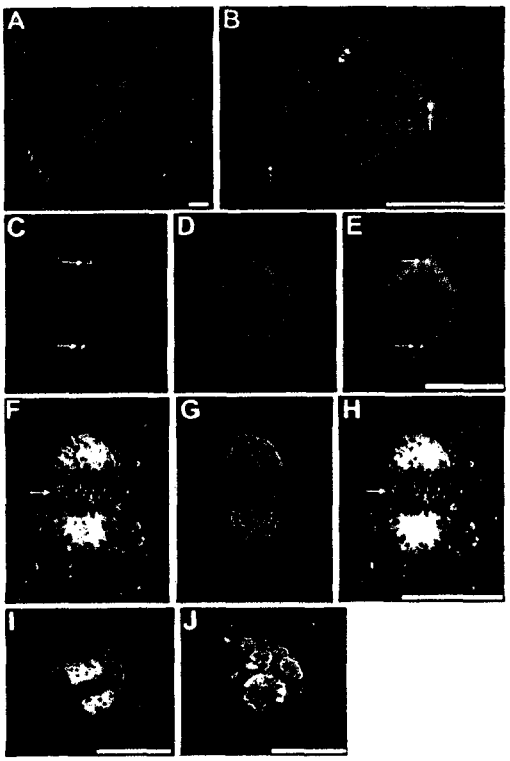

Figure 1
Localization of Kinesin-5-like proteins (A-H) and morphology of short bipolar and multipolar spindles (I, J). Microtubules are in green in all images. Kinesin-5-like proteins are in red in A-C, E, F, H. Condensed chromatin is in blue in I and J. (A) 17-h old zygote in interphase. (B) Thallus cell of a 2-day old embryo entering prophase. (C-H) Two metaphase spindles are shown; anti-Kinesin-5 signal (C, F), microtubules (D, G), and merged images (E, H). In F and H, anti-Kinesin-5 signal was collected with increased amplifier gain and adjusted for contrast and brightness to enhance visualization of the weak signal; microtubule signal was not enhanced. Arrows indicate Kinesin-5-like motors colocalizing with microtubules in B and E, at the spindles poles and midzone in C and F, respectively. (I, J) Effect of monastrol treatment on metaphase spindles. Condensed chromatin is associated with short bipolar spindles in I and multipolar spindles in J following treatment with monastrol. Secondary antibodies commonly stick to zygotes' extracellular adhesive and is seen in A. Scale bars equal 10 μm.

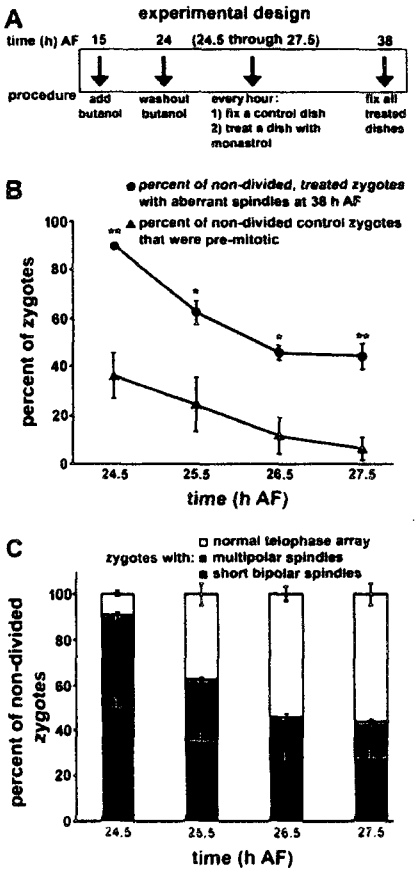

Figure 2
Developmental progression of spindle formation and spindle morphology. (A) Experimental design. Zygotes were treated with 1-butanol at 15 h AF and released by washout at 24 h AF. At hourly intervals from 24.5 to 27.5 h AF, a control dish was fixed and another dish was treated with monastrol. At 38 h AF, the monastrol-treated zygotes were fixed and labeled. (B) Percent of butanol-synchronized control zygotes that had not yet formed spindles (triangles) at the indicated times, and the percent of monastrol-treated zygotes with aberrant spindles at 38 h AF (circles). Cells that had divided were not included in this analysis. Control and treated populations were significantly different at all time points (single asterisk indicates $P < 0.05$ and double asterisks indicate $P < 0.01$). (C) Percent of telophase, short bipolar and multipolar spindles in monastrol-treated zygotes. The vast majority of the zygotes in telophase divided normally by 48 h AF. Standard error bars are shown.

terns observed in animals [14,15]. We interpret this localization pattern to be *bona fide* for several reasons. First, a tBLASTn search of the related brown alga *E. siliculosis* genome database [16] with full length human Kinesin-5 (KIF11) produced a match of 37% identity and 51% similarity across 239 amino acid residues, including half of the human KIF11 coiled-coil domain to which the antibody was made. Second, the *S. compressa* Kinesin-5-like motor is likely to be structurally and functionally similar to the human motor protein since both are sensitive to monastrol. Third, while anti-Kinesin-5-positive signal is seen most heavily at the forming spindle poles during prophase and at metaphase spindle poles, it is never observed to colocalize with centrosomes in interphase cells. This suggests that the strong association with the spindle poles is not due to non-specific centrosomal labeling. Finally, the weak labeling at the spindle midzone is consistent with the monastrol-induced spindle abnormalities described below. While these observations do not prove that the Kinesin-5 antibody exclusively binds to Kinesin-5 proteins, they strongly suggest it.

Disruption of Kinesin-5-like proteins leads to aberrant spindle morphology

Previous findings showed that addition of monastrol prior to entry into mitosis resulted in multipolar spindles and numerous cytasters, indicating that the putative Kinesin-5 motor is needed for proper spindle assembly [12]. In order to determine whether Kinesin-5-like proteins also function to maintain bipolarity in already established spindles, populations of zygotes were synchronized during mitosis (Fig. 2A). This was accomplished by application of 1-butanol, which reversibly arrests zygotes in metaphase with condensed chromatin and unseparated spindle poles [13]. 1-butanol was applied to zygotes prior to mitotic entry (15 h after fertilization) and by 24 h after fertilization nearly all zygotes had arrested in metaphase (data not shown). Zygotes were released from 1-butanol arrest by washout from 24 to 24.5 h after fertilization, and control zygotes were fixed at hourly intervals thereafter to assess spindle maturation. Simultaneously, another sample was treated with monastrol; the later the time of monastrol addition the more mature the spindles were at the time of treatment. The monastrol-treated zygotes were allowed to develop until 38 h after fertilization and were then fixed and labeled to analyze spindle morphologies. Interestingly, attempts to label Kinesin-5-like proteins in monastrol-treated zygotes were unsuccessful; perhaps due to reduced affinity of Kinesin-5-like proteins for microtubules in the presence of monastrol [8].

Regardless of the time of application, monastrol treatment led to the formation of very short, but still bipolar, spindles and also to multipolar spindles (Fig. 1I and 1J). Multipolar spindles have also been observed following Kinesin-5 gene disruption in higher plants and in invertebrate cells [10,14]. Cytasters were infrequently found in cells possessing short bipolar spindles. The maximal pole-to-pole distances of monastrol-treated and control spindles were measured. Short bipolar spindles were approximately half the length of untreated control spindles (Table 1). In contrast to animals [9], spindles of *S. compressa* rarely collapsed fully to monasters.

Following 1-butanol washout at 24 h after fertilization, control zygotes entered mitosis very rapidly; most had formed spindles within 30 min. The percent of zygotes that were pre-mitotic dropped from 36.6 ± 9.3% at 30 min after washout to 6.6 ± 4.8% at 3.5 h after washout (Fig. 2B). The percent of aberrant (short bipolar plus multipolar) spindles in the monastrol-treated zygotes was significantly higher than the percent of zygotes containing pre-mitotic spindles at the time of drug addition (Fig. 2B). Thus, the aberrant spindles must not arise exclusively from zygotes entering mitosis and improperly assembling a spindle. That is, a large portion of disrupted spindles must have originated from pre-formed bipolar spindles that partially collapsed or broke apart. This suggests that in brown algae, Kinesin-5-like proteins are required for maintenance of spindle integrity.

Spindle morphology and progression through the cell cycle were analyzed in greater detail in the monastrol-treated populations. As expected, the later monastrol was added, the greater the percentage of zygotes that progressed to telophase by 38 h after fertilization (Fig. 2C), suggesting these zygotes were past metaphase when drug was applied. Thus, the percentage of aberrant spindles decreased with later treatment time. The percentage of zygotes with multipolar spindles declined more steeply with time than did the percentage with short bipolar spindles.

Table 1: Spindle pole-to-pole distance in control and monastrol-treated zygotes

Spindle category	Distance (μm) ± SE
Washout control spindles	17.39 ± 0.12
Short bipolar spindles in monastrol-treated zygotes	7.75 ± 0.44†
Multipolar spindles in monastrol-treated zygotes*	19.22 ± 0.24

† indicates significant ($P < 0.01$) difference from controls or multipolar spindles
* greatest distance between two spindle poles

These findings suggest that monastrol treatment may have different effects on cells entering mitosis compared to those that already possess a spindle. We previously reported that treatment of young zygotes with monastrol well before entry into mitosis resulted in nearly all cells forming multipolar spindles [12]. Thus, spindle pole breakup and formation of multipolar spindles may preferentially occur as spindles are assembled. The current data are consistent with this hypothesis. The percentage of cells that were pre-mitotic at the time of drug addition was quite similar to the percentage of cells forming multipolar spindles following treatment. Furthermore, zygotes treated later in mitosis tended to form relatively more short spindles than multipolar spindles. An interesting possibility is that the formation of short spindles is due to shortening of bipolar spindles upon drug addition, whereas the formation of multipolar spindles is due to improper assembly of spindles, leading to spindle pole breakup prior to achievement of bipolarity. It does however remain a formal possibility that monastrol-treated spindles form properly but break apart or collapse while trying to maintain bipolarity.

Discussion

Kinesin-5 motors are highly conserved throughout the eukaryote lineage [1]. Interestingly, while the localization and function of these motors in *S. compressa* and animals are similar, they are distinct from those of higher plants, protists, and invertebrates. In *S. compressa* and animals, Kinesin-5-like motors are sequestered within the nucleus during interphase and localize to the spindle poles during mitosis, but in higher plants these motors decorate cortical microtubules throughout the cell cycle [10]. Furthermore, disruption of motor function with monastrol induces spindle abnormalities in both *S. compressa* and animal cells, but has little effect on higher plant or Dictyostelium cells [9-12,17]. These observations suggest that the mechanisms by which brown algae build and maintain bipolar spindles are more closely related to mechanisms operating in animal cells than to those of vascular plants. While the extent of this relatedness has yet to be fully understood, it may be due in part to ancient conserved mechanisms of spindle formation possessed by centrosomal organisms but lacking in non-centrosomal ones. There is, however, a difference between the abnormal spindles formed in *S. compressa* and animal cells. Animal cells exclusively form monasters whereas the algal zygotes produce multipolar and short bipolar spindles, and to a lesser degree monasters. The lower incidence of monasters may indicate that in brown algae additional forces, perhaps provided by other motors, function to maintain some degree of spindle pole separation in the absence of Kinesin-5-like activity.

Abbreviations

(AF): after fertilization; (ASW): artificial sea water.

Competing interests

The authors declare that they have no competing interests.

Authors' contributions

NTP and ACM carried out the experiments, NTP and DLK wrote the manuscript, and DLK raised the funds. All authors have read and approved the final manuscript.

Acknowledgements

This work was supported by NSF awards IOB-0414089 and IOS-0817045 to DLK.

References

1. Kikkawa M: **The role of microtubules in processive kinesin movement.** *Trends Cell Biol* 2008, **18(3)**:128-135.
2. Miki H, Okada Y, Hirokawa N: **Analysis of the kinesin superfamily: insights into structure and function.** *Trends Cell Biol* 2005, **15(9)**:467-476.
3. Lawrence CJ, Dawe RK, Christie KR, Cleveland DW, Dawson SC, Endow SA, Goldstein LSB, Goodson HV, Hirokawa N, Howard J, *et al.*: **A standardized kinesin nomenclature.** *J Cell Biol* 2004, **167(1)**:19-22.
4. Sawin KE, Mitchison TJ: **Mutations in the kinesin-like protein Eg5 disrupting localization to the mitotic spindle.** *Proc Natl Acad Sci USA* 1995, **92(10)**:4289-4293.
5. Brier S, Lemaire D, DeBonis S, Forest E, Kozielski F: **Identification of the protein binding region of S-Trityl-L-cysteine, a new potent inhibitor of the mitotic Kinesin Eg5.** *Biochem* 2004, **43**:13072-13082.
6. DeBonis S, Simorre JP, Crevel I, Lebeau L, Skoufias DA, Blangy A, Ebel C, Gans P, Cross R, Hackney DD, Wade RH, Kozielski F: **Interaction of the mitotic inhibitor monastrol with human Kinesin Eg5.** *Biochem* 2003, **42**:338-349.
7. Maliga Z, Kapoor TM, Mitchison TJ: **Evidence that monastrol is an allosteric inhibitor of the mitotic kinesin Eg5.** *Chem & Biol* 2002, **9(9)**:989-996.
8. Cochran JC, Gatial JE III, Kapoor TM, Gilbert SP: **Monastrol inhibition of the mitotic kinesin Eg5.** *J Biol Chem* 2005, **280**:12658-12667.
9. Kapoor TM, Mayer TU, Coughlin ML, Mitchison TJ: **Probing spindle assembly mechanisms with monastrol, a small molecule inhibitor of the mitotic kinesin, Eg5.** *J Cell Biol* 2000, **150(5)**:975-988.
10. Bannigan A, Scheible W-R, Lukowitz W, Fagerstrom C, Wadsworth P, Somerville C, Baskin TI: **A conserved role for kinesin-5 in plant mitosis.** *J Cell Sci* 2007, **120(16)**:2819-2827.
11. Tikhonenko I, Nag DK, Martin N, Koonce M: **Kinesin-5 is not essential for mitotic spindle elongation in Dictyostelium.** *Cell Motil Cytoskel* 2008, **65(11)**:853-862.
12. Peters NT, Kropf DL: **Kinesin-5 motors are required for organization of spindle microtubules in Silvetia compressa zygotes.** *BMC Plant Biol* 2006, **6(19)**:1-10.
13. Peters NT, Logan KO, Miller AC, Kropf DL: **Phospholipase D signaling regulates microtubule organization in the fucoid alga Silvetia compressa.** *Plant Cell Physiol* 2007, **48**:1764-1774.
14. Sharp DJ, Brown HM, Kwon M, Rogers GC, Holland G, Scholey JM: **Functional Coordination of Three Mitotic Motors in Drosophila Embryos.** *Mol Biol Cell* 2000, **11(1)**:241-253.
15. Kapitein LC, Peterman EJG, Kwok BH, Kim JH, Kapoor TM, Schmidt CF: **The bipolar mitotic kinesin Eg5 moves on both microtubules that it crosslinks.** *Nature* 2005, **435(7038)**:114-118.
16. ***E. siliculosis* genome database** [http://www.genoscope.cns.fr/spip/Whole-genome-random-shotgun.html]
17. Touitou I, Lhomond G, Pruliere G: **Boursin, a sea urchin bimC kinesin protein, plays a role in anaphase and cytokinesis.** *J Cell Sci* 2001, **114(3)**:481-491.

CHAPTER 7

THE MICROTUBULE PLUS-END BINDING PROTEIN EB1 FUNCTIONS IN ROOT RESPONSES TO TOUCH AND GRAVITY SIGNALS IN ARABIDOPSIS

The Plant Cell, Vol. 20: 396–410, February 2008, www.plantcell.org © 2008 American Society of Plant Biologists

The Microtubule Plus-End Binding Protein EB1 Functions in Root Responses to Touch and Gravity Signals in *Arabidopsis*

Sherryl R. Bisgrove,[a,1] Yuh-Ru Julie Lee,[b] Bo Liu,[b] Nick T. Peters,[c] and Darryl L. Kropf[c]

[a] Department of Biological Sciences, Simon Fraser University, Burnaby, British Columbia, Canada V5A 1S6
[b] Section of Plant Biology, University of California, Davis, California 95616
[c] Biology Department, University of Utah, Salt Lake City, Utah 84112

Microtubules function in concert with associated proteins that modify microtubule behavior and/or transmit signals that effect changes in growth. To better understand how microtubules and their associated proteins influence growth, we analyzed one family of microtubule-associated proteins, the END BINDING1 (EB1) proteins, in *Arabidopsis thaliana* (EB1a, EB1b, and EB1c). We find that antibodies directed against EB1 proteins colocalize with microtubules in roots, an observation that confirms previous reports using EB1-GFP fusions. We also find that T-DNA insertion mutants with reduced expression from *EB1* genes have roots that deviate toward the left on vertical or inclined plates. Mutant roots also exhibit extended horizontal growth before they bend downward after tracking around an obstacle or after a 90° clockwise reorientation of the root. These observations suggest that leftward deviations in root growth may be the result of delayed responses to touch and/or gravity signals. Root lengths and widths are normal, indicating that the delay in bend formation is not due to changes in the overall rate of growth. In addition, the genotype with the most severe defects responds to low doses of microtubule inhibitors in a manner indistinguishable from the wild type, indicating that microtubule integrity is not a major contributor to the leftward deviations in mutant root growth.

INTRODUCTION

Since plants are sessile, they respond to changes in the environment by modifying their growth. Changes in growth are usually effected by altering patterns of cell expansion and cell division, and microtubules are key players in both processes. In addition, the microtubule arrays found in plants are strikingly different from the arrays found in other eukaryotes. Higher plant cells lack centrosomes, and microtubules in expanding interphase cells are found beneath the plasma membrane in parallel arrays that encircle the cell. Cell elongation is perpendicular to the microtubules, which are thought to regulate expansion by influencing cell wall properties, while the wall mechanically constrains the direction of expansion (reviewed in Wasteneys and Fujita, 2006). Plant microtubules also behave differently from those of other eukaryotes in mitosis. Prior to entering mitosis, a preprophase band of microtubules, actin, and associated proteins assembles in the cortex at the position of the future division site. Upon entry into mitosis, the preprophase band gives way to the mitotic spindle and the cell cortex becomes devoid of microtubules. Without centrosomes, plant spindles are barrel-shaped with unfocused poles and no astral microtubules. As cells exit anaphase, the spindle breaks down and a unique cytokinetic structure, the phragmoplast, assembles in the center of the cell. The phragmoplast is a cylindrical array composed of actin filaments and opposing sets of parallel microtubules that control cell plate deposition. As cytokinesis proceeds, the phragmoplast and cell plate expand centrifugally and fuse to the mother cell wall at the site marked by the preprophase band. After cytokinesis, cortical microtubules reappear and are organized into parallel arrays (for reviews, see Wasteneys, 2002; Gardiner and Marc, 2003).

How microtubules are regulated and how they influence growth are key questions in plant cell biology. Microtubules are dynamic structures that are usually growing or shrinking within the cell. The dynamic nature of microtubules provides the flexibility that allows rearrangements into different arrays. Microtubules also function in concert with a fleet of microtubule-associated proteins that modify microtubule dynamics and influence microtubule interactions with other subcellular structures (Niethammer et al., 2007). To understand how microtubules and their associated proteins influence plant growth, we are analyzing one family of microtubule associated proteins, the END BINDING1 (EB1) proteins in *Arabidopsis thaliana*.

EB1 belongs to a group of microtubule-associated proteins that are known as microtubule plus-end tracking proteins because they preferentially accumulate at the rapidly growing or plus ends of microtubules. Although EB1 has been intensively studied in animal and fungal cells, how it functions remains enigmatic (Vaughan, 2005). Recent work has shown that EB1 proteins bind to microtubule plus ends at the seam that joins the tubulin protofilaments into a tube-shaped structure (Sandblad et al., 2006). In addition to microtubules, EB1 also interacts with several other proteins, including many of the known microtubule plus-end tracking proteins. This observation has led to the proposal that EB1 is an integrator of protein complex assembly

[1] Address correspondence to sbisgrov@sfu.ca.
The author responsible for distribution of materials integral to the findings presented in this article in accordance with the policy described in the Instructions for Authors (www.plantcell.org) is: Sherryl R. Bisgrove (sbisgrov@sfu.ca).
www.plantcell.org/cgi/doi/10.1105/tpc.107.056846

on microtubules (Vaughan, 2005; Lansbergen and Akhmanova, 2006). In some cases, EB1 facilitates delivery of its interacting partners to specific subcellular sites. Examples include the axonal targeting of a voltage-gated potassium channel in neuronal cells (Gu et al., 2006), the delivery of DRhoGEF2 (a guanine nucleotide exchange factor) to target sites in the cell cortex in *Drosophila melanogaster* (Rogers et al., 2004), the melanophilin-dependent transfer of melanosomes from microtubule plus ends to actin at the distal ends of melanocytes (Wu et al., 2005), and the delivery of connexin to adherens junctions in animal cells (Shaw et al., 2007). EB1 proteins are also involved in microtubule searching of the cytoplasm for specific capture sites (Su et al., 1995; Morrison et al., 1998; Tirnauer et al., 1999, 2002a; Bloom, 2000; Miller et al., 2000; Tirnauer and Bierer, 2000; Nakamura et al., 2001). Capture sites often contain F-actin, and EB1 proteins can therefore link the microtubule and actin cytoskeletons in specific cellular domains (Goode et al., 2000; Carvalho et al., 2003). EB1-mediated microtubule search and capture is thought to facilitate mitotic spindle alignment and assembly, microtubule binding to chromosomes, and cargo delivery to specific sites within the cell (Bloom, 2000; Bienz, 2001; Hayles and Nurse, 2001; Schroer, 2001; Schuyler and Pellman, 2001; Segal and Bloom, 2001; Tirnauer et al., 2002a, 2002b; Galjart and Perez, 2003; Green et al., 2005). While bound to microtubules, EB1 proteins also influence microtubule dynamics. Recent in vitro analyses indicate that EB1 affects dynamics by suppressing shortening of the microtubule plus ends (Manna et al., 2008).

Although EB1 has been the object of intense scrutiny in yeast and cultured animal cells, analyses in multicellular systems are just beginning. So far, *eb1* mutants have been described in *Dictyostelium discoideum* and *D. melanogaster*, and in both organisms the phenotypes are surprisingly mild. Rehberg and Graf (2002) found that a *Dictyostelium eb1* null mutant was viable but had defects in spindle formation that slowed the progression into metaphase. Mutants were able to overcome many of the spindle defects after prolonged cultivation. In the first genetic study of EB1 in a developing metazoan, Elliott et al. (2005) showed that hypomorphic Dm *EB1* mutants did not display any obvious defects in spindle assembly or mitosis but did have neuromuscular defects.

In plants, several groups have reported subcellular localization patterns of green fluorescent protein (GFP) fusions to At EB1 proteins (Chan et al., 2003, 2005; Mathur et al., 2003; Van Damme et al., 2004a, 2004b; Abe and Hashimoto, 2005; Dhonukshe et al., 2005; Dixit et al., 2006). These analyses show that plant EB1-GFP fusions colocalize with microtubules and exhibit microtubule plus end tracking ability. In addition, Van Damme et al. (2004b) have shown that overexpression of one EB1 family member increased microtubule polymerization rates, indicating that EB1 proteins can influence microtubule dynamics in plant cells.

Complete analysis of the role of EB1 proteins in plants requires analysis of mutant phenotypes. The existence of *Arabidopsis eb1* mutants has been reported in a review article (Kaloriti et al., 2007). Here, we find that *Arabidopsis eb1* mutants have root growth defects. Mutant roots deviate toward the left when grown on vertically oriented or inclined agar plates. Mutant roots also exhibit delayed responses to gravity after tracking around an obstacle in their path or after a 90° clockwise rotation of the root. These delays suggest that EB1 plays a role in initiating downward bends in response to gravity and/or touch signals, and this may be the reason for the enhanced leftward deviations in root growth observed in mutants. We also find that EB1 antibodies colocalize with microtubules in roots, an observation that confirms previous reports using At EB1-GFP fusions.

RESULTS

Surveys of the *Arabidopsis* genome reveal three *EB1* genes, designated *EB1a* (At3g47690), *EB1b* (At5g62500), and *EB1c* (At5g67270) (Figure 1A; Chan et al., 2003; Gardiner and Marc, 2003; Mathur et al., 2003; Meagher and Fechheimer, 2003; Bisgrove et al., 2004). Each gene is predicted to code for 31.7-, 32.7-, and 35.8-kD proteins that are 54 to 63% similar and 37 to 41% identical to human EB1 (National Center for Biotechnology Information accession number AAC09471) at the amino acid level. Each predicted protein also contains two domains that are conserved in EB1 proteins from diverse organisms. Microtubule binding has been mapped to the calponin homology domain near the N terminus, while the coiled-coil EB1 domain is involved in protein–protein interactions (Bu and Su, 2003; Figure 1B). The *Arabidopsis* EB1 family members are closely related to each other. At the amino acid level, EB1a is 78% identical to EB1b, and EB1c is more divergent; it is 49% identical to EB1a and EB1b. Most of the sequence identity maps to the conserved calponin homology and EB1 domains of the proteins.

To determine where *EB1* genes are expressed, several organs were assayed for the presence or absence of transcripts. RT-PCR experiments revealed that *EB1* genes are expressed in multiple plant tissues (Figure 1C). All three *EB1* genes are expressed in cotyledons, leaves, flowers, siliques, and roots, and two family members, *EB1a* and *EB1c*, were detected in stems. Coexpression of multiple *EB1* genes in the same tissues raises the possibility that the genes could have overlapping functions. Curiously, cDNA from some organs yielded more PCR product than others. Although these experiments were not quantitative in nature, this observation raises the possibility that expression from *EB1* genes varies across different organs. Lower expression levels could be due to either a uniform reduction in expression throughout the organ or a restriction of expression to a subset of cells within the organ. Hence, the weaker PCR bands observed in roots could be due to a confinement of expression to actively elongating or dividing cells.

EB1 Proteins Colocalize with Microtubules in Roots

Previous reports have shown that GFP-tagged At EB1 proteins colocalize with microtubules and track microtubule plus ends in plant cells (Chan et al., 2003, 2005; Mathur et al., 2003; Van Damme et al., 2004a, 2004b; Abe and Hashimoto, 2005; Dhonukshe et al., 2005; Dixit et al., 2006). We used an alternative approach to assess EB1 localization. Affinity-purified polyclonal antibodies were generated against bacterially expressed full-length EB1c, the most divergent of the three family members (Figure 1B). Protein gel blot analysis of bacterially expressed proteins showed that the antibodies recognized both EB1c and

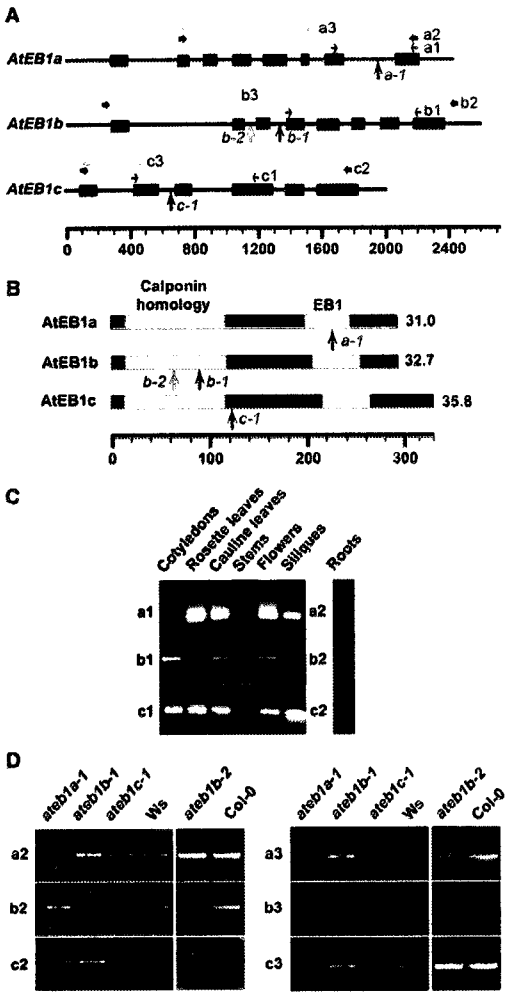

Figure 1. Expression Analysis of *EB1* Genes.

(A) *EB1* genes, with introns designated as lines and exons as boxes. Horizontal arrows mark the positions of the PCR primers used in RT-PCR experiments (primers are not drawn to scale). Thin black arrows indicate the a1, b1, and c1 primer pairs, thick black arrows represent the a2, b2, and c2 primer pairs, and gray arrows represent a3, b3, and c3 primer pairs (corresponding to *EB1a*, *EB1b*, and *EB1c*, respectively). Scale is in nucleotides.

(B) Predicted EB1 proteins contain conserved calponin homology and EB1 domains (gray boxes). Vertical arrows in **(A)** and **(B)** designate the sites of T-DNA insertions. Black arrows mark the insertion sites in plants from the Ws genetic background, while the gray arrow represents the insertion site of the *eb1b-2* allele in the Col-0 background.

EB1a (Figure 2A). Although EB1b was not tested, because EB1a shares 78% sequence identity with EB1b and only 49% identity with EB1c, the antibodies most likely cross-react with all three EB1 family members. The antibodies also detected a major band around 35 kD in protein extracts from wild-type seedlings (Figure 2B). Since the three EB1 proteins are very close in size, this band is most likely an unresolved triplet.

EB1 localization was examined in wild-type root tips where the antibodies labeled microtubules in preprophase bands, mitotic spindles, and phragmoplasts (Figure 3). Localization to mitotic and cytokinetic arrays in plant cells has previously been reported for At EB1 fusions to GFP (Chan et al., 2003, 2005; Mathur et al., 2003; Van Damme et al., 2004a; Dhonukshe et al., 2005). EB1 antibodies labeled microtubules throughout these arrays, a pattern that could reflect either EB1 localization along the lengths of microtubules or preferential localization to the ends of short microtubules that are distributed throughout the arrays. In the preprophase band, EB1 appears to be more abundant toward the center of the band. Changes in microtubule dynamics have been observed during preprophase band formation, and one model proposes that dynamic microtubules are recruited into the preprophase band by a search and capture mechanism (Dhonukshe and Gadella, 2003; Vos et al., 2004). Preferential localization to the center of the preprophase band suggests that EB1 proteins could play a role in this recruitment process. The EB1 antibodies labeled microtubules in the mitotic spindle, as has previously been observed for EB1 proteins in other eukaryotic cells (Berrueta et al., 1998; Morrison et al., 1998; Rehberg and Graf, 2002; Rogers et al., 2002; Tirnauer et al., 2002b), including plants (Chan et al., 2003, 2005; Van Damme et al., 2004a). In the phragmoplast, EB1 antibodies label more abundantly in the midzone, suggesting that EB1 proteins are biased toward microtubule plus ends. In many interphase cells, the nuclear region labeled intensely and a more diffuse, punctuate pattern was observed in the cytoplasm. Perinuclear and cytoplasmic microtubules were also visible in these cells. Although the significance of nuclear-associated EB1 is not clear, a transient perinuclear array of microtubules (the radial array) has been detected in plant cells that are exiting cytokinesis (Hasezawa et al., 1991), and it is possible that EB1 proteins are associated with these microtubules. Nuclear labeling of GFP-tagged EB1a has also been reported in cytokinetic *Arabidopsis* suspension cells (Chan et al., 2003, 2005). In addition, nuclear labeling has also been reported for an At EB1c-GFP fusion in interphase *Arabidopsis* and BY-2 cells (Dixit et al., 2006). Although not visible in this photograph, occasional EB1 puncta were observed in association with the cortical microtubules of interphase root tip cells. Previous studies with At EB1-GFP fusions report numerous EB1 puncta in the

(C) RT-PCR analyses using RNA from wild-type (Ws) plants indicate that *EB1* genes are coexpressed in multiple plant organs.

(D) RT-PCR analyses using RNA isolated from flowers indicate that full-length transcripts are undetectable in each homozygous *eb1* mutant line (left panel). However, partial transcripts corresponding to sequences 5′ of the insertion site are detected (right panel). In **(C)** and **(D)**, the PCR primer pairs used in each analysis are indicated to the left of the appropriate lanes.

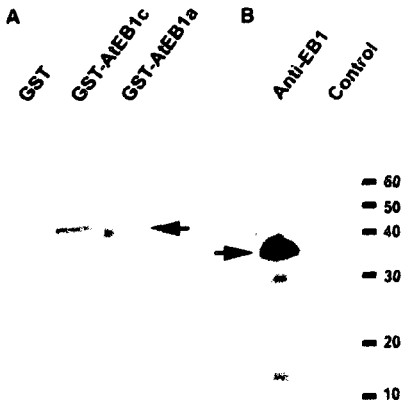

Figure 2. EB1 Antibodies Recognize Multiple EB1 Family Members.

(A) Protein gel blot analysis of bacterially expressed GST, GST-EB1c, and GST-EB1a.

(B) Protein gel blot analysis of wild-type plant extract with anti-EB1 and secondary antibody only (Control). The lower bands on the blot are due to nonspecific labeling of the secondary antibodies, since they are present on blots probed with secondary antibodies alone (Control lane). Arrows indicate the positions of major 35-kD bands corresponding to EB1 proteins.

cortex of elongating interphase cells (Chan et al., 2003; Van Damme et al., 2004b; Dhonukshe et al., 2005; Dixit et al., 2006). Why interphase cells in the root tip would have fewer cortical EB1 puncta than other cell types is not clear. Perhaps there is a shift toward EB1 accumulation on cortical microtubules as cells exit the cell cycle and enter the elongation zone of the root.

EB1c-Enriched Antibodies Preferentially Label Microtubule Plus Ends

We also investigated the labeling patterns associated with a pool of antibodies more specific for EB1c, the original antigen. To enrich for EB1c-specific antibodies, a column containing bacterially expressed EB1a protein was used to remove antibodies that recognize epitopes common to EB1a and EB1c from the pool. When used as a probe in protein gel blot analyses, the anti-EB1c enriched pool clearly detected a band at ~35 kD from plants carrying intact versions of the *EB1c* gene (Figure 4A). Bands were barely detectable in samples from mutants carrying the *eb1c-1* allele, suggesting that the pool is significantly enriched for EB1c-specific antibodies. When used on dividing *Arabidopsis* cells, the EB1c labeling was biased toward the midzones of spindles and phragmoplasts, where the plus ends of microtubules are more concentrated (Figures 4B to 4I). Scans of fluorescence intensity across the phragmoplast confirmed that EB1c labeling was most intense in the midline of the phragmoplast, between opposing sets of microtubules (Figure 4E).

Identification of Plants Carrying T-DNA Insertions in *EB1* Genes

To assess the effects of altering *EB1* expression on plant growth and development, we isolated plants carrying T-DNA insertions in each of the three *EB1* genes from the BASTA population at the Wisconsin Knockout Facility (Krysan et al., 1999; Weigel et al., 2000). The alleles were designated *eb1a-1*, *eb1b-1*, and *eb1c-1*. Each line was backcrossed to wild-type Wassilewskija (Ws) plants three times, and the genotypes of F1 and F2 progeny were verified by PCR using primers specific for *EB1* genes and the T-DNA insert (see Methods). The PCR fragments were sequenced to determine the positions of the T-DNA insertions in each gene (Figures 1A and 1B). To test for the presence of T-DNA insertions at additional sites in the

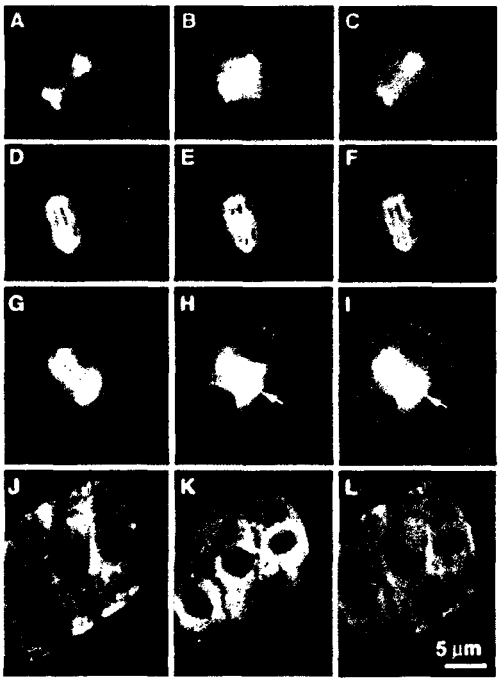

Figure 3. EB1 Proteins Colocalize with Microtubules in Meristematic Root Tip Cells.

Root tip squashes double labeled with monoclonal antitubulin ([A], [D], [G], and [J]) and polyclonal anti-EB1 ([B], [E], [H], and [K]) imaged by epifluorescence microscopy. Merged images ([C], [F], [I], and [L]) are false colored with microtubules in red and EB1 in green. EB1 colocalizes with microtubules in the preprophase band ([A] to [C]), the mitotic spindle ([D] to [F]), and the phragmoplast ([G] to [I]). In an interphase cell with a radial array of microtubules, EB1 antibodies label the nuclear region and the cytoplasm in a punctuate pattern. Bar in [L] = 5 μM and applies to all cells.

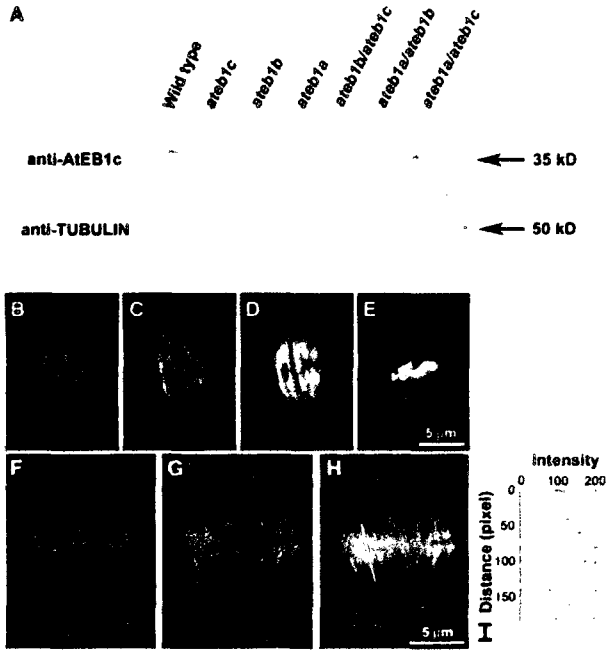

Figure 4. An Anti-EB1c-Enriched Pool of Antibodies Labels Microtubules in a Spindle and the Phragmoplast.

(A) Protein gel blot analysis of extracts from mutant and wild-type plants probed with the anti-EB1c pool of antibodies (top panel). Labeling is reduced or absent in samples from seedlings carrying the *eb1c-1* allele. Probing with anti-tubulin antibodies reveals that all lanes contain approximately equivalent amounts of protein (bottom panel). Arrows mark the positions of bands corresponding to At EB1c (~35 kD) and tubulin (~50 kD).
(B) to **(E)** Labeling with EB1c antibodies is biased toward microtubule plus ends in a metaphase spindle from an *Arabidopsis* root tip cell and in a phragmoplast from an *Arabidopsis* suspension cell. Both cells were double-labeled with anti-EB1c-enriched antibodies **([B]** and **[F])** and anti-tubulin antibodies **([C]** and **[G])** and were imaged by confocal microscopy. The spindle was also labeled with 4′,6-diamidino-2-phenylindole to visualize chromosomes at the metaphase plate **(E)**. Merged images **([D]** and **[H])** and single labels are false colored with EB1c in green and microtubules in red. Intensity scans across the phragmoplast **(E)** show that EB1c is concentrated toward the midzones, near the plus ends of microtubules. The white line marks the position of the intensity scan.

genome, F2 progeny from backcrosses to Ws plants were grown on Basta-containing agar plates. Since Basta resistance is conferred by the T-DNA insert, F2 plants from a line with an insertion at a single site will segregate 3 resistant to 1 sensitive, while lines with multiple unlinked insertions will have a higher number of Basta-resistant F2 plants. For all three lines, F2 progeny from backcrosses exhibit 3:1 segregation for Basta resistance. These lines, therefore, carry either a single T-DNA insertion or multiple closely linked insertions. The *eb1b-2* allele was identified using the SIGnAL T-DNA Express *Arabidopsis* gene mapping tool at the Salk Institute website (http://signal.salk.edu/cgi-bin/tdnaexpress). The WiscDsLox331A08 line in the Columbia (Col-0) genetic background was found to carry an insertion in the *EB1b* gene; it was designated as *eb1b-2*, and the corresponding seeds were obtained from The Arabidopsis Information Resource (TAIR; Garcia-Hernandez et al., 2002; Alonso et al., 2003). Progeny from plants heterozygous for the *eb1b-2* allele also segregate 3 resistant to 1 sensitive when grown on Basta-containing agar plates.

Insertional lines were also analyzed for the presence of *EB1* transcripts by RT-PCR. First, PCR primers located on opposite sides of the T-DNA insertion site were used (a2, b2, and c2 primer pairs; Figure 1). We were unable to detect transcripts corresponding to genes carrying T-DNA insertions, indicating that *EB1* gene activity is disrupted in mutants (Figure 1D). We also analyzed mutants for the presence of partial transcripts using primer pairs located 5′ of the T-DNA insertion site (a3, b3, and c3 primers; Figure 1). In every case, transcripts corresponding to sequences 5′ of the T-DNA insertion were detected, indicating that transcription from mutant genes is not completely abolished. The locations of the T-DNAs within the genes predict that if truncated proteins were translated from the partial transcripts, the proteins would be missing at least part of the conserved EB1 domain. The *eb1a-1* insertion is located in the middle of the EB1

domain, the *eb1b-1* and *eb1b-2* insertions fall in the calponin homology domain, and in *eb1c-1*, the T-DNA is located 3′ of the calponin homology domain (Figure 1B). These mutations, therefore, may not be completely devoid of gene function.

Root Growth Is Affected in *eb1* Mutants

Plants homozygous for *eb1a-1*, *eb1b-1*, *eb1b-2*, or *eb1c-1* are all fertile, with leaves, flowers, and stems similar in appearance to wild-type organs at the gross morphological level. Double and triple mutant combinations were generated with the *eb1a-1*, *eb1b-1*, and *eb1c-1* lines in the Ws genetic background. In every case, plants were fertile and obvious defects in aerial structures were not apparent (data not shown). To assess possible root growth defects, three analyses were conducted. First, seedlings were grown on agar plates that were oriented vertically. Under these conditions, *eb1* mutants exhibited root growth that skewed toward the left of the plate when viewed from above the agar surface (Figure 5). The most pronounced skewing was observed in *eb1b-1* mutants. All mutant combinations that were homozygous for *eb1b-1* showed skewing that was significantly different from wild-type roots ($P \leq 0.01$) when the average angle at which roots deviated from the vertical direction was measured. Roots of *eb1a-1* and *eb1c-1* mutants also skewed to the left, but less dramatically than *eb1b-1*, and only *eb1c-1* mutants had skewing angles significantly different from the wild type ($P \leq 0.01$).

Second, on agar plates inclined by 45°, all *eb1* genotypes exhibited leftward-oriented root growth that was significantly different from wild-type plants ($P \leq 0.01$). On inclined plates, root skewing was again most pronounced in genotypes homozygous for *eb1b-1* (Figure 5). Double and triple mutant combinations skewed about the same amount as single mutants. Although skewing is reduced in the Col-0 genetic background, *eb1b-2* roots also exhibit significantly more leftward deviation in growth than Col-0 ($P = 0.002$; Figure 6). Third, on inclined plates containing a higher agar concentration (1.6% rather than 0.8%) all *eb1* genotypes had roots that skewed toward the left (data not shown). Plants homozygous for *eb1b-1* again showed the most dramatic defects; they tended to form leftward (clockwise) oriented loops more often than wild-type roots (Figure 7). Closer examination of loops revealed that they were associated with epidermal cell files that were twisted into left-handed helices (Figure 7B). Occasionally, loops with twisted epidermal cell files were also observed in wild-type roots. The amount of twisting in mutant and wild-type loops appeared identical, and mutant loops were not associated with excessive twisting of epidermal cell files. These analyses suggest that *EB1* family members influence root growth. Individual homozygous mutants all had a root skewing phenotype, indicating that intact *EB1* family members were not able to compensate for mutated genes. *eb1b-1* mutants had the most severe defects, suggesting that either *EB1b* plays a larger role in root growth or the *eb1b-1* allele retains less function than the *eb1a-1* and *eb1c-1* alleles.

Because *eb1b-1* mutants exhibited the strongest phenotype, we chose this line to assess root growth in heterozygous plants. Thirty-five F2 progeny from crosses between wild-type and *ateb1b-1* plants were analyzed on inclined 0.8% agar plates and then genotyped either by PCR or by testing the F3 progeny from individual F2 plants for Basta resistance. We found that homozygous *eb1b-1* roots exhibited the most pronounced leftward skewing; on average their roots skewed 44° (C.I. = 4.5°) to the left of a vertical vector. Heterozygous roots skewed significantly less than homozygotes (Student's *t* test, $P = 0.01$) with an average skewing angle of 36° (C.I. = 6°). Skewing in wild-type roots (31°, C.I. = 9°) was slightly, but not significantly, less than heterozygous plants (Student's *t* test, $P = 0.24$). Therefore, *eb1b-1* is recessive.

eb1b Mutants Exhibit Defects in Response to Gravity/Touch Stimuli

Roots growing on inclined agar plates respond to a combination of touch and gravity stimuli, and mutants with altered responses to these stimuli often exhibit skewed root growth and/or loop formation (Okada and Shimura, 1990; Rutherford and Masson, 1996). To investigate the responses of *eb1* mutants to touch and/or gravity, we monitored the ability of roots to navigate around an obstacle placed in their path. Plants were grown on vertically oriented plates. After 9 d, a cover slip was inserted into the agar just in front of the root tip, plates were rotated to position root tips parallel with the gravity vector, and roots were observed after they had navigated around the barrier. As previously described (Massa and Gilroy, 2003), wild-type roots tracked across the cover slip, and when they reached the edge, they curved downwards in response to gravity (Figure 8A). *eb1* mutants also grew across the cover slip. However, when they reached the edge, many roots did not bend down but instead continued to grow horizontally before forming a downward curvature (Figure 8B). On average, wild-type Ws roots formed a bend within 0.25 mm (C.I. = 0.04) of the edge of the cover slip (Figure 8C). *eb1a-1* and *eb1c-1* roots grew 0.37 (C.I. = 0.11) and 0.35 (C.I. = 0.05) mm, respectively, beyond the edge of the cover slip, a distance that is significantly greater than wild-type plants ($P \leq 0.01$ by Student's *t* test). *eb1b-1* and triple mutants continued to grow horizontally for a much longer distance than any of the other genotypes. *eb1b-1* roots grew an average of 0.69 mm (C.I. = 0.21), and triple mutants grew ~0.72 mm (C.I. = 0.27) before forming downward bends. Delays were also observed in *eb1b-2* roots. Wild-type Col-0 plants formed bends ~0.2 mm (C.I. = 0.03) from the edge of the cover slip, while *eb1b-2* roots continued to grow horizontally for ~0.36 mm (C.I. = 0.13) before they bent down.

To assess whether mutant roots are also delayed in their response to a change in the gravity vector, seedlings on vertical agar plates were rotated to reorient the root tip horizontally. Roots were photographed prior to rotation and again after gravitropic bends were completed. The two images were superimposed in Photoshop, and the distance from the root tip before reorientation to the downward bend that formed afterwards was measured. Triple and *eb1b-1* mutants were chosen for these analyses since they exhibited the longest delays in the obstacle navigation assay described above. When roots were rotated in the clockwise direction, the left side of the root was positioned on the top, and both *eb1b-1* and triple mutants exhibited significant delays before forming downward bends ($P \leq 0.05$ and 0.01, respectively, by Student's *t* test; Figure 8D). Wild-type roots grew ~0.43 mm (C.I. = 0.14) before bending down, while *eb1b-1* and

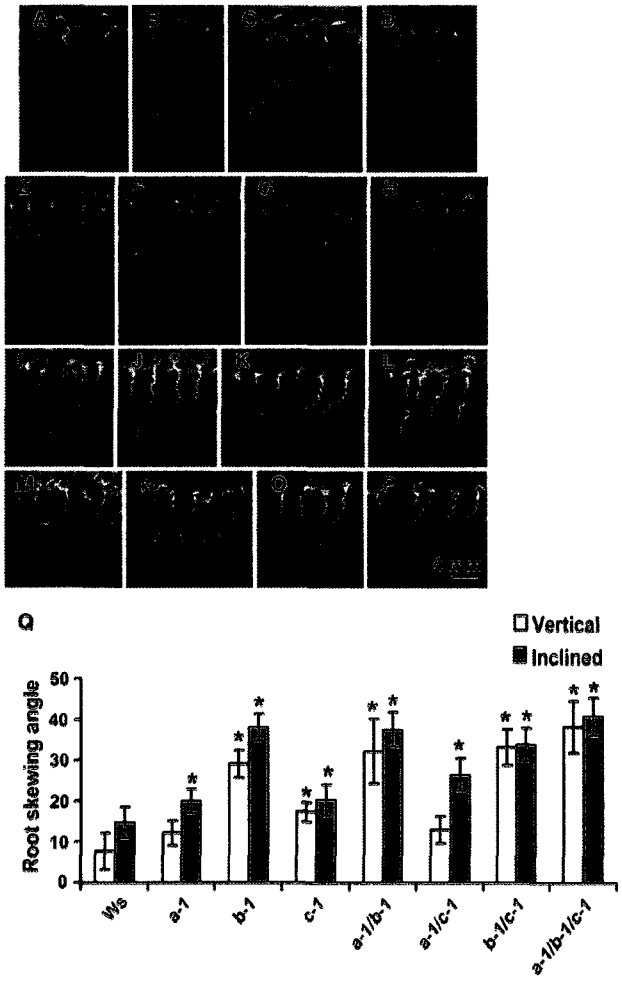

Figure 5. Roots of *eb1* Mutants Skew toward the Left.

On both vertically oriented ([A] to [H]) and inclined ([I] to [P]) agar plates, wild-type (Ws) roots grow down with a slight leftward deviation when viewed from above the agar surface ([A] and [I]). All *eb1* genotypes exhibit leftward deviations in growth that are stronger than the wild type, *eb1a-1* ([B] and [J]), *eb1b-1* ([C] and [K]), *eb1c-1* ([D] and [L]), *eb1a-1/eb1b-1* ([E] and [M]), *eb1a-1/eb1c-1* ([F] and [N]), *eb1b-1/eb1c-1* ([G] and [O]), and *eb1a-1/eb1b-1/eb1c-1* ([H] and [P]). The average angle at which roots deviated from the vertical direction (root skewing angle) was determined for each genotype on both vertically (open bars) and inclined (gray filled bars) agar plates (Q). Angles are reported in degrees, and confidence intervals (C.I.s) are calculated at P = 0.01. On vertically oriented plates, $n = 186$ (10 to 31 seedlings per genotype), and on inclined plates $n = 316$ (32 to 48 seedlings per genotype). Asterisks denote average angles that are significantly different from the wild type ($P \leq 0.01$) by Student's *t* test.

triple mutants grew 0.64 (C.I. = 0.39) and 0.89 (C.I. = 0.42) mm, respectively. By contrast, rotating roots in the counterclockwise direction positioned the left side of the root on the bottom, and mutant roots were able to bend down with kinetics similar to wild-type plants.

Overall Elongation Is Normal in *eb1* Roots

To determine whether *eb1* mutants have general defects in root expansion, we analyzed root growth and root tip morphology. Mutant root tips appeared morphologically normal, and root

widths and elongation rates were similar to the wild type (Figure 9). Mutant roots grew at a slightly faster rate than the wild type, but statistical analysis indicated that this difference was not significant ($P > 0.01$). Only *eb1c-1* roots grown on inclined agar plates were slightly, but significantly ($P < 0.01$), thinner than the wild type. The fact that root widths and growth rates were normal in *eb1* mutants indicates that the primary defect is not in the regulation of overall root expansion. In addition, observations at the cellular level failed to reveal any obvious defects in cell size, shape, or organization in mutant roots (data not shown).

Microtubule Stability in *eb1* Roots

Since directional biases in root growth are sometimes associated with changes in microtubule stability (for example, Ishida and Hashimoto, 2007; Ishida et al., 2007), we assessed the sensitivities of *eb1* mutants to the microtubule inhibitors oryzalin and taxol. Treating *Arabidopsis* seedlings with low doses of microtubule inhibitors is known to alter microtubule dynamics (Nakamura et al., 2004). Adding oryzalin, a microtubule destabilizing agent, to the growth medium inhibited root elongation in a

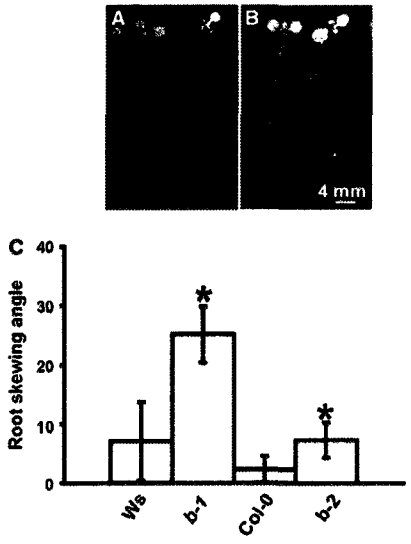

Figure 6. In the Col-0 Genetic Background, *eb1b-2* Mutant Roots Also Deviate toward the Left.

(A) and **(B)** When grown on inclined 0.8% agar plates, Col-0 roots **(A)** exhibit a slight deviation toward the left, and this leftward skewing is enhanced in the *eb1b-2* allele **(B)**.

(C) The average root skewing angle was determined for the wild type (Ws and Col-0, open bars) as well as for *eb1b-1* and *eb1b-2* mutants (gray bars). Angles are reported in degrees, and C.I.s are calculated at $P = 0.01$. $n = 79$ (9 to 27 seedlings per genotype), and asterisks denote average angles that are significantly different from the wild type ($P \leq 0.01$) by Student's *t* test.

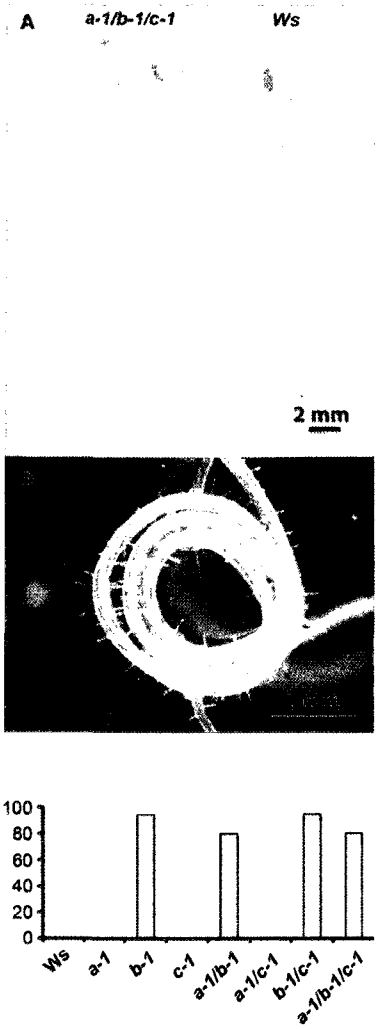

Figure 7. Mutant Roots Form Clockwise Oriented Loops and Coils on Inclined Plates with a High Concentration of Agar (1.6%).

(A) A triple mutant has formed a clockwise coil (seedling on the left), while the wild-type seedling (right) has not.

(B) Epidermal cell files in the coil of a *triple* mutant root are twisted into left-handed helices.

(C) A representative experiment showing a percentage of cells forming loops and/or coils. Greater than 75% of roots homozygous for *eb1b-1* formed loops and/or coils, while the same structures were not observed in the other genotypes. In this experiment, $n = 160$ (15 to 23 seedlings per genotype). Although the proportions of roots that form loops varies between experiments, *eb1b* mutants always form loops at much higher frequencies than the other genotypes.

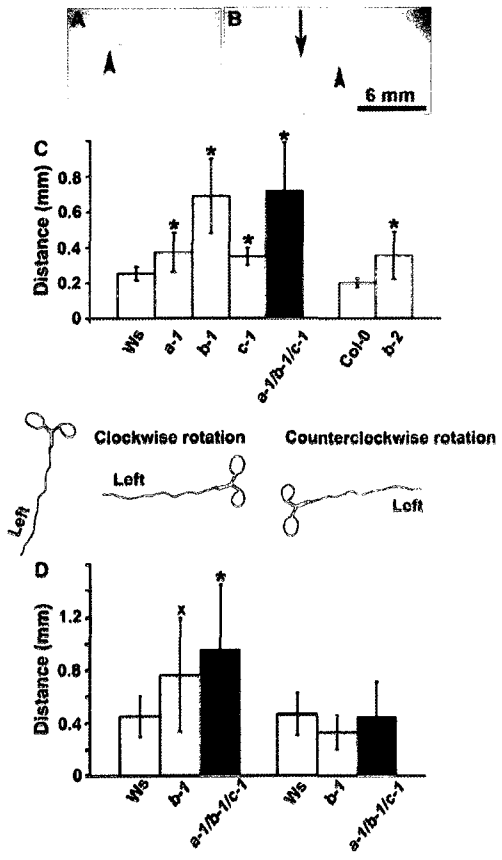

Figure 8. Analysis of Bend Formation in Roots Navigating around a Barrier or after a 90° Reorientation of the Root Tip.

(A) and **(B)** Wild-type roots **(A)** track across the barrier and at the edge they immediately bend down. *eb1b-1* mutants **(B)** continue to grow horizontally beyond the edge of the barrier. Arrowheads in denote the edge of the cover slip, and the arrow in **(B)** indicates the position of the downward gravitropic bend.

(C) The average distance between the edge of the cover slip and downward curvature was calculated for each genotype. $n = 306$ (18 to 88 seedlings per genotype).

(D) *eb1* roots exhibit delays in bend formation when seedlings are rotated clockwise but not when they are rotated counterclockwise. The average distance between the position of the root tip at the time of rotation and the subsequent downward curvature was determined for each genotype. For clockwise rotations, $n = 39$ (10 to 15 roots per genotype), and for counterclockwise rotations $n = 36$ (10 to 16 roots per genotype).

The asterisk and the "X" denote average angles that are significantly different from the wild type by Student's t test ($P \leq 0.01$ and ≤ 0.05, respectively). Open bars denote wild-type plants (either Ws or Col-0), gray bars indicate single *eb1* mutants, and black bars represent triple mutants. C.I.s are reported at $P = 0.01$.

dose-dependant manner for all of the genotypes tested (Figure 10A). At each concentration of oryzalin, root elongation was inhibited by about the same amount in *eb1a-1*, *eb1b-1*, *eb1b-2*, Ws, and Col-0, indicating that these genotypes are all equally sensitive to the drug. Root elongation in *eb1c-1* and triple mutants, by contrast, was more severely inhibited at 0.2 and 0.1 μM oryzalin, respectively, indicating that these genotypes are more sensitive to oryzalin treatment. In addition to decreasing root elongation, 0.1 μM oryzalin also increased the amount of leftward skewing exhibited by *eb1a-1*, *eb1b-1*, *eb1b-2*, Ws, and Col-0 roots. For each mutant, root skewing was increased by about the same amount as it was in the corresponding wild-type plant. By contrast, oryzalin did not increase root skewing in *eb1c-1* or triple mutants. In 0.1 μM oryzalin, *eb1c-1* roots skewed about the same amount as they did in DMSO controls. Triple mutants skewed less in oryzalin than they did in DMSO, although these roots were also much shorter and may not have grown enough to exhibit much leftward deviation in growth. Taxol, a drug that stabilizes microtubules, also inhibited root elongation and increased leftward skewing. In taxol, however, all of the genotypes responded in a similar fashion (Figure 10B). Analysis of variance was used to statistically test for genotypic differences in root skewing responses to either oryzalin or taxol treatment (Zar, 1974). This analysis revealed significant differences only between the wild type and *eb1c-1* or triple mutants in oryzalin ($P = 0.0182$ for *eb1c-1* and $P = 0.0007$ for triple mutants). It is important to note that the responses of *eb1b-1*, the genotype that exhibits the most skewing, were statistically indistinguishable from those of wild-type plants. We also observed cortical microtubules in wild-type and triple mutant roots fixed and labeled with antitubulin antibodies and were unable to detect differences in microtubule organization (Figure 10C). Thus, we were unable to correlate the *eb1* root skewing phenotype with a change in the integrity of cortical microtubules.

DISCUSSION

The ability of a plant to direct root growth through the soil is vitally important for survival, and roots change the direction of their growth in response to a myriad of signals. Gravity, gradients of moisture and nutrients, as well as rocks and other impediments in the soil trigger bends that redirect root growth in a more favorable direction. Here, we report that roots of *eb1* mutants exhibit delays in the initiation of downward bends after growing around an obstacle or after a 90° clockwise reorientation of the root. The fact that bend initiation is delayed suggests that mutants are slow to perceive, transmit, and/or respond to signals that induce downward root bending. *eb1* roots also have a greater tendency to form loops when grown on tilted agar plates, a phenotype that has also been associated with gravitropic defects (Okada and Shimura, 1990; Mullen et al., 1998b; Ferrari et al., 2000; Rashotte et al., 2001).

In the literature, the stability and organization of microtubules has been associated with directional biases in root growth (Furutani et al., 2000; Hashimoto, 2002; Thitamadee et al., 2002; Sedbrook et al., 2004; Abe and Hashimoto, 2005; Ishida et al., 2007; Ishida and Hashimoto, 2007). For the *eb1* alleles described here, however, microtubule defects do not appear to

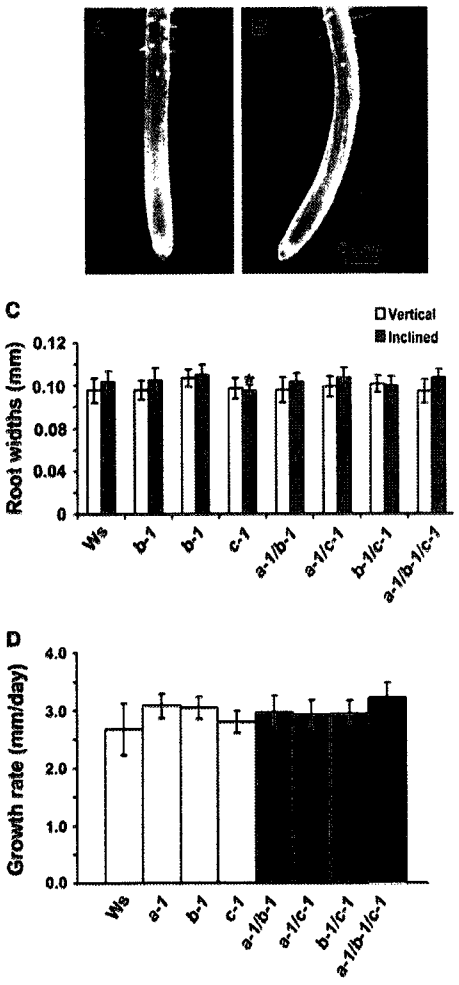

Figure 9. Root Elongation and Morphology Is Not Altered in *eb1* Mutants.

(A) and **(B)** Wild-type **(A)** and triple mutant **(B)** root tips are morphologically similar.

(C) Average root widths, measured at the base of the elongation zone where root hair emergence begins, are similar for all genotypes, regardless of whether they are grown on vertically oriented (white bars) or inclined (gray bars) agar plates. The asterisk indicates a slight, but significant ($P < 0.01$ by Student's *t* test), difference between *eb1c-1* and the wild type. On vertically oriented plates, $n = 217$ (19 to 39 seedlings per genotype), and on inclined plates $n = 239$ (27 to 33 seedlings per genotype).

(D) When grown on vertically oriented plates, the elongation rate of mutants did not deviate significantly from the wild type (white bar), although mutant roots grew at slighter faster rates. Light-gray bars denote single *eb1* mutants, dark-gray bars indicate double mutants, and the triple mutant is shown in black. $n = 238$ (16 to 40 seedlings measured per genotype). Widths are reported in millimeters, elongation rates in millimeters/day, and C.I.s are calculated at $P = 0.01$.

be linked to the deviations in root growth. This conclusion is based on the fact that the genotype with the strongest leftward growth bias, *eb1b-1*, responds to microtubule inhibitors in a manner that is statistically indistinguishable from wild-type plants. Of the *eb1* single mutant lines examined, only *eb1c-1* roots are more sensitive to microtubule disruption. Why this is the case is not clear, although the observation does indicate that EB1 family members influence microtubules in different ways. Others have reported different effects of individual EB1 homologs on microtubules. Van Damme et al. (2004b) found that overexpression of EB1a:GFP increased microtubule polymerization rates and overexpression of EB1b:GFP did not. Mathur et al. (2003) report that overexpressed mouse EB1:GFP labeled entire microtubules and reduced their growth rates, but overexpression of At EB1b:GFP did not.

Delays in bend initiation could explain the enhanced leftward deviations in root growth that occur when *eb1* mutants are grown on the surface of an agar plate. On inclined or vertically oriented agar surfaces, *Arabidopsis* roots grow in a waving pattern that is thought to be produced through a combination of normal root tip circumnutatory movements and growth responses to touch and gravity signals (Okada and Shimura, 1990; Rutherford and Masson, 1996). The tilted agar surface seems to act as a barrier; a root growing vertically downward touches the surface of the agar, triggering an obstacle avoidance response that bends the root away from the downward trajectory. The agar surface also impedes movement of the root tip, causing the root to bend as cells behind the tip continue to elongate (Thompson and Holbrook, 2004). In either case, the root senses that its growth direction is no longer vertical and responds by reorienting the direction of growth downwards until the tip once again contacts the agar surface, triggering another cycle of bending (Okada and Shimura, 1990; Rutherford and Masson, 1996; Sedbrook, 2004). We find that when *eb1* root tips encounter an obstacle and rotate away from the gravity vector, they undergo prolonged horizontal growth rather than immediately bending down. If similar delays occurred each time a mutant root tip encountered the agar surface, they would, over time, produce a root that deviated from the vertical more than the wild type.

Although bend initiation is delayed in mutant roots after encountering obstacles or after clockwise reorientations, there is no delay when roots are rotated in the counterclockwise direction. Why the delay would depend on which way the root is rotated is not clear, but it may be related to the directional growth bias that is present in wild-type plants. Ws roots have a growth bias that causes their tips to rotate more toward the left as they circumnutate down the plate (for reviews, see Migliaccio and Piconese, 2001; Oliva and Dunand, 2007). Clockwise reorientations place the left flanks of roots on top. Because of the leftward growth bias, these roots tend to circumnutate upwards and their tips would hit the agar surface before they could circle around

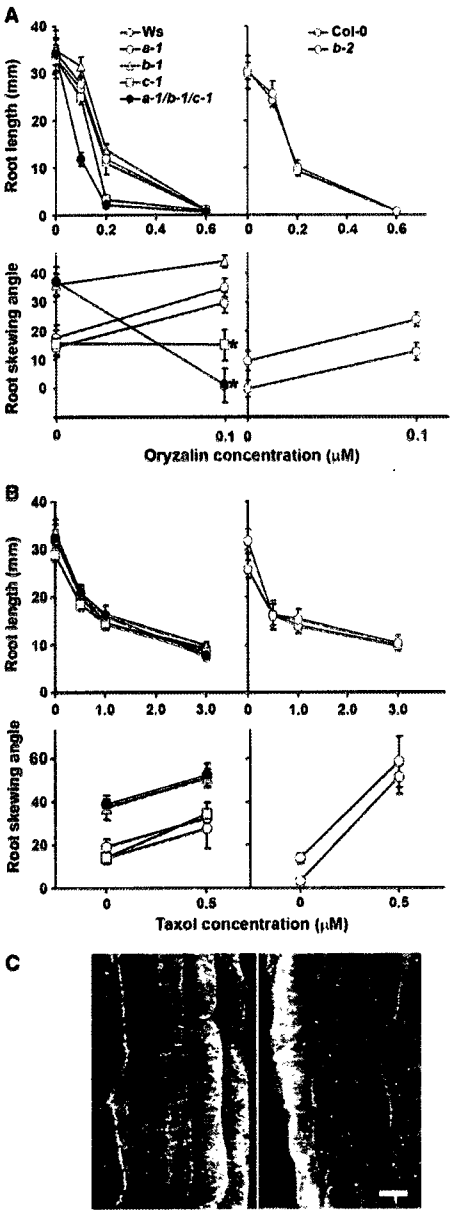

Figure 10. Microtubule Integrity in *eb1* Roots.

(A) and **(B)** Several *eb1* genotypes were germinated on agar plates containing different concentrations of oryzalin **(A)** or taxol **(B)**. On the third day, the position of the root tip was marked and the seedlings were allowed to continue growth for a total of 7 d, at which time root skewing angles and the amount of growth between day 3 and day 7 were measured. For all genotypes tested, root growth decreased with increasing concentrations of oryzalin or taxol (top panels in **[A]** and **[B]**), although *eb1c-1* and triple mutants were more sensitive to oryzalin than were the other genotypes. Low concentrations of oryzalin or taxol in the medium (0.1 and 0.5 μM, respectively) increased root skewing angles in all genotypes except *eb1c-1* and the triple mutant (bottom panels in **[A]** and **[B]**). Open circles denote wild-type plants (either Ws or Col-0), gray symbols indicate single mutants, and black circles designate triple mutants.

(C) Microtubules, visualized by immunofluorescence and confocal microscopy, in triple mutant (left panel) and Ws root cells (right panel) are similar in appearance.

into the downward direction. Contact with the agar provides a touch stimulus that is thought to modulate gravitropism and bend the root away from the surface (Massa and Gilroy, 2003). If mutants have trouble responding to gravity after contact with the agar surface, they would exhibit delays in downward bend formation. Wild-type roots, on the other hand, have no problems responding to gravity and they would form downward bends without delay. By contrast, counterclockwise reorientations position the left flanks of roots on the bottom. This time circumnutation rotates the tips downwards without interference from the agar, and both mutants and wild-type plants form downward bends without delay.

How might EB1 proteins function in the initiation of root bending? A bend is initiated when cells across the root begin elongating at different rates. In roots that have been reoriented into a horizontal plane, cell elongation increases on the upper flank and decreases on the lower flank, causing the root to bend down (Mullen et al., 1998a). Changes in elongation rates are thought to be effected via alterations in the extensibility of the cell wall (McQueen-Mason et al., 2007). The fact that *eb1* roots exhibit extended horizontal growth before they initiate a bend suggests that there are delays in triggering changes in elongation rates across the root. However, overall elongation appears to be normal since mutant roots are the same lengths and widths as wild-type plants. One possibility is that EB1 proteins are involved in relaying the signals that effect changes in cell elongation rates across the root. In animal and fungal cells, EB1 facilitates the delivery of certain proteins, including signaling molecules and ion channels, to specific places in the cell (Rogers et al., 2004; Vaughan, 2005; Wu et al., 2005; Gu et al., 2006; Lansbergen and Akhmanova, 2006; Shaw et al., 2007). By analogy, At EB1 could target proteins that trigger changes in cell expansion rates to their sites of action in elongating root cells.

The root growth phenotype observed for *eb1* mutants is rather mild given the roles proposed for EB1 proteins in cultured animal and fungal cells. However, it is important to note that budding and fission yeast lines carrying null mutations in *EB1* genes are viable even though each organism carries only one *EB1* homolog in its genome (Chen et al., 2000; Miller et al., 2000). In addition, mild *eb1* phenotypes have also been reported for both of the nonplant multicellular organisms that have been examined. In

Dictyostelium, a null *eb1* mutant was viable but its cells progressed through metaphase more slowly than the wild type (Rehberg and Graf, 2002). In addition, hypomorphic *Drosophila EB1* mutants form fully viable larvae that pupate and develop into morphologically normal adults with neuromuscular defects (Elliott et al., 2005).

Why *Arabidopsis eb1* mutants exhibit mild phenotypes is not clear. Perhaps there are other microtubule-associated proteins that overlap functionally with EB1 in plant cells. This is the case in *Schizosaccharomyces pombe*, where spindle defects were unveiled in cells carrying mutations in both the *S. pombe* EB1 homolog (*MINICHROMOSOME ALTERED LOSS3*) and *MICROTUBULE OVEREXTENDED1* (*MOE1*), another microtubule-associated protein (Chen et al., 2000). A *MOE1* homolog is present in the *Arabidopsis* genome (Bisgrove et al., 2004), and analyses of *eb1 moe1* double mutants could provide additional information about At EB1 functions. It is also possible that the mutant lines reported here do not carry null alleles, since all of the mutants express partial transcripts that could encode proteins with some functional capabilities. Whatever the reason for the mild phenotypes in *Arabidopsis*, these alleles do reveal a role for EB1 proteins in root responses to gravity and/or touch signals, a result that may not have been apparent in lines with more severe defects.

METHODS

Plants and Growth Conditions

Wild-type Ws seeds were obtained from TAIR (http://www.Arabidopsis.org/), and *eb1* alleles were identified by screening the BASTA population at the Wisconsin Knockout Facility according to protocols on the website (http://www.biotech.wisc.edu/*Arabidopsis*/default.htm; Krysan et al., 1999; Weigel et al., 2000). For phenotypic analyses, seeds were sterilized using the vapor phase method outlined in Clough and Bent (1998) and placed on either 0.8 or 1.6% Phytablend agar plates containing half-strength Murashige and Skoog (MS) medium (Sigma-Aldrich) with 0.5 g MES per liter and a pH of 5.8. Seeds were vernalized in the dark at 4°C for 3 to 7 d and then grown at 20°C under either constant light or a 16-h-light/8-h-dark cycle. Drug sensitivities were assayed by germinating seedlings on 0.8% Phytablend agar plates containing half-strength MS and one of 25 mg/L glufosinate-ammonium (Pestanal; Sigma-Aldrich), paclitaxel, or oryzalin. For protein isolation, seeds were germinated for 3 d in the dark with shaking (200 rpm) in half-strength MS liquid medium supplemented with 1% sucrose. To analyze root growth, seedlings were photographed using a Toshiba 4.0 megapixel digital camera, and measurements were made using either Photoshop or ImageJ. Statistical analyses were performed in Excel (Student's *t* tests) or JMP 6 (analysis of variance testing).

PCR Analyses

RNeasy and DNeasy kits (Qiagen) kits were used to extract RNA and DNA from plant organs. RNA was reverse transcribed using the Promega reverse transcription system and the oligo(dT) primers provided in the kit. The product from the reverse transcription reaction was diluted 100-fold and used as a template in PCR amplification using Ex Taq polymerase (TaKaRa). The primers used for PCR amplification were as follows: a1 forward 5′-CAAGCTCCGGGATGTAGAGA-3′, a1 reverse 5′-TCCAGTTGTTCTCCGTTTCC-3′, b1 forward 5′-AGCCATTGGAAGTCAACAGG-3′, b1 reverse 5′-TTTGCATCGGTTGCGTATAA-3′, c1 forward 5′-GTCGAAGAGGCTTGTTCAGG-3′, c1 reverse 5′-TGAGTACCGGTGTTGTTGGA-3′, a2 forward 5′-GCTGTGCAATGTCAGATGCT-3′, a2 reverse 5′-TCCAGTTGTTCTCCGTTTCC-3′, b2 forward 5′-CGTTTCAGAGAGGGGTTCAA-3′, b2 reverse 5′-TTGTGCAAACATCCTCTCCA-3′, c2 forward 5′-*ATTGGGATGATGGATTCTGC-3′*, *c2 reverse* 5′-*AAGGCGTTGTCTTGG*AGAGA-3′, a3 forward 5′-GTCGAAGAGGCTTGTTCAGG-3′, a3 reverse 5′-TGAGATCCACGAGCTCCTTC-3′, b3 forward 5′-TTGTTTTCGGTTTCACCTAACC-3′, b3 reverse 5′-CCAACATTTGACATTGCACAG-3′, c3 forward 5′-GCCGTTAGAGAGAGACAGATCG-3′, and c3 reverse 5′-GCTGGCCTCCATTAACAGAA-3′. The identities of amplification products were verified by excising and sequencing bands from agarose gels.

T-DNA insertional alleles and wild-type plants were genotyped by PCR using Ex Taq polymerase and the following primers: JL202 5′-CATTTTATAATAACGCTGCGGACATCTAC-3′ (T-DNA insertion), At3g47690F 5′-ACCCATTTCTTCTATCGCTCTCGTTTCCA-3′, At3g47690R 5′-CCAGCCATTGTTCGTCACCCTTCTACTTA-3′, At5g62500F 5′-GCTTCTCCGTCCTTTTCTCTGCTTCAGTT-3′, At5g62500R 5′-TTCGGTTCAGTTCACTGTAAAACCAAAAA-3′, At5g67270F 5′-TTGAATTGAAAACTCCGCTCTCGTCTCTT-3′, and At5g67270R 5′-CGGTTCTTGCGTTTGTCTTTCTGTTCCTC-3′.

Preparation of EB1 Antibodies

Glutathione *S*-transferase (GST) fusion protein constructs were made by PCR amplifying EB1 coding sequences from the cDNA clones 188D24 and U23125, corresponding to EB1c and EB1a, respectively, using Vent DNA polymerase (New England Biolabs). To make the GST-EB1c construct, the following primers were used: ateb5e 5′-CGGGAATTCTGGGCTACGAACATTGGG-3′ and sp6 5′-ATTTAGGTGACACTATAG-3′. The amplified DNA fragment was digested with *Eco*RI and *Hin*DIII and then cloned into the pGEX-KG vector (Guan and Dixon, 1991) at the corresponding restriction enzyme sites. The GST-EB1a construct was amplified from U23125 using the following primers: III47690.5r 5′-CGGAATTCAAATGGCGACGAACATC-3′ and III47690.3x 5′-AGAGACTCGAGGGCTTGAGTCTTTTCTTC-3′. The amplified fragment was then digested with *Eco*RI and *Xho*I and cloned into pGEX-KG at the corresponding sites. Both fusion proteins were expressed in the *Escherichia coli* strain BL21(DE3)pLysS (Novagen). GST fusion proteins were affinity purified with glutathione-sepharose as described by the manufacturer (Pierce Chemical).

The GST-EB1c fusion protein was used as an antigen to raise polyclonal antibodies in rabbits at the Comparative Pathology Laboratory (University of California, Davis, CA). To purify antibodies, three recombinant proteins, GST, GST-EB1c, and GST-EB1a, were conjugated to AminoLink coupling gel (Pierce Chemical), and antibodies were subjected to affinity purification with these columns according to the manufacturer's instructions. The GST column was used to remove anti-GST antibodies. The GST-EB1c column was used to purify antibodies with affinity for all three EB1 family members. To enrich for EB1c-specific antibodies, the GST-EB1a column was used to deplete the pool of antibodies that recognize epitopes common to EB1a and EB1c. AtEB1c-specific antibodies were then purified once more with the GST-EB1c column.

Immunoblotting

Protein extracts were prepared from plant tissues as described previously (Liu et al., 1996), separated by SDS-PAGE, and then transferred to nitrocellulose membranes prior to immunoblotting. The secondary antibody was alkaline phosphatase-conjugated goat anti-rabbit IgG (Bio-Rad), and a colorimetric detection method using nitro blue tetrazolium chloride/5-bromo-4-chloro-3-indolyl phosphate substrate solution (Bio-Rad) was used.

Immunofluorescence Microscopy

Whole-mount roots were prepared using a modification of the freeze shatter protocol outlined in Wasteneys et al. (1997). Briefly, roots were

fixed for 1 to 2 h at room temperature under a vacuum in PEM buffer (50 mM PIPES, 2 mM EGTA, and 2 mM $MgSO_4$, pH 7.2) containing 1.5% (v/v) formaldehyde, 0.5% (v/v) gluteraldehyde, and 5% (v/v) DMSO. Fixed roots were rinsed two to three times with PEM and then placed on slides coated with poly-L-lysine (Sigma-Aldrich), a cover slip was clipped to the slide over the root, and the assembly was briefly immersed in liquid nitrogen. While still frozen, the eraser on the end of a pencil was used to apply pressure to the cover slip and roots, the cover slip was removed, and the roots were digested 30 min at room temperature in PEM, pH 5.5, containing 1% (w/v) cellulase Y-6 (ICN), pectolyase Y-23 (ICN), and 0.1 mM phenylmethyl sulfonyl fluoride (Sigma-Aldrich). Tissue was rinsed in PEM, pH 7.2, incubated 10 min in −20°C methanol, and then rehydrated in PBS (2.8 mM NaCl, 54 mM KCl, 200 mM Na_2HPO_4, 36 mM KH_2PO_4, and 2% [w/v] sodium azide, pH 7.3) and incubated for 20 min in PBS with 1 mg/mL sodium borohydride. Prior to antibody addition, roots were rinsed in PBS and then incubated for 30 min in incubation buffer (PBS with 50 mM glycine added). Antibodies (monoclonal DM1A; Sigma-Aldrich) to label microtubules as well as the secondary antibodies Alexa Fluor 488 goat anti-rabbit and Alexa Fluor 546 goat anti-mouse (Molecular Probes) were applied overnight at room temperature in incubation buffer. Finally, roots were rinsed in incubation buffer, incubated for 20 min in −20°C methanol, mounted in 1 part benzyl alcohol:2 parts benzyl benzoate, and imaged using a Zeiss LSM 510 confocal microscope or an Olympus IMT-2 equipped with fluorescence and a Photometrics CoolSnap CCD camera.

Squashed root cells were prepared according to the method described by Palevitz (1988). Briefly, *Arabidopsis thaliana* roots were fixed in 4% paraformaldehyde in PEM buffer, followed by digestion with 1% cellulase in PEM. The *Arabidopsis* suspension cell line, generated in the laboratory of Luca Comai at the University of Washington, was provided to us by the laboratory of Richard Michelmore. The cells were grown in MS basal medium supplemented with 4.2 mg/L naphthylacetic acid and 0.02 mg/L kinetin at 21°C and processed as described previously (Liu et al., 1996). Both root squashes and tissue cultured cells were labeled with anti-EB1 and DM1a antibodies followed by fluorescein isothiocyanate–conjugated goat anti-rabbit IgG (Sigma-Aldrich) and Texas Red X-conjugated goat anti-mouse IgG (Molecular Probes). Images were collected under a Leica TCS SP2 confocal microscope (Leica Microsystems). All figures were assembled using the Photoshop 7.0 program (Adobe Systems).

Accession Numbers

Sequence data from this article can be found in the Arabidopsis Genome Initiative or GenBank/EMBL databases under the following accession numbers: At4g47690, NM_114637, At5g62500, NM_125644, At5g67270, and NM_126127.

ACKNOWLEDGMENTS

We gratefully acknowledge three undergraduate researchers for conducting some of the experimental analyses reported here. Adam Carrick assisted in the isolation of *eb1* mutant alleles, John Reich analyzed EB1 gene expression in wild-type plants by RT-PCR, and Michele Barakat assayed root growth on vertical and inclined agar plates. The work was supported by a Natural Sciences and Engineering Research Council of Canada Postdoctoral Fellowship (PDF-219981-1999) and Discovery Grant (Application 331017) awarded to S.R.B., a University of Utah Seed Grant and a National Science Foundation Grant (IOB-0414089) awarded to D.L.K., and a National Research Initiative of the USDA Cooperative State Research, Education, and Extension Service grant (2005-35304-16031) awarded to Y.-R.J.L. and B.L.

Received November 9, 2007; revised January 20, 2008; accepted January 31, 2008; published February 15, 2008.

REFERENCES

Abe, T., and Hashimoto, T. (2005). Altered microtubule dynamics by expression of modified α-tubulin protein causes right-handed helical growth in transgenic *Arabidopsis* plants. Plant J. **43:** 191–204.

Alonso, J.M., et al. (2003). Genome-wide insertional mutagenesis of *Arabidopsis thaliana*. Science **301:** 653–657.

Berrueta, L., Kraeft, S.-K., Tirnauer, J.S., Schuyler, S.C., Chen, L.B., Hill, D.E., Pellman, D., and Bierer, B.E. (1998). The adenomatous polyposis coli-binding protein EB1 is associated with cytoplasmic and spindle microtubules. Proc. Natl. Acad. Sci. USA **95:** 10596–10601.

Bienz, M. (2001). Spindles cotton on to junctions, APC and EB1. Nat. Cell Biol. **3:** E1–E3.

Bisgrove, S.R., Hable, W.E., and Kropf, D.L. (2004). +TIPs and microtubule regulation. The beginning of the plus end in plants. Plant Physiol. **136:** 3855–3863.

Bloom, K. (2000). It's a kar9ochore to capture microtubules. Nat. Cell Biol. **2:** E96–E98.

Bu, W., and Su, L.-K. (2003). Characterization of functional domains of human EB1 family proteins. J. Biol. Chem. **278:** 49721–49731.

Carvalho, P., Tirnauer, J.S., and Pellman, D. (2003). Surfing on microtubule ends. Trends Cell Biol. **13:** 229–237.

Chan, J., Calder, G., Fox, S., and Lloyd, C. (2005). Localization of the microtubule end binding protein EB1 reveals alternative pathways of spindle development in Arabidopsis suspension cells. Plant Cell **17:** 1737–1748.

Chan, J., Calder, G.M., Doonan, J.H., and Lloyd, C.W. (2003). EB1 reveals mobile microtubule nucleation sites in *Arabidopsis*. Nat. Cell Biol. **5:** 967–971.

Chen, C.-R., Chen, J., and Chang, E.C. (2000). A conserved interaction between Moe1 and Mal3 is important for proper spindle formation in *Schizosaccharomyces pombe*. Mol. Biol. Cell **11:** 4067–4077.

Clough, S.J., and Bent, A.F. (1998). Floral dip: A simplified method for *Agrobacterium*-mediated transformation of *Arabidopsis thaliana*. Plant J. **16:** 735–743.

Dhonukshe, P., and Gadella, T.W.J.J. (2003). Alteration of microtubule dynamic instability during preprophase band formation revealed by yellow fluorescent protein-CLIP170 microtubule plus-end labeling. Plant Cell **15:** 596–611.

Dhonukshe, P., Mathur, J., Hulskamp, M., and Gadella, T.J. (2005). Microtubule plus-ends reveal essential links between intracellular polarization and localized modulation of endocytosis during division-plane establishment in plant cells. BMC Biol. **3:** 11–25.

Dixit, R., Chang, E., and Cyr, R. (2006). Establishment of polarity during organization of the acentrosomal plant cortical microtubule array. Mol. Biol. Cell **17:** 1298–1305.

Elliott, S.L., Cullen, F., Wrobel, N., Kernan, M.J., and Ohkura, H. (2005). EB1 is essential during *Drosophila* development and plays a crucial role in the integrity of chordotonal mechanosensory organs. Mol. Biol. Cell **16:** 891–901.

Ferrari, S., Piconese, S., Tronelli, G., and Migliaccio, F. (2000). A new *Arabidopsis thaliana* root gravitropism and chirality mutant. *Plant Sci.* **158:** 77–85.

Furutani, I., Watanabe, Y., Prieto, R., Masukawa, M., Suzuki, K., Naoi, K., Thitamadee, S., Shikanai, T., and Hashimoto, T. (2000). The *SPIRAL* genes are required for directional control of cell elongation in *Arabidopsis thaliana*. Development **127:** 4443–4453.

Galjart, N., and Perez, F. (2003). A plus-end raft to control microtubule dynamics and function. Curr. Opin. Cell Biol. **15:** 48–53.

Garcia-Hernandez, M., et al. (2002). TAIR: A resource for integrated *Arabidopsis* data. Funct. Integr. Genomics **2:** 239–253.

Gardiner, J., and Marc, J. (2003). Putative microtubule-associated proteins from the Arabidopsis genome. Protoplasma **222:** 61–74.

Goode, B.L., Drubin, D.G., and Barnes, G. (2000). Functional cooperation between the microtubule and actin cytoskeletons. Curr. Opin. Cell Biol. **12:** 63–71.

Green, R.A., Wollman, R., and Kaplan, K.B. (2005). APC and EB1 function together in mitosis to regulate spindle dynamics and chromosome alignment. Mol. Biol. Cell **16:** 4609–4622.

Gu, C., Zhou, W., Puthenveedu, M.A., Xu, M., Jan, Y.N., and Jan, L.Y. (2006). The microtubule plus-end tracking protein EB1 is required for Kv1 voltage-gated K^+ channel axonal targeting. Neuron **52:** 803–816.

Guan, K.L., and Dixon, J.E. (1991). Eukaryotic proteins expressed in *Escherichia coli:* An improved thrombin cleavage and purification procedure of fusion proteins with glutathione S-transferase. Anal. Biochem. **192:** 262–267.

Hasezawa, S., Marc, J., and Palevitz, B.A. (1991). Microtubule reorganization during the cell cycle in synchronized BY-2 tobacco suspensions. Cell Motil. Cytoskeleton **18:** 94–106.

Hashimoto, T. (2002). Molecular genetic analysis of left-right handedness in plants. Philos. Trans. R. Soc. Lond. B Biol. Sci. **357:** 799–808.

Hayles, J., and Nurse, P. (2001). A journey into space. Nat. Rev. Mol. Cell Biol. **2:** 647–656.

Ishida, T., and Hashimoto, T. (2007). An *Arabidopsis thaliana* tubulin mutant with conditional root-skewing phenotype. J. Plant Res. **120:** 635–640.

Ishida, T., Kaneko, Y., Iwano, M., and Hashimoto, T. (2007). Helical microtubule arrays in a collection of twisting tubulin mutants of *Arabidopsis thaliana.* Proc. Natl. Acad. Sci. USA **104:** 8544–8549.

Kaloriti, D., Galva, C., Parupalli, C., Khalifa, N., Galvin, M., and Sedbrook, J.C. (2007). Microtubule associated proteins in plants and the processes they manage. J. Int. Plant Biol. **49:** 1164–1173.

Krysan, P.J., Young, J.C., and Sussman, M.R. (1999). T-DNA as an insertional mutagen in Arabidopsis. Plant Cell **11:** 2283–2290.

Lansbergen, G., and Akhmanova, A. (2006). Microtubule plus end: A hub of cellular activities. Traffic **7:** 499–507.

Liu, B., Cyr, R.J., and Palevitz, B.A. (1996). A kinesin-like protein, KatAp, in the cells of *Arabidopsis* and other plants. Plant Cell **8:** 119–132.

Manna, T., Honnappa, S., Steinmetz, M.O., and Wilson, L. (2008). Suppression of microtubule dynamic instability by the +TIP protein EB1 and its modulation by the CAP-Gly domain of $p150^{Glued}$. Biochemistry **47:** 779–786.

Massa, G.D., and Gilroy, S. (2003). Touch modulates gravity sensing to regulate the growth of primary roots of *Arabidopsis thaliana.* Plant J. **33:** 435–445.

Mathur, J., Mathur, N., Kernebeck, B., Srinivas, B.P., and Hulskamp, M. (2003). A novel localization pattern for an EB1-like protein links microtubule dynamics to endomembrane organization. Curr. Biol. **13:** 1991–1997.

McQueen-Mason, S.J., Le, N.T., and Brocklehurst, D. (2007). Expansins. In The Expanding Cell, J.-P. Verbelen and K. Vissenberg, eds (Berlin/Heidelberg, Germany: Springer-Verlag), pp. 117–138.

Meagher, R.B., and Fechheimer, M. (September 30, 2003). The *Arabidopsis* cytoskeletal genome. In The Arabidopsis Book, C.R. Somerville and E.M. Meyerowitz, eds (Rockville, MD: American Society of Plant Biologists), doi/10.1199/tab.0096, http://www.aspb.org/publications/arabidopsis/.

Migliaccio, F., and Piconese, S. (2001). Spiralizations and tropisms in Arabidopsis roots. Trends Plant Sci. **6:** 561–565.

Miller, R.K., Cheng, S.-C., and Rose, M.D. (2000). Bim1p/Yeb1p mediates the Kar9p-dependent cortical attachment of cytoplasmic microtubules. Mol. Biol. Cell **11:** 2949–2959.

Morrison, E.E., Wardleworth, B.N., Askham, J.M., Markham, A.F., and Meredith, D.M. (1998). EB1, a protein which interacts with the APC tumour suppressor, is associated with the microtubule cytoskeleton throughout the cell cycle. Oncogene **17:** 3471–3477.

Mullen, J.L., Ishikawa, H., and Evans, M.L. (1998a). Analysis of changes in relative elemental growth rate patterns in the elongation zone of *Arabidopsis* roots upon gravistimulation. Planta **206:** 598–603.

Mullen, J.L., Turk, E., Johnson, K., Wolverton, C., Ishikawa, H., Simmons, C., Soll, D., and Evans, M.L. (1998b). Root-growth behavior of the *Arabidopsis* mutant *rgr1.* Roles of gravitropism and circumnutation in the waving/coiling phenomenon. Plant Physiol. **118:** 1139–1145.

Nakamura, M., Naoi, K., Shoji, T., and Hashimoto, T. (2004). Low concentrations of propyzamide and oryzalin alter microtubule dynamics in *Arabidopsis* epidermal cells. Plant Cell Physiol. **45:** 1330–1334.

Nakamura, M., Zhou, X.Z., and Lu, K.P. (2001). Critical role for the EB1 and APC interaction in the regulation of microtubule polymerization. Curr. Biol. **11:** 1062–1067.

Niethammer, P., Kronja, I., Kandels-Lewis, S., Rybina, S., Bastuaebs, P., and Karsenti, E. (2007). Discrete states of a protein interaction network govern interphase and mitotic microtubule dynamics. PLoS Biol. **5:** e29.

Okada, K., and Shimura, Y. (1990). Reversible root tip rotation in *Arabidopsis* seedlings induced by obstacle-touching stimulus. Science **250:** 274–276.

Oliva, M., and Dunand, C. (2007). Waving and skewing: How gravity and the surface of growth media affect root development in Arabidopsis. New Phytol. **176:** 37–43.

Palevitz, B.A. (1988). Cytochalasin-induced reorganization of actin in *Allium* root cells. Cell Motil. Cytoskeleton **9:** 283–298.

Rashotte, A.M., DeLong, A., and Muday, G.K. (2001). Genetic and chemical reductions in protein phosphatase activity alter auxin transport, gravity response, and lateral root growth. Plant Cell **13:** 1683–1697.

Rehberg, M., and Graf, R. (2002). *Dictyostelium* EB1 is a genuine centrosomal component required for proper spindle formation. Mol. Biol. Cell **13:** 2301–2310.

Rogers, S.L., Rogers, G.C., Sharp, D.J., and Vale, R.D. (2002). *Drosophila* EB1 is important for proper assembly, dynamics, and positioning of the mitotic spindle. J. Cell Biol. **158:** 873–884.

Rogers, S.L., Wiedemann, U., Hacker, U., Turck, C., and Vale, R.D. (2004). *Drosophila* RhoGEF2 associates with microtubule plus ends in an EB1-dependent manner. Curr. Biol. **14:** 1827–1833.

Rutherford, R., and Masson, P.H. (1996). *Arabidopsis thaliana sku* mutant seedlings show exaggerated surface-dependent alteration in root growth vector. Plant Physiol. **111:** 987–998.

Sandblad, L., Busch, K.E., Tittmann, P., Gross, H., Brunner, D., and Hoenger, A. (2006). The *Schizosaccharomyces pombe* EB1 homolog Mal3p binds and stabilizes the microtubule lattice seam. Cell **127:** 1415–1424.

Schroer, T.A. (2001). Microtubules don and doff their caps: Dynamic attachments at plus and minus ends. Curr. Opin. Cell Biol. **13:** 92–96.

Schuyler, S.C., and Pellman, D. (2001). Microtubule "plus-end-tracking proteins": The end is just the beginning. Cell **105:** 421–424.

Sedbrook, J.C. (2004). MAPs in plant cells: Delineating microtubule growth dynamics and organization. Curr. Opin. Plant Biol. **7:** 632–640.

Sedbrook, J.C., Ehrhardt, D.W., Fisher, S.E., Scheible, W.-R., and Somerville, C. (2004). The Arabidopsis *SKU6/SPIRAL* gene encodes a plus end-localized microtubule-interacting protein involved in directional cell expansion. Plant Cell **16:** 1506–1520.

Segal, M., and Bloom, K. (2001). Control of spindle polarity and orientation in *Saccharomyces cerevisiae.* Trends Cell Biol. **11:** 160–166.

Shaw, R.M., Fay, A.J., Puthenveedu, M.A., von Zastrow, M., Jan, Y.-N., and Jan, L.Y. (2007). Microtubule plus-end-tracking proteins target gap junctions directly from the cell interior to adherens junctions. Cell **128:** 547–560.

Su, L.K., Burrell, M., Gyuris, J., Brent, R., Wiltshire, R., Trent, J., Vogelstein, B., and Kinzler, K.W. (1995). APC binds to the novel protein EB1. Cancer Res. **55:** 2972–2977.

Thitamadee, S., Tuchihara, K., and Hashimoto, T. (2002). Microtubule basis for left-handed helical growth in Arabidopsis. Nature **417:** 193–196.

Thompson, M.V., and Holbrook, N.M. (2004). Root-gel interactions and the root waving behavior of *Arabidopsis*. Plant Physiol. **135:** 1822–1837.

Tirnauer, J.S., and Bierer, B.E. (2000). EB1 proteins regulate microtubule dynamics, cell polarity, and chromosome stability. J. Cell Biol. **149:** 761–766.

Tirnauer, J.S., Canman, J.C., Salmon, E.D., and Mitchison, T. (2002b). EB1 targets to kinetochores with attached polymerizing microtubules. Mol. Biol. Cell **13:** 4308–4316.

Tirnauer, J.S., Grego, S., Salmon, E.D., and Mitchison, T. (2002a). EB1-microtubule interactions in *Xenopus* egg extracts: Role of EB1 in microtubule stabilization and mechanisms of targeting to microtubules. Mol. Biol. Cell **13:** 3614–3626.

Tirnauer, J.S., O'Toole, E., Berrueta, L., Bierer, B.E., and Pellman, D. (1999). Yeast Bim1p promotes the G1-specific dynamics of microtubules. J. Cell Biol. **145:** 993–1007.

Van Damme, D., Bouget, F.-Y., Van Poucke, K., Inze, D., and Geelen, D. (2004a). *Molecular dissection of plant cytokinesis and phragmoplast structure: A survey of GFP-tagged proteins.* Plant J. **40:** 386–398.

Van Damme, D., Van Poucke, K., Boutant, E., Ritzenthaler, C., Inze, D., and Geelen, D. (2004b). In vivo dynamics and differential microtubule-binding activities of MAP65 proteins. Plant Physiol. **136:** 3956–3967.

Vaughan, K.T. (2005). TIP maker and TIP marker; EB1 as a master controller of microtubule plus ends. J. Cell Biol. **171:** 197–200.

Vos, J.W., Dogterom, M., and Emons, A.M.C. (2004). Microtubules become more dynamic but not shorter during preprophase band formation: A possible "search and capture" mechanism for microtubule translocation. Cell Motil. Cytoskeleton **57:** 246–258.

Wasteneys, G., and Fujita, M. (2006). Establishing and maintaining axial growth: wall mechanical properties and the cytoskeleton. J. Plant Res. **119:** 5–10.

Wasteneys, G.O. (2002). Microtubule organization in the green kingdom: Chaos or self-order? J. Cell Sci. **115:** 1345–1354.

Wasteneys, G.O., Willingale-Theune, J., and Menzel, D. (1997). Freeze shattering: A simple and effective method for permeabilizing higher plant cell walls. J. Microsc. **188:** 51–61.

Weigel, D., et al. (2000). Activation tagging in *Arabidopsis*. Plant Physiol. **122:** 1003–1013.

Wu, X.S., Tsan, G.L., and Hammer III, J.A. (2005). Melanophilin and myosin Va track the microtubule plus end on EB1. J. Cell Biol. **171:** 201–207.

Zar, J.H. (1974). Biostatistical Analysis. (Englewood Hills, NJ: Prentice-Hall).

CHAPTER 8

DISCUSSION

Early development in *S. compressa* is an extremely critical period of its life cycle. The forces of the intertidal zone can be quite harsh; the relatively fast rise and fall of the tides demand an efficient and accurate anchoring mechanism, dependent upon proper establishment and maintenance of zygotic polarity. The egg cell forms a default polar axis upon fertilization, so it can grow a rhizoid and attempt to attach to the rocky substratum even when no environmental vectors are detected (Hable and Kropf, 2000). Before sensing environmental cues, the zygote begins to anchor itself to the substratum using a polyphenolic-based primary adhesive (Hable and Kropf, 1998; Vreeland et al., 1993). The zygote then integrates multiple vectors before choosing a new, more suitable, polar axis to direct deposition of adhesive asymmetrically towards the rocks to strengthen attachment. This polar axis remains labile and capable of disassembling and reassembling according to perception of new vectorial cues (Kropf, 1992). At germination the polar axis becomes fixed and rhizoid outgrowth commences; a subsequent change in light direction will redirect rhizoid growth but no additional rhizoids will emerge. The polar axis also establishes the position of the spindle, which subsequently determines cell plate placement (Bisgrove and Kropf, 2001a; Bisgrove and Kropf, 2004). The resulting asymmetric cell division creates distinct cell fates corresponding to the rhizoid and thallus lineages. The focus of my research has been to examine microtubule function and regulation during these early developmental processes.

8.1 Research summary and interpretation

Since little was known about microtubule array morphology during polarity establishment, I first conducted experiments aimed at assessing microtubule organization. For this I employed two experimental approaches. I first modified existing

immunoflourescence protocols to optimize preservation of microtubules and found microtubule bundles extend from their point of nucleation at centrosomes out to and along the cell cortex. I then utilized high pressure freezing to confirm these results. Microtubule arrays appeared to be nucleated exclusively from centrosomes; I did not observe any evidence for cortical nucleation, in contrast to a recent report (Corellou et al., 2005). Strikingly, I found that early in the polarization process microtubule arrays were asymmetrically oriented. They were highly spatially and temporally correlated with deposition of polar adhesive, a marker of the rhizoid pole. The initially broad microtubule arrays became increasingly focused toward the rhizoid pole as early development proceeded. These data suggested that microtubules, in contrast to established dogma, likely play an important role during polarity establishment in brown algae.

I therefore set out to identify the functional role(s) of microtubules during polarity establishment. Recent evidence from our lab suggested microtubules may play a role in organization of the endomembrane system (Hadley et al., 2006). I showed that microtubules were indeed required for organization of the endoplasmic reticulum and for efficient deposition of asymmetric adhesive (Chapter 2). Asymmetric microtubule arrays were highly spatially correlated with endoplasmic reticulum asymmetry, and their colocalization became more focused toward the rhizoid pole as polarization progressed. Statistical analysis showed that the correlation between microtubule and endoplasmic reticulum positioning was highly significant. Additional studies showed that reorientation of the polarizing light vector led to redistribution of microtubules followed by retargeting of the endoplasmic reticulum and adhesive deposition. Finally, inhibitor studies were conducted. I found that while disruption of microtubules led to aggregation of

endoplasmic reticulum and loss of asymmetry, inhibition of F-actin function did not uncouple the strong colocalization of microtubules and endoplasmic reticulum. This work demonstrates that microtubules, not F-actin, are responsible for endoplasmic reticulum organization.

Since microtubules appeared to perform important roles during early development in *S. compressa*, I next began to identify the signaling pathways which regulate microtubule array morphology. The PLD and PLC phospholipid signaling pathways have been shown to regulate cytoskeletal function in other lineages (Jenkins and Frohman, 2005; Meijer and Munnik, 2003; Munnik, 2001; Oude Weernink et al., 2007). Inhibitors are also available to help dissect the function of the PLD and PLC pathways. To disrupt the PLD pathway, 1-butanol was applied to zygotes during the polarization process. Treatment with 1-butanol led to immediate and dramatic cellular effects. Within 30 minutes of application microtubule arrays appeared almost completely fragmented. Over the next 2 hours, these short fragmented microtubule elements aggregated in the cortex of zygotes and formed large structures resembling lightning bolts. No centrosomally-nucleated microtubules were observed following 1-butanol treatment. Consistent with earlier studies using the microtubule-disrupting agents taxol and oryzalin (Hadley et al., 2006), zygotes treated with 1-butanol still germinated and grew a rhizoid tip, albeit more slowly and less well focused. These cells ultimately arrested in mitosis, unable to form a bipolar mitotic spindle. Since disruption of F-actin or endomembrane trafficking blocks germination, my results suggested that the PLD pathway primarily signals to microtubules, and not directly to F-actin or the endomembrane system. Wash out of 1-butanol rescued zygotes and the vast majority went on to divide successfully. The rapid

reversibility of 1-butanol provided a novel tool for synchronizing zygotes and this tool was employed to study spindle assembly (Chapter 6).

I also addressed the roles of the highly conserved PLC signaling pathway. Since the formation of PA derived from the PLC pathway is based on phosphorylation by DAGK, I sought to employ specific inhibitors of DAGK. Treatment of polarizing *S. compressa* zygotes with the DAGK inhibitor R59022 led to microtubule and developmental defects. In contrast to 1-butanol treatment, the microtubule arrays of *S. compressa* did not heavily fragment under R59022 treatment. Instead, the microtubule arrays formed long linear bundles, exclusively in the cortex. Additionally, R59022 treatment blocked rhizoid outgrowth, known to be dependent on F-actin and endomembrane trafficking. Therefore, the PLC signaling pathway in brown algae appears to have multiple targets and is likely more diverse than the PLD pathway.

Cortical localization of microtubules following PLD or PLC pathway disruption may have resulted from either cortical nucleation sites or aggregation of microtubules/microtubule fragments at the plasma membrane. We have not uncovered any evidence of cortical nucleation sites for microtubules from either conventional or high pressure freezing fixation techniques. Instead, the plus ends of radially oriented microtubule arrays may interact with the plasma membrane, and as microtubules elongate along the cell cortex they likely become laterally stabilized by MAPs. When microtubule arrays become fragmented or perturbed, as under PLD or PLC pathway disruption, cortical interactions may still occur and produce the heavily bundled and exclusively cortical appearance of microtubule arrays.

The PLD and PLC pathways impact a variety of targets in other systems (Jenkins and Frohman, 2005; Meijer and Munnik, 2003; Munnik, 2001; Oude Weernink et al., 2007). Inhibition of the PLD pathway disrupts F-actin organization in animals, higher plants, slime molds, and red algae (Jenkins and Frohman, 2005; Li et al., 2009; Meijer and Munnik, 2003; Mikami K, 2009; Zouwail et al., 2005). However, PLD disruption does not affect F-actin-based processes in *S. compressa,* yet it strongly disrupts microtubule arrays and microtubule-based processes. Thus, PLD signaling in stramenopiles, compared to other systems, appears to have evolved primarily microtubule-specific targets.

In contrast, the PLC signaling pathway is more pleiotropic in *S. compressa.* Inhibition of DAGK not only disrupts microtubules and microtubule-dependent processes, but also F-actin and endomembrane-based processes. In animals and red algae, PLC disruption blocks F-actin-based processes (Li et al., 2009; Wang, 2004). In higher plants microtubule-based defects are observed when PLC signaling is disrupted (Meijer and Munnik, 2003). There are several possible reasons why the PLC pathway has taken on diverse functional roles in brown algae. The PLC pathway yields multiple signaling molecules including IP_3, DAG, and PA (Wang, 2004), and each may have unique downstream targets. PA produced from different pathways need not be functionally equivalent as a signaling molecule (Hodgkin et al., 1998; Testerink and Munnik, 2005). The fatty acid chain length and degree of saturation may impose an additional layer of signaling specificity to the two pathways. Also, the apparent functional expansion of the PLC pathway may have compensated for a more restricted PLD pathway. Future work

should help elucidate whether the observed variation in the targets of the PLD and PLC pathways are directly related to variation in the PA molecule itself.

In my final line of investigation, I initiated studies on the roles of MAPs during early development. As a starting point, I tested the function of plus-end-directed kinesin motor proteins. Kinesins are a diverse group of microtubule-associated proteins which have a variety of functions, ranging from vesicle trafficking to microtubule severing to spindle organization (Lawrence et al., 2004). Since spindle formation is critical for placement of the division plane in *S. compressa*, I chose to study Eg5 because of its known role in spindle assembly and maintenance. Two approaches were taken; first, antibodies were used to assess the localization of Eg5 during the cell cycle. Second, a small molecule inhibitor, monastrol, was applied to block Eg5 function. This work constitutes the first time kinesin motors have been studied in stramenopiles.

Immunolocalization studies showed that Eg5 was sequestered within the nucleus during interphase. During mitosis, Eg5 motors were localized to spindle poles and weakly to the spindle midzone. Monastrol treatment did not affect microtubule organization during interphase. Instead, Eg5 was shown to be necessary for formation of spindles, as well as maintenance of spindle bipolarity. Treatment of zygotes prior to metaphase led to high proportions of multipolar spindles and cytasters, while treatment after spindle formation led to high proportions of short bipolar spindles. I hypothesize that during formation of a spindle Eg5 functions to maintain spindle pole integrity and once a bipolar spindle is formed, Eg5 maintains pole separation through interactions with interdigitating microtubules at the midzone.

Curiously, while the localization of Eg5 in *S. compressa* is similar to animals (Crevel et al., 1997; Kapitein et al., 2005), the mitotic functions of Eg5 appear to be more like those of higher plants (Bannigan et al., 2007). Eg5 is localized to the nucleus during interphase and then associates with spindle poles during mitosis in both animals and *S. compressa* (Kapitein et al., 2005). In contrast, Eg5 has been show to associate along the length of microtubules during interphase and with the spindle during mitosis in Arabidopsis (Bannigan et al., 2007). Interestingly, a temperature-sensitive mutation in the Eg5 homologue in Arabidopsis induced multipolar spindles or monasters during mitosis, much as we found in *S. compressa* (Bannigan et al., 2007). In animals, Eg5 inhibition causes spindle collapse but does not induce formation of multipolar spindles (Miyamoto et al., 2003). Apparently, both higher plants and brown algae utilize Eg5 for maintaining spindle pole integrity and spindle bipolarity. Further studies will be needed to adequately address the evolution of Eg5 localization and function across other lineages of the tree of life.

8.2 Model of early development

My work has focused on examining the roles of microtubules during early development in *S. compressa*, and has provided novel insights and new avenues for future work. From these findings I propose a revised model, presented in Figure 8.1, of the cellular and physiological processes that orchestrate early development in *S. compressa*.

Development begins with the release of sessile symmetric egg cells and small motile sperm from receptacles (Kropf, 1994). Fertilization establishes a default axis with the rhizoid pole at the site of sperm entry (Hable and Kropf, 2000). A patch of F-actin

Figure 8.1 Model of Early Development in *S. compressa*
Important aspects of polarization and early development are represented, see text for details. Heavily outlined boxes depict stages of early development. Thinly lined boxes represent sequential or simultaneous steps in early development determined from previous studies. Double thinly lined boxes correspond to my hypothesized aspects of polarization. Grayed boxes represent my original work from this thesis. Arrows depict regulatory interactions: solid arrows represent direct interactions, dashed arrows represent indirect microtubule-based interactions, and dotted arrows represent potential F-actin-based interactions. The question mark indicates a potential direct regulatory interaction from the PLC pathway to F-actin organization.

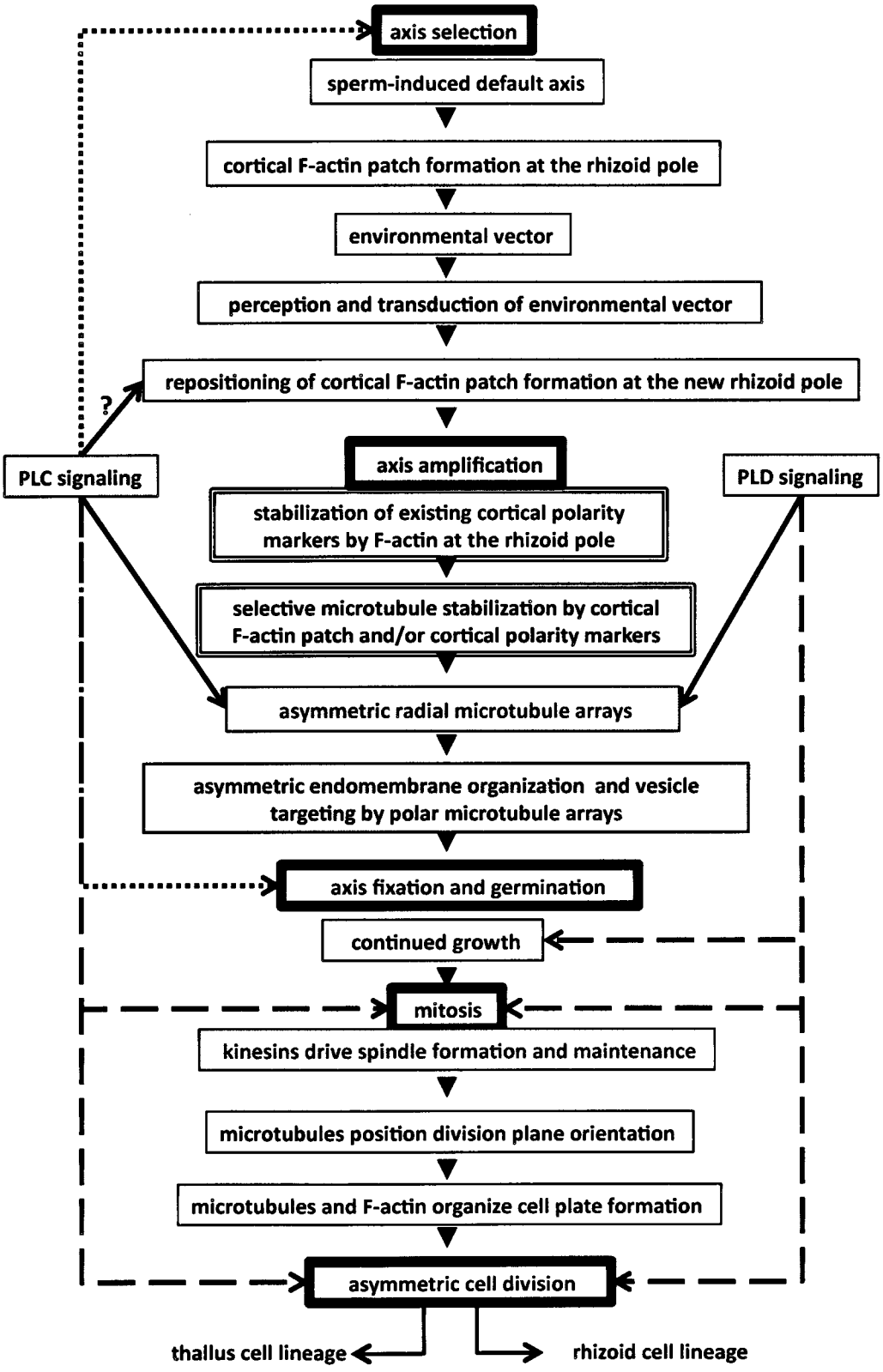
axis selection
sperm-induced default axis
cortical F-actin patch formation at the rhizoid pole
environmental vector
perception and transduction of environmental vector
repositioning of cortical F-actin patch formation at the new rhizoid pole
?
PLC signaling
axis amplification
PLD signaling
stabilization of existing cortical polarity markers by F-actin at the rhizoid pole
selective microtubule stabilization by cortical F-actin patch and/or cortical polarity markers
asymmetric radial microtubule arrays
asymmetric endomembrane organization and vesicle targeting by polar microtubule arrays
axis fixation and germination
continued growth
mitosis
kinesins drive spindle formation and maintenance
microtubules position division plane orientation
microtubules and F-actin organize cell plate formation
asymmetric cell division
thallus cell lineage
rhizoid cell lineage

marks the site of sperm entry (Alessa and Kropf, 1999). Environmental vectors, typically light, can override the default axis and establish a new polar axis (Brownlee et al., 2001). The sperm-induced F-actin patch depolymerizes and a new F-actin patch forms in the cortex of the new rhizoid pole (Hable et al., 2003). Any polar axis is likely amplified as soon as an F-actin patch forms. I hypothesize that during amplification, binding to F-actin stabilizes cortical polarity markers and both may act to selectively stabilize microtubule plus ends. Local capture by F-actin/or polarity markers results in asymmetric microtubule arrays early in the amplification process. These asymmetric arrays progressively focus toward the rhizoid pole as more microtubules are captured. The arrays organize the endoplasmic reticulum and are responsible for its asymmetric distribution. Microtubules transport vesicles containing calcium and proton channels to the rhizoid pole. Localized vesicle secretion, dependent on F-actin, feeds forward to amplify the polar axis by inserting ion channels at the rhizoid pole and thus amplify polarizing ion gradients. In addition, microtubule plus ends deliver polarity markers preferentially to the F-actin patch at the rhizoid pole, which further aid in the capture of microtubules and axis amplification.

Germination is due to localized cell wall loosening and continued secretion at the rhizoid pole (Bisgrove and Kropf, 2001b). At first mitosis, kinesin motors are required for organization of the mitotic spindle. Eg5 organizes spindle poles and maintains pole-to-pole separation. Interdigitating microtubules define the plane of cell division and deliver vesicles to the division zone where F-actin is required for cell plate formation (Bisgrove and Kropf, 2001a). The resulting, asymmetric, cell division yields thallus and rhizoid cell lineages, with the thallus cell giving rise to the vegetative stipe and

reproductive fronds while the rhizoid cell lineage becomes the holdfast to anchor the alga down in the rocks.

Phospholipid signaling pathways function throughout the cell cycle. My work suggests that PLD signaling strongly and directly regulates microtubules, and thereby indirectly regulates cell growth, mitosis, and cell division, all microtubule-dependent processes. The PLC pathway has multiple targets including microtubules, and perhaps regulates F-actin and/or endomembrane-based processes. The impending genomic and genetic tools being developed for brown algae should provide the tools needed to comprehensively examine early development and build off of the foundation of work presented here.

8.3 Thoughts on evolution of microtubule morphology and function

Although brown algae are evolutionarily quite distant from animals, their organization and utilization of microtubules during early development appear similar (Motomura, 1989; Oakley, 1989). Both systems possess microtubule-nucleating centrosomes and asymmetric, radially oriented, microtubule arrays that organize the endoplasmic reticulum and transport vesicles (Cuschieri, 2007; Hehnly and Stamnes, 2007; Kollu et al., 2009; Motomura, 1989; Oakley, 1989). Thus, the ancestral state of microtubule organization and function is likely similar to modern day animals and stramenopiles, and must have evolved prior to their divergence many millions of years before the crown group radiation. In contrast, higher plants have lost centrosomes and disperse their MTOCs throughout the cortex of the cell (Smirnova, 2003). Because of this, higher plants typically have parallel cortical microtubule arrays that help orient deposition of cellulose, directing cell shape (Lucas and Shaw, 2008). In higher plants, F-

actin has acquired functions originally performed by microtubules, including movement of vesicles, cytoplasmic streaming, and in organization of the endoplasmic reticulum (Wasteneys, 2000).

8. 4 References

Alessa, L., and Kropf, D.L. (1999). F-actin marks the rhizoid pole in living *Pelvetia compressa* zygotes. Development *126*, 201-209.

Bannigan, A., Scheible, W.-R., Lukowitz, W., Fagerstrom, C., Wadsworth, P., Somerville, C., and Baskin, T.I. (2007). A conserved role for kinesin-5 in plant mitosis. J. Cell Sci. *120*, 2819-2827.

Bisgrove, S.R., and Kropf, D.L. (2001a). Asymmetric cell division in fucoid algae: a role for cortical adhesions in alignment of the mitotic apparatus. J. Cell Sci. *114*, 4319-4328.

Bisgrove, S.R., and Kropf, D.L. (2001b). Cell wall deposition during morphogenesis in fucoid algae. Planta *212*, 648-658.

Bisgrove, S.R., and Kropf, D.L. (2004). Cytokinesis in brown algae: Studies of asymmetric division in fucoid zygotes. Protoplasma *223*, 163-173.

Brownlee, C., Bouget, F.-Y., and Corellou, F. (2001). Choosing sides: establishment of polarity in zygotes of fucoid algae. Cell Dev. Biol. *12*, 345-351.

Corellou, F., Coelho, S.M.B., Bouget, F.-Y., and Brownlee, C. (2005). Spatial re-organisation of cortical microtubules in vivo during polarisation and asymmetric division of *Fucus* zygotes. J. Cell Sci. *118*, 2723-2734.

Crevel, I.M.T.C., Lockhart, A., and Cross, R.A. (1997). Kinetic evidence for low chemical processivity in ncd and Eg5. J. Molec. Biol. *273*, 160-170.

Cuschieri, L., Nguyen, T., Vogel, J. (2007). Control at the cell center: the role of spindle poles in cytoskeletal organization and cell cycle regulation. Cell Cycle *6*, 2788-2794.

Hable, W.E., and Kropf, D.L. (1998). Roles of secretion and the cytoskeleton in cell adhesion and polarity establishment in *Pelvetia compressa* zygotes. Dev. Biol. *198*, 45-56.

Hable, W.E., and Kropf, D.L. (2000). Sperm entry induces polarity in fucoid zygotes. Development *127*, 493-501.

Hable, W.E., Miller, N.R., and Kropf, D.L. (2003). Polarity establishment requires dynamic actin in fucoid zygotes. Protoplasma *221*, 193-204.

Hadley, R., Hable, W.E., and Kropf, D.L. (2006). Polarization of the endomembrane system is an early event in fucoid zygote development. BMC Plant Biol. *6*, 1-10.

Hehnly, H., and Stamnes, M. (2007). Regulating cytoskeleton-based vesicle motility. FEBS Letters *581*, 2112-2118.

Hodgkin, M.N., Pettitt, T.R., Martin, A., Michell, R.H., Pemberton, A.J., and Wakelam, M.J.O. (1998). Diacylglycerols and phosphatidates: which molecular species are intracellular messengers? Trends Biochem. Sci. *23*, 200-204.

Jenkins, G., and Frohman, M. (2005). Phospholipase D: a lipid centric review. CMLS *62*, 2305-2316.

Kapitein, L.C., Peterman, E.J.G., Kwok, B.H., Kim, J.H., Kapoor, T.M., and Schmidt, C.F. (2005). The bipolar mitotic kinesin Eg5 moves on both microtubules that it crosslinks. Nature *435*, 114-118.

Kollu, S., Bakhoum, S.F., and Compton, D.A. (2009). Interplay of microtubule dynamics and sliding during bipolar spindle formation in mammalian cells. Curr. Biol. *11*, 21-32.

Kropf, D. (1992). Establishment and expression of cellular polarity in fucoid zygotes. Microbiol. Rev. *56*, 316-339.

Kropf, D.L. (1994). Cytoskeletal control of cell polarity in a plant zygote. Dev. Biol. *165*, 361-371.

Lawrence, C.J., Dawe, R.K., Christie, K.R., Cleveland, D.W., Dawson, S.C., Endow, S.A., Goldstein, L.S.B., Goodson, H.V., Hirokawa, N., Howard, J., *et al.* (2004). A standardized kinesin nomenclature. J. Cell Biol. *167*, 19-22.

Li, L., Saga, N., and Mikami, K. (2009). Ca2+ influx and phosphoinositide signalling are essential for the establishment and maintenance of cell polarity in monospores from the red alga Porphyra yezoensis. J. Exp. Bot. *60*, 3477-3489.

Lucas, J., and Shaw, S.L. (2008). Cortical microtubule arrays in the *Arabidopsis* seedling. Curr.Opin. Plant Biol. *11*, 94-98.

Meijer, H., and Munnik, T. (2003). Phospholipid-based signaling in plants. Annu. Rev. Plant Biol. *54*, 265-306.

Mikami K, L.L., Takahashi M, Saga N. (2009). Photosynthesis-dependent Ca2+ influx and functional diversity between phospholipases in the formation of cell polarity in migrating cells of red algae. Plant Signal. Behav. *4*, 911-913.

Miyamoto, D., Perlman, Z., Mitchison, T., and Shirasu-Hiza, M. (2003). Dynamics of the mitotic spindle--potential therapeutic targets. Prog. Cell Cycle Res. *5*, 349-360.

Motomura, T. (1989). Ultrastructural study of sperm in *Laminaria angustata (Laminariales, Phaeophyta)*, especially on the flagellar apparatus. Jpn. J. Phycol. *37*, 105-116.

Munnik, T., Musgrave, A. (2001). Phospholipid signaling in plants: holding on to phospholipase D. Sci. Signlaing *4*, 42.

Oakley, C.E.O., B. R. (1989). Identification of γ-tubulin, a new member of the tubulin superfamily encoded by mipA gene of *Aspergillus nidulans*. Nature *338*, 662-664.

Oude Weernink, P., López de Jesús, M., and Schmidt, M. (2007). Phospholipase D signaling: orchestration by PIP2 and small GTPases. Naunyn-Schmiedeberg's Arch. Pharmacol. *374*, 399-411.

Smirnova, E.A. (2003). Spindle pole formation in higher plant cells. Cell Biol. Inter. *27*, 273-274.

Testerink, C., and Munnik, T. (2005). Phosphatidic acid: a multifunctional stress signaling lipid in plants. Trends Plant Sci. *10*, 368-375.

Vreeland, V., Grotkopp, E., Espinosa, S., Quiroz, D., Laetsch, W.M., and West, J. (1993). The pattern of cell wall adhesive formation by *Fucus* zygotes. Hydrobiologia *260/261*, 485-491.

Wang, X. (2004). Lipid signaling. Curr. Opin. Plant Biol. *7*, 329-336.

Wasteneys, G.O. (2000). The cytoskeleton and growth polarity. Curr. Opin. Plant Biol. *3*, 503-511.

Zouwail, S., Pettitt, T.R., Dove, S.K., Chibalina, M.V., Powner, D.J., Haynes, L., Wakelam, M.J.O., and Insall, R.H. (2005). Phospholipase D activity is essential for actin localization and actin-based motility in *Dictyostelium*. Biochem. J. *389*, 207-214.